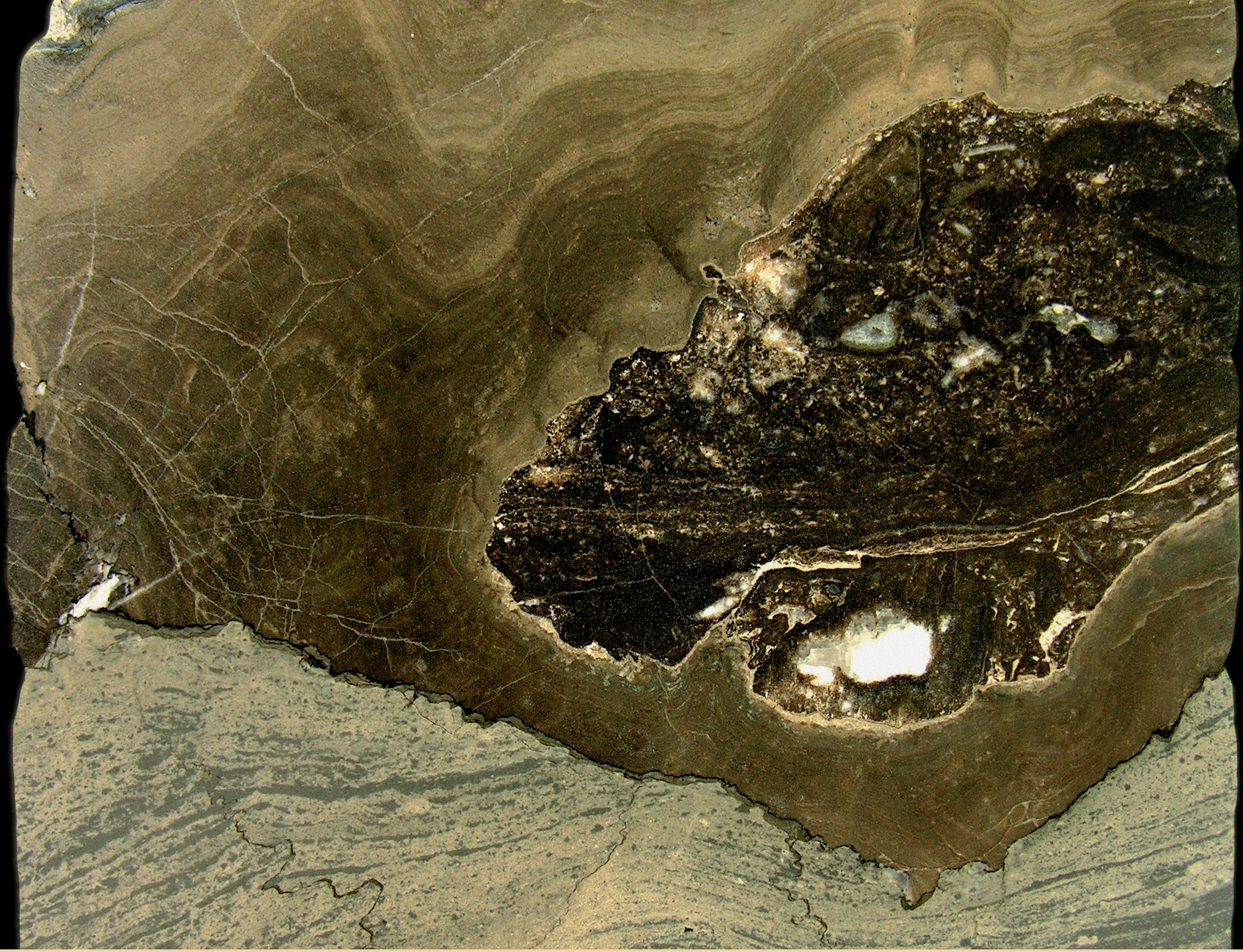

Upper part of the gas-bearing Zechstein Limestone reef in western Poland (Kościan 20 well, depth 2151.3 m): laminated fenestral mudstone covered by stromatolite, which is encrusting bioclastic limestone with anhydrite nodules. Sample length 12 cm. Photo by Pawel Raczyński.

Chapter 8 Zechstein

Authors
Tadeusz Marek Peryt (PGI), Mark Geluk (Shell E&P Int B.V.), Anders Mathiesen (GEUS), Josef Paul (University of Göttingen; retired) and Kevin Smith (BGS)

Contributors
Andrzej Gąsiewicz (PGI), Marek Jasionowski (PGI), Valentinas Kadunas (Institute of Geology and Geography, Vilnius), Paweł Raczyński (University of Wrocław) and Paweł Zdanowski (POGC)

Bibliographic reference
Peryt, T.M., Geluk, M.C., Mathiesen, A., Paul, J. & Smith, K., 2010. Zechstein. *In:* Doornenbal, J.C. and Stevenson, A.G. (editors): Petroleum Geological Atlas of the Southern Permian Basin Area. EAGE Publications b.v. (Houten): 123-147.

1 Introduction

Zechstein rocks extend across the entire SPBA area from the UK to Latvia, Lithuania (see Section 4) and western Belarus in the east (**Figure 8.1**). The depositional area is delineated by several Variscan highs, including the London-Brabant and Rhenish massifs in the south and the Mid North Sea and Ringkøbing-Fyn highs in the north. The evolution of the Northern Permian Basin, which lies to the north of the Mid North Sea and Ringkøbing-Fyn highs, is described in detail in the Millennium Atlas (Glennie et al., 2003). During the Zechstein, there may have been connections between the Northern and Southern Permian basins across the intervening highs (Jenyon et al., 1984; Glennie et al., 2003). There were also local contemporaneous highs within the SPB area during the Permian, but their influence on facies distribution gradually decreased as Zechstein sediments were deposited. Areas where the Zechstein is absent are mostly related to erosion, either at the regional pre-Cretaceous unconformity or during uplift associated with basin inversion in the Late Cretaceous.

The Zechstein inland sea was established by rapid flooding of a Late Permian intracontinental topographic depression. At about 257.5 Ma (Brauns et al., 2003), a catastrophic transgression from the Barents Sea inundated both the Northern and Southern Permian basins and brought fully marine conditions for the first time since the Early Carboniferous (Ziegler, 1990a; Taylor, 1998; Glennie et al., 2003). Through a combination of rifting and eustatic sea-level rise, (Glennie & Buller, 1983), this rapid flooding had a loading effect on the lithosphere that caused further regional subsidence and overstepping of the Rotliegend Basin margins (Ziegler, 1990a; Geluk, 1999a; McCann et al., 2008b). The correlation of Zechstein strata with the global Permian timescale is still under debate. Early Wuchiapingian conodonts in the Kupferschiefer (e.g. Legler et al., 2005) would seem to indicate that the duration of the Zechstein was longer than is accepted in this chapter. Another unresolved question concerns the nature of the marine ingression into the SPB, as foraminiferal (Peryt & Peryt, 1975, 1977) and ostracod microfauna (Ivanov, 1975) of Tethyan and Uralian affinities suggest an additional alternate source. These microfauna first appear within the basal Zechstein deposits of the Polish and Lithuanian areas of the SPB. In contrast, the fauna in England are clearly of Boreal affinity (Hollingworth & Pettigrew, 1988).

Tectonism played a minor local role during Zechstein deposition. Synsedimentary tectonic features are reported from basal Zechstein anhydrite platforms bordering the main salt basin (Wolf, 1985; Ziegler, 1989; Geluk, 1999a), mainly along the southern margin of the SPB. Here, the Zechstein depressions are aligned with west-north-west and north-north-east-oriented lineaments and are thought to have originated from minor transtensional movements enhanced by the loading effect of rapidly deposited evaporites (Geluk, 1999a, 2005). A second phase of tectonic movements towards the end of the Permian resulted in a disconformity in the upper Zechstein (Geluk, 1999a).

There are numerous papers dealing with aspects of the Zechstein Basin (e.g. Füchtbauer & Peryt, 1980; Depowski, 1981; Harwood & Smith, 1986; Peryt, 1987a; Schröder et al., 1991b) as well as syntheses of parts, or the entire basin (e.g. Ziegler, 1990a; Kiersnowski et al., 1995; Geluk, 2005; McCann et al., 2008b). This chapter presents a review based on both published and unpublished studies (**Table 8.1**). Zechstein outcrops are limited (**Figure 8.2**), therefore research has usually focussed on subsurface data (mostly core material and seismic data) although outcrops in areas such as the Harz Mountains and Lithuania have been studied in detail. In addition to papers of regional importance, reference is made to publications dealing with local aspects of the facies and sedimentology of particular Zechstein members.

Table 8.1 Benchmark papers summarising data from various countries and regions.

Lithuania and the Kaliningrad Region	Suveizdis (1975); Suveizdis & Katinas (1990); Kadunas (2001)
Poland	
– General	Wagner (1994); Dadlez et al. (1998);
– NE and northern Poland	Peryt (1989a); Peryt et al. (1992)
– NW Poland	Wagner (1976, 1979, 1987)
– SW Poland	Peryt (1977, 1978a, 1981a); Śliwiński (1988); Peryt & Kasprzyk (1992); Raczyński (1996, 1997)
– Central Poland (Holy Cross Mts)	Kostecka (1966); Pawłowska (1968, 1978); Rubinowski (1978); Peryt & Rup (1987); Gąsiewicz et al. (1991)
– East Poland	Peryt (1990)
Germany	Richter-Bernburg (1955a); Boigk et al. (1960); Füchtbauer (1964); Trusheim (1964); Sannemann et al. (1978); Paul (1987); Kulick & Paul (1987); Langbein & Seidel (1995); Becker (2002); Hug (2004)
Denmark	Clark & Tallbacka (1980); Sønderholm (1987); Stemmerik et al. (1987); Stemmerik & Frykman (1989); Vejbæk (1997); Evans et al. (2003)
The Netherlands	Van Adrichem Boogaert & Burgers (1983); Clark (1986); Van der Baan (1990); Geluk et al. (1997); Geluk (2005)
North Sea	Cameron et al. (1992); Taylor (1998)
United Kingdom	Smith (1994, 1995)

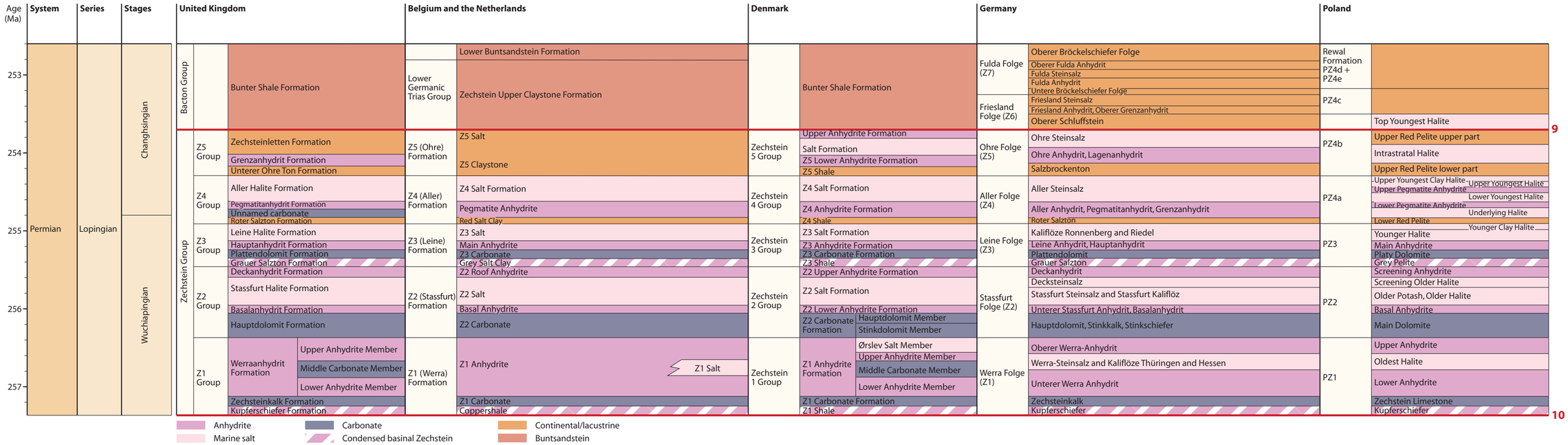

Figure 8.1 Tectonostratigraphic correlation chart of the Zechstein. See Table 8.2 for detailed correlation. The red line at the base of the Kupferschiefer/Z1 Shale (10) is the lithostratigraphic horizon used to map the depth to the base of the Zechstein. See Figures 1.5 and 8.2.

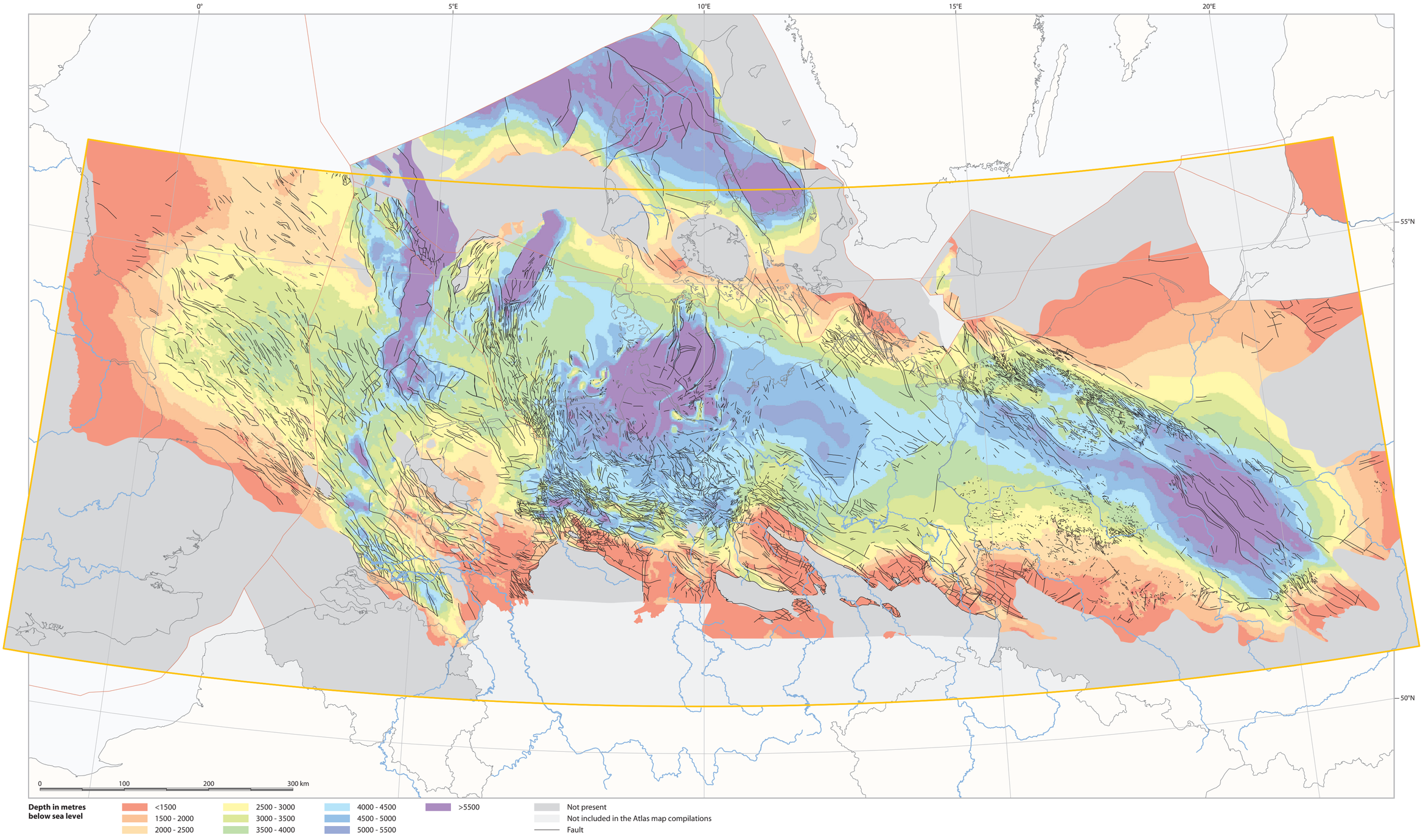

Figure 8.2 Depth to the base of the Zechstein. The lithostratigraphic horizon is shown as Horizon 10 on Figures 1.5 and 8.1.

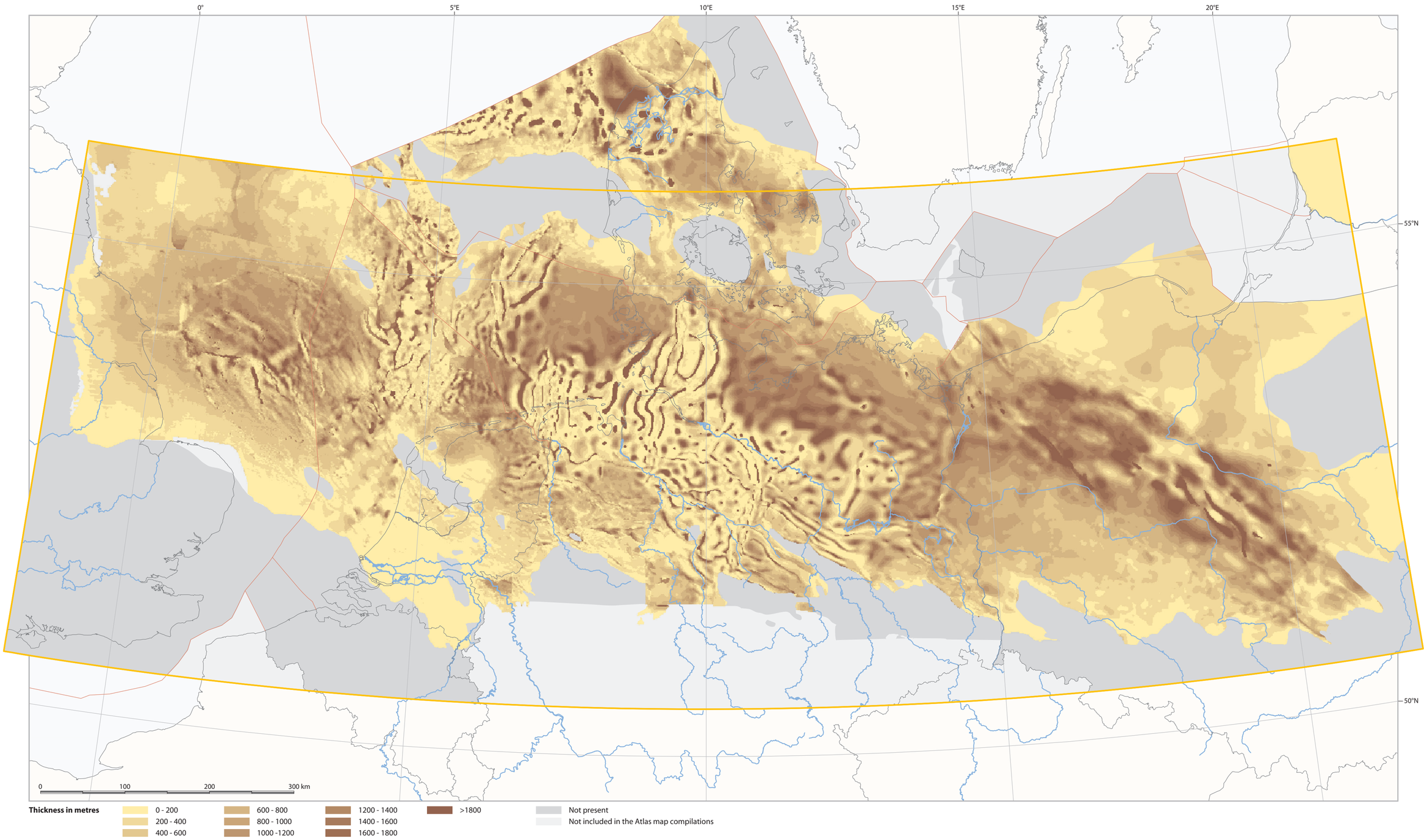

Figure 8.3 Thickness of the Zechstein.

2 Stratigraphy

Regional stratigraphic correlation of Zechstein strata is relatively straightforward as sedimentation throughout the SPB area follows the classical model of cyclic chemical precipitation in a giant saline basin (Richter-Bernburg, 1955a, 1955b). Traditionally, four evaporitic cycles have been identified, known as the Z1-Werra, Z2-Stassfurt, Z3-Leine, and Z4-Aller Series (Richter-Bernburg, 1955b), although younger cycles (Ohre Z5, Friesland Z6, and Fulda Z7) have been recognised subsequently in the axial parts of the Anglo-Dutch and North German basins (Kulick & Paul, 1987; Best, 1989; Geluk et al., 1997; Käding, 2000; Geluk, 2005) (**Figure 8.1**; **Table 8.2**).

There is a consensus that the three predominantly marine lower cycles are of different magnitude to the younger cycles, during which salt deposition appears to have been driven more by short-term climatic variation (Wagner, 1994; Geluk et al., 1997). The depositional thickness of the Zechstein is thought to have reached up to 1500-2000 m in the Polish Trough, the Anglo-Dutch and North German basins (Olsen, 1987; Wagner, 1994; Taylor, 1998), gradually thinning towards the basin margins (**Figure 8.3**). Due to widespread post-Permian salt movement and erosion, present-day thicknesses are very variable and do not have a clear relationship with the original thicknesses of Zechstein deposits.

Correlation of Zechstein sequences with global standard stages using faunal evidence is difficult because of the absence of index fossils, but there are reasons to suggest that the Zechstein corresponds to the last 5 to 7 Ma of the Permian (Menning, 1995). Menning et al. (2005) proposed that the duration of the Zechstein, based on magnetostratigraphy and radiometric data, was about 2.8 Ma. This is supported by strontium isotope data from Zechstein anhydrites, which indicate that the Zechstein anhydrites of the upper part of the Werra and the Stassfurt and Leine cyclothems are latest Permian in age and represent a time interval less than 2 Ma (Denison & Peryt, 2009).

The Zechstein Group is traditionally divided into cycles reflecting progressive evaporation: at the base of a cycle are normal marine sediments followed by sediments that indicate increasing salinity (Richter-Bernburg, 1955a). The accompanying environmental changes were oscillatory, which resulted in the cyclicity (often of regional extent) of both carbonate (e.g., Peryt, 1984; Peryt & Dyjaczyński, 1991; Strohmenger & Strauss, 1996) and evaporite deposition (e.g. Czapowski, 1998; Richter-Bernburg, 1985; Taylor, 1980; Peryt et al., 2005).

Zechstein stratigraphy is well defined across most of the SPB. Regional stratigraphic correlation was initially established by Richter-Bernburg (1955a) and Lotze (1957), and has been subsequently refined by many authors including Van Adrichem Boogaert & Kouwe (1993), Wagner (1994), Kiersnowski et al. (1995) and Taylor (1998). The base of the Zechstein is marked by the Kupferschiefer, one of the principal correlation units in north-west European stratigraphy. The unit is widespread between the UK and Lithuania and from central Germany northwards to Denmark (Kiersnowski et al., 1995) where it represents a period of basinwide euxinic conditions and can therefore be considered an excellent time-marker. The Kupferschiefer has been dated in central Germany at 257.3±1.6 Ma based on Re/Os isotopes (Brauns et al., 2003). Two other regionally extensive correlation markers are the Grey Salt Clay at the base of the Zechstein 3 cycle and the Red Salt Clay at the base of the Zechstein 4 cycle. These markers, which represent almost isochronous flooding events, help to establish a reliable basinwide correlation.

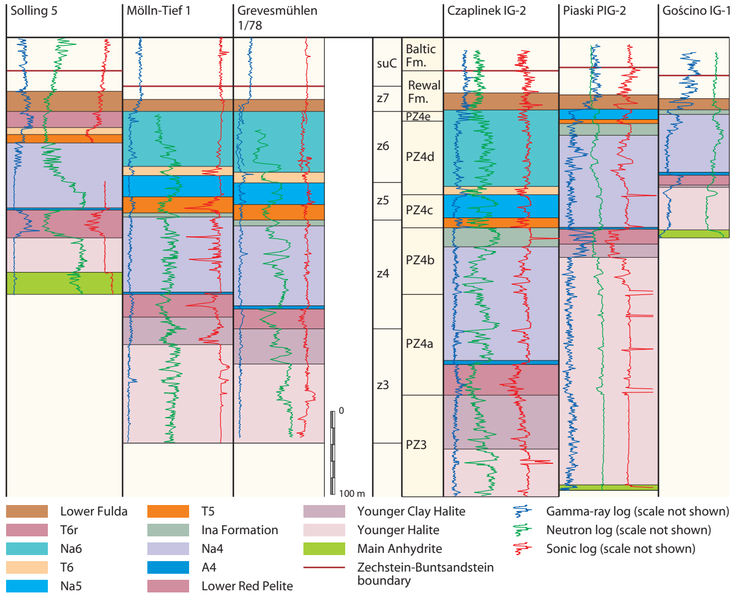

Figure 8.4 Correlation of Z3-Z7 deposits in Germany and Poland (after Käding, 2000). See Figures 8.5 and 8.21 for explanation of abbreviations.

There are two major discrepancies in the interpretation of the Zechstein interval between different countries. Firstly, there is a much wider definition of the Zechstein 4 cycle in Poland (PZ4), where it includes correlatives of Zechstein 5 and younger formations. In Poland, the fourth cyclothem (PZ4) is subdivided into five subcyclothems (from PZ4a to PZ4e), but the correlation of these subcyclothems with subdivisions in Germany is a matter of debate (Wagner & Peryt, 1997; Käding, 2000, 2003, 2005). **Figure 8.1** shows the correlation of the Polish and German sections proposed by Käding (2000), which assumes that the Rewal Formation in Poland (and specifically in the Czaplinek IG-2 borehole) corresponds to the Fulda Formation in Germany. However, Peryt & Wagner (1998) suggested that the Fulda Formation probably corresponds to subcyclothem PZ4d in the Polish Basin, which was deposited as part of a lowstand systems tract in an intracontinental salt lake; in this case, the subcyclothem PZ4e would be the youngest evaporite deposit in the entire Zechstein Basin. Käding (2000, 2003, 2005) assumed that the subcyclothems PZ4a and PZ4b in Poland correspond to cyclothem Z4 in Germany, and strata above the Z4 cycle in Germany are an equivalent of the subcyclothem PZ4c in Poland.

The second discrepancy is in the definition of the Zechstein-Buntsandstein boundary. In the Netherlands, Germany and Poland, this boundary is placed at about the same stratigraphic level (Best, 1989; Röhling, 1993; Van Adrichem Boogaert & Kouwe, 1993; Wagner, 1994; Geluk et al., 1996, 1997; Lokhorst et al., 1998; Käding, 2000; Roman, 2004). In the UK, it was formerly taken much lower, at the top of the uppermost evaporite beds (Johnson et al., 1994; Geluk, 2005), but recent regional correlations with the Permian succession in and around the Irish Sea (Jackson & Johnson, 1996) have raised the possibility that at least the basal Bröckelschiefer Member of the UK Triassic in the southern North Sea should be included in the Zechstein succession.

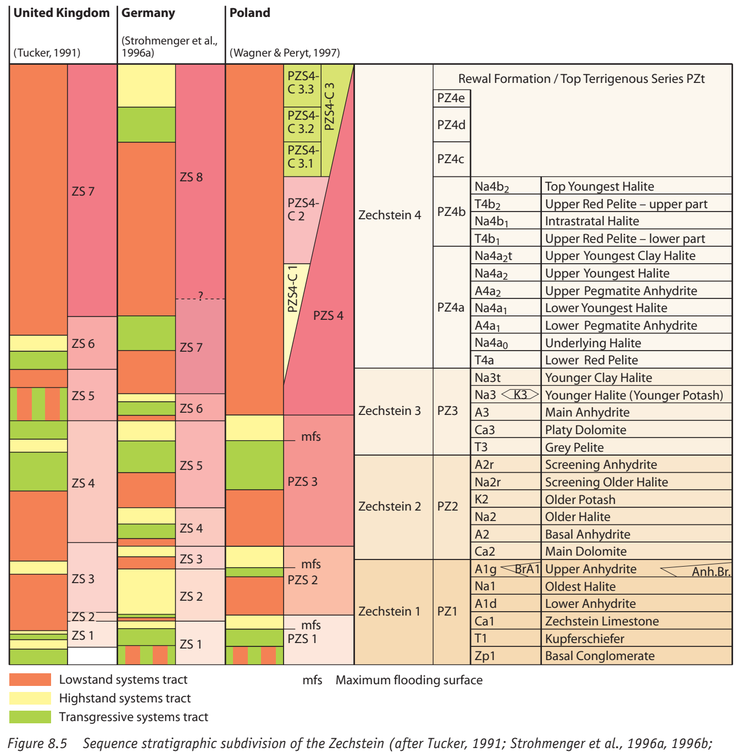

Figure 8.5 Sequence stratigraphic subdivision of the Zechstein (after Tucker, 1991; Strohmenger et al., 1996a, 1996b; Wagner & Peryt, 1997).

2.1 Sequence stratigraphy

An alternative to the classic Zechstein stratigraphy based on the concept of evaporite cycles (cyclothems) was published by Tucker (1991), who correlated evaporites with sea-level lowstands during which marginal gypsum wedges (e.g. Hartlepool Anhydrites, English Zechstein 1 cycle) or basin-centre halite fills (Fordon Evaporites, English Zechstein 2 cycle) were formed. These evaporites grade upwards into carbonates of the transgressive and highstand systems tracts. Seven depositional sequences have been distinguished by Tucker (1991) in north-east England and the adjoining North Sea area (**Figure 8.5**). These were originally regarded as third-order sequences by Tucker (1991); however, Goodall et al. (1992) pointed out that the entire Zechstein interval lies within the typical duration of third-order eustatic cycles (1-10 Ma), which would suggest that the sequences are actually fourth-order sequences (*sensu* Mitchum & van Wagoner, 1991). Goodall et al. (1992) also suggested that the carbonate-dominated lower part of the Zechstein is related to a third-order sea-level rise, whereas the upper part originated during a third-order fall. Tucker (1992) argued that, considering the deposition rate of shallow-water carbonates (averaging 60 m/Ma (Schlager, 1981)), the Zechstein carbonate formations could each represent a timespan of one million years or more. If so, the four previously identified sequences (Z1-Z4) (Tucker, 1991) could still be third-order sequences, whereas the three thin and evaporite-dominated upper sequences could represent parasequences of one third-order sequence (Tucker, 1992). The Zechstein sequence as a whole is carbonate-rich at the base and evaporite-rich at the top, which could have originated during a single second-order sea-level rise and fall respectively (Tucker, 1992).

Strohmenger et al. (1996b) refined the sequence stratigraphy of the lowermost Zechstein units (Z1 and Z2) using facies analysis, geometric relationships and stacking patterns seen on seismic-reflection data from the southern margin of the German Zechstein Basin in the area of the Weser and Ems rivers. Wagner & Peryt (1997) distinguished four depositional sequences in the Polish Zechstein, of which the first commenced during the deposition of the upper portion of the Rotliegend and the fourth continued into the lower part of the Buntsandstein (**Figure 8.5**). The same authors also proposed an alternative subdivision because of significant differences between the Polish Zechstein and that of the areas studied by Tucker (1991) and Strohmenger et al. (1996a, 1996b). These differences have prompted a different way of looking at the Zechstein division (see Wagner & Peryt, 1997 and Peryt & Wagner, 1998 for detailed discussion).

A lithostratigraphic subdivision is used in the stratigraphic description below, although reference is made to the sequence stratigraphy where necessary.

2.2 Stratigraphic and structural development

2.2.1 Zechstein 1 (Z1)

During the initial Zechstein transgression, the topmost parts of the Rotliegend dune sands were reworked to form the so-called Weissliegend. These 10 to 50 m-thick, grey to white sandstones are structurally featureless and show evidence of soft-sediment deformation. In their uppermost part, bioturbation and a marine fauna indicate that the sandstones originated in a shallow-marine, probably wave-dominated environment. However, in the southern North Sea area, there is evidence that increased fluvial activity during the latest Rotliegend caused at least part of this reworking (K.W. Glennie, pers. comm., in Geluk, 2005). The Weissliegend sandstones are therefore interpreted as aeolian sands reworked and redeposited by flash floods and wave action. The initial transgression also resulted in local deposition of the Basal Conglomerate. In the former Rotliegend playa lake, the uppermost red beds have thin sporadic layers characterised by marine shells that record short-lived pre-Zechstein ingressions of the Boreal Sea into the Permian basins of central Europe (Hoffmann et al., 1989; Legler, 2005). In southern Germany, the fluvial white Rotliegend sandstones beneath the Zechstein deposits are also termed Weissliegend. Here, the colour of the sandstones is most likely to have been the result of reducing conditions caused by solutions percolating from the overlying Zechstein strata (Paul, 2010).

The Weissliegend sandstone locally grades into limestone in Germany and Poland. The basal limestone is known as the Mutterflöz or Border Dolomite in Germany and was deposited only in shallow-water environments. All of these basal Zechstein units are overlain by the Kupferschiefer (or Marl Slate in England) followed by the Zechstein Limestone, Lower Anhydrite, Oldest Halite and Upper Anhydrite. Sediments of the Z1 Group were deposited across the entire basin (**Figure 8.7**) and onlap the margins such that progressively younger units form the base of the Zechstein. In the basin centre, the base-Zechstein deposits are a condensed succession of anhydrites and carbonates some 50 m thick; however, they may have had primary thicknesses of more than 500 m in marginal sub-basins on the platform. Water depths

Cycles	Group	Durham	Yorkshire	UK Southern North Sea
EZ5	Eksdale	Roxby Formation (Upper Marls)	Roxby Formation	Zechsteinletten Formation
			Littlebeck Anhydrite Formation (Upper or Saliferous Marls)	Grenzanhydrit Formation
			Sleights Siltstone Formation	Unterer Ohre Ton Formation
EZ4	Staintondale	Sherburn Anhydrite Formation (Upper Anhydrite)	Sneaton Halite Formation (Upper Halite)	Aller Halite Formation
			Sherburn Anhydrite Formation (Upper Anhydrite)	Pegmatitanhydrit Formation
			Upgang Formation	Unnamed carbonate
	Teeside	Rotten Marl Formation (Rotten Marl)	Rotten or Carnallitic Marl Formation (Rotten or Carnallitic Marl)	Roter Salzton Formation
EZ3		Boulby Halite Formation (Main Salt)	Boulby Halite Formation (Middle Halite)	Leine Halite Formation
		Billingham Anhydrite Formation (Billingham Main Anhydrite)	Billingham Anhydrite Formation (Billingham Main Anhydrite)	Hauptanhydrit Formation
	Aislaby	Seaham Formation (part of Upper Magnesian Limestone)	Brotherton Formation (Upper Magnesian Limestone)	Plattendolomit Formation
			Grauer Salzton	Grauer Salzton Formation
EZ2		Edlington Formation (Middle Marls or Lower Evaporites)	Edlington Formation	Deckanhydrit Formation
			Fordon Evaporite Formation (Middle Marls) in West (Lower Evaporites) in East	Stassfurt Halite Formation
				Basalanhydrit Formation
		Roker Dolomite Formation (Hartlepool and Roker Dolomite) (part of Upper Magnesian Limestone)	Kirkham Abbey Formation	Hauptdolomit Formation
		Concretionary Limestone Formation (Concretionary Limestone) (part of Upper Magnesian Limestone)		
EZ1	Don	Hartlepool Anhydrite Formation (Hartlepool Anhydrite)	Hayton Anhydrite Formation	Werraanhydrit Formation — Upper Anhydrite Member
				Middle Carbonate Member
				Lower Anhydrite Member
		Ford Formation (Middle Magnesian Limestone)	Sprotbrough Member	Zechsteinkalk Formation
			Cadeby Formation (‘upper subdivision’)	
		Raisby Formation (Lower Magnesian Limestone)	(Lower Magnesian Limestone)	
			Wetherby Member (‘lower subdivision’)	
		Marl Slate Formation (Marl Slate)	Marl Slate Formation (Marl Slate)	Kupferschiefer Formation

Symbols used in Poland		Kaliningrad region (Zagorodnykh et al., 2001)		Lithuania (Kadunas, 2001)
PZ4		Kornevskaya Suite		
PZ3	A3	Mamonovskaya Suite		Šventapilis (Mamonovo)
	Ca3	Galindaskaya Site		Galinda
PZ2	Na2 + A2	Aystmarskaya Suite		Aistmarės
	Ca2	Guryevskaya Suite		Žalgiriai
PZ1	A1g + Na1 + A1d	Pregolskaya Suite		Prieglis
	Ca1	Muravyevskaya Suite	Upper Sub-suite	Naujoji Akmenė
	T1		Middle Sub-suite	Sasnava
	Z1congl		Lower Sub-suite	Kalvarija

Table 8.2 Correlation of Zechstein strata.

UK Southern North Sea Johnson et al., 1994		The Netherlands Van Adrichem Boogaert & Kouwe, 1993		Denmark Clark & Tallbacka, 1980		Germany		Poland Wagner & Peryt, 1997	
						Fulda-Folge (Z7)	Obere Bröckelschiefer-Folge	Rewal Formation	
							Oberer Fulda-Anhydrit	PZ4e	
							Fulda-Steinsalz	PZ4d	
							Fulda-Anhydrit		
							Untere Bröckelschiefer-Folge		
						Friesland-Folge (Z6)	Friesland-Steinsalz	P4c	
							Friesland-Anhydrit, Oberer Grenzanhydrit		
							Oberer Schluffstein		
Zechsteinletten Formation				Zechstein 5 Group	Z5 Upper Anhydrite Formation	Ohre-Folge (Z5)	Ohre-Steinsalz	PZ4b	Top Youngest Halite
					Z5 Salt Formation				Upper Red Pelite – upper part
Grenzanhydrit Formation		Z5 (Ohre) Formation			Z5 Lower Anhydrite Formation		Ohre-Anhydrit, Lagenanhydrit		Intrastratal Halite
Unterer Ohre Ton Formation					Z5 Shale		Salzbrockenton		Upper Red Pelite – lower part
Aller Halite Formation		Z4 (Aller) Formation	Z4 Salt	Zechstein 4 Group	Z4 Salt Formation	Aller-Folge (Z4)	Aller-Steinsalz, Jüngstes Steinsalz	PZ4a	Upper Youngest Clay Halite
									Upper Youngest Halite
									Upper Pegmatite Anhydrite
									Lower Youngest Halite
Pegmatitanhydrit Formation			Pegmatite-Anhydrite		Z4 Anhydrite Formation		Aller-Anhydrit, Pegmatitanhydrit, Grenzanhydrit		Lower Pegmatite Anhydrite
Unnamed carbonate									Underlying Halite
Roter Salzton Formation			Red Salt Clay		Z4 Shale		Roter Salzton		Lower Red Pelite
Leine Halite Formation		Z3 (Leine) Formation	Z3 Salt	Zechstein 3 Group	Z3 Salt Formation	Leine-Folge (Z3)	Leine-Steinsalz Kaliflöze	PZ3	Younger Clay Halite
							Ronnenberg Riedel, Jüngeres Steinsalz		Younger Halite
Hauptanhydrit Formation			Main Anhydrite		Z3 Anhydrite Formation		Leine-Anhydrit, Hauptanhydrit		Main Anhydrite
Plattendolomit Formation			Z3 Carbonate		Z3 Carbonate Formation		Plattendolomit		Platy Dolomite
Grauer Salzton Formation			Grey Salt Clay		Z3 Shale		Grauer Salzton		Grey Pelite
Deckanhydrit Formation		Z2 (Stassfurt) Formation	Z2 Roof Anhydrite	Zechstein 2 Group	Z2 Upper Anhydrite Formation	Stassfurt-Folge (Z2)	Deckanhydrit	PZ2	Screening Anhydrite
Stassfurt Halite Formation			Z2 Salt		Z2 Salt Formation		Decksteinsalz		Screening Older Halite
Basalanhydrit Formation							Stassfurt-Steinsalz Kaliflöz		Older Potash
							Stassfurt, Älteres Steinsalz		Older Halite
Hauptdolomit Formation			Basal Anhydrite		Z2 Lower Anhydrite Formation		Unterer Stassfurt-Anhydrit, Basalanhydrit		Basal Anhydrite
			Ca2 Carbonate		Z2 Carbonate Hauptdolomit Member		Hauptdolomit, Stinkkalk, Stinkschiefer		Main Dolomite
Werraanhydrit Formation	Upper Anhydrite Member	Z1 (Werra) Formation	Z1 Anhydrite	Zechstein 1 Group	Ørslev Salt Member	Werra-Folge (Z1)	Oberer Werra-Anhydrit	PZ1	Upper Anhydrite
					Upper Anhydrite Member				
	Middle Carbonate Member				Middle Carbonate Member		Werra-Steinsalz Kaliflöze Thüringen Hessen, Ältestes Steinsalz		Oldest Halite
	Lower Anhydrite Member				Lower Anhydrite Member		Unterer Werra-Anhydrit		Lower Anhydrite
Zechsteinkalk Formation			Z1 Carbonate		Z1 Carbonate Formation		Zechsteinkalk		Zechstein Limestone
Kupferschiefer Formation			Coppershale		Z1 Shale		Kupferschiefer		Kupferschiefer

of more than 200 m have been estimated based on the architecture of the Z1 anhydrite platform (Cameron et al., 1992; Taylor, 1998). The infill of the Zechstein Basin is characterised by a series of sigmoidal units, the thickest of which gradually moved basinward causing a shift of facies boundaries during the Z1 and Z2 cycles.

Both deep- and shallow-water facies have been identified in the Kupferschiefer deposits (Oszczepalski & Rydzewski, 1987; Paul, 1987). The deep-water facies is consistently between 20 and 60 cm thick and is a sequence of alternating organic-rich shale with planar laminae of clay and planar- and wavy-laminated dolomitic-calcareous clays. The floor of the deep-water facies was situated mainly within the anaerobic zone or at its transition into the dysaerobic zone. The shallow-water facies are characterised by varied thicknesses of mainly planar- and wavy-laminated dolomitic-calcareous marl, mostly deposited in dysaerobic (in Poland) and aerobic (in Germany) environments. The sediments contain plant, reptile and lingula brachiopod remains, suggesting a nearshore brackish environment, and bivalves, echinoids, and foraminifera that indicate a marine environment; both freshwater and marine fish remains are common (Jowett et al., 1987). There are reworked marine benthic fauna in the slope facies of the Kupferschiefer, which is characterised by laminated black shales with calcareous tempestites (Paul, 1982b). The formation is absent on intrabasinal swells and in basin-margin areas where normal marine fauna occur. These coeval deposits developed in a calcareous facies formed in well-aerated waters above the chemocline.

There is a consensus that reducing conditions were established shortly after the Zechstein transgression. Nutrient-rich waters, whether freshwater from continental areas (McCann et al., 2008b) or upwelled by trade-winds (Brongersma-Sanders, 1971), led to high organic productivity in surface waters and, together with the high evaporation rates, the development of permanent stagnant bottom-water conditions. After the initial transgression, water depths in the axial parts of the SPB may have been 200 to 300 m (Ziegler, 1990a). The rate of deposition of the Kupferschiefer was estimated to be 30 to 40 cm in 17 ka (Hirst & Dunham, 1963). There are three carbonate-clay cycles in Germany, which can be traced from eastern Germany to the Lower Rhine Sub-basin, probably due to productivity fluctuations that partly depended on climatic variation (Paul, 2006). The Kupferschiefer and adjacent strata host very rich copper deposits, which are mined in south-west Poland.

The Kupferschiefer is overlain by the Zechstein Limestone, which was deposited in oxygenated waters. In marginal areas and intrabasinal highs, the Zechstein Limestone is up to 100 m thick and is of shallow-water facies with a rich fauna of close affinity to the Arctic faunal province (Hollingworth & Pettigrew, 1988). The Zechstein microfauna in Poland and Lithuania also include Tethys-related species (Peryt & Peryt, 1977; Suveizdis, 1975), suggesting at least a temporary connection with the Tethys Ocean.

The Zechstein Limestone carbonate platform and slope deposits are up to 120 m-thick carbonates and marls, in contrast to the 5 to 10 m-thick carbonates in the sediment-starved basinal setting (Wagner, 1994; Taylor, 1998; Geluk et al., 2000) (**Figure 8.7**). A carbonate platform was also present along the Mid North Sea and Ringkøbing-Fyn highs (Taylor, 1998). The number of subcycles in the carbonate vary (Peryt, 1984; Pöhlig, 1986; Paul, 1987; Śliwiński, 1988; Becker & Bechstädt, 2006) and may not correlate due to local palaeogeographical or tectonic control (Peryt, 1986a); in south-west Poland, three subcycles can be identified within the carbonate-platform area (**Figures 8.8** & **8.9**). All of the cycles are asymmetrical, with a sharp return to open-sea conditions indicating either rapid transgression or slow sedimentation during the transgression. Basal Zechstein sedimentation was controlled mainly by cyclic glacial eustasy and associated sea-level changes, progradation of carbonate platforms, and by inherited relief, especially during and immediately after the Zechstein Sea transgression.

The lower parts of the carbonate-platform sections are mainly carbonate mudstones and wackestones, whereas packstones and grainstones are common in the upper part (see Section 5). Carbonate buildups developed in a belt a few hundred metres to a few kilometres (up to 12 km) wide and consist of boundstones and packstones (Kerkmann, 1969; Lorenc, 1975; Peryt, 1978b; Paul, 1980, 1996, 2005; Smith, 1981a, 1981b, 1989, 1994, 1995; Hollingworth & Tucker, 1987). The buildups are generally found along the basin margin (e.g. in Thüringia, south-east Germany, they are around 2 km from the palaeocoastline: Paul, 1995), or above

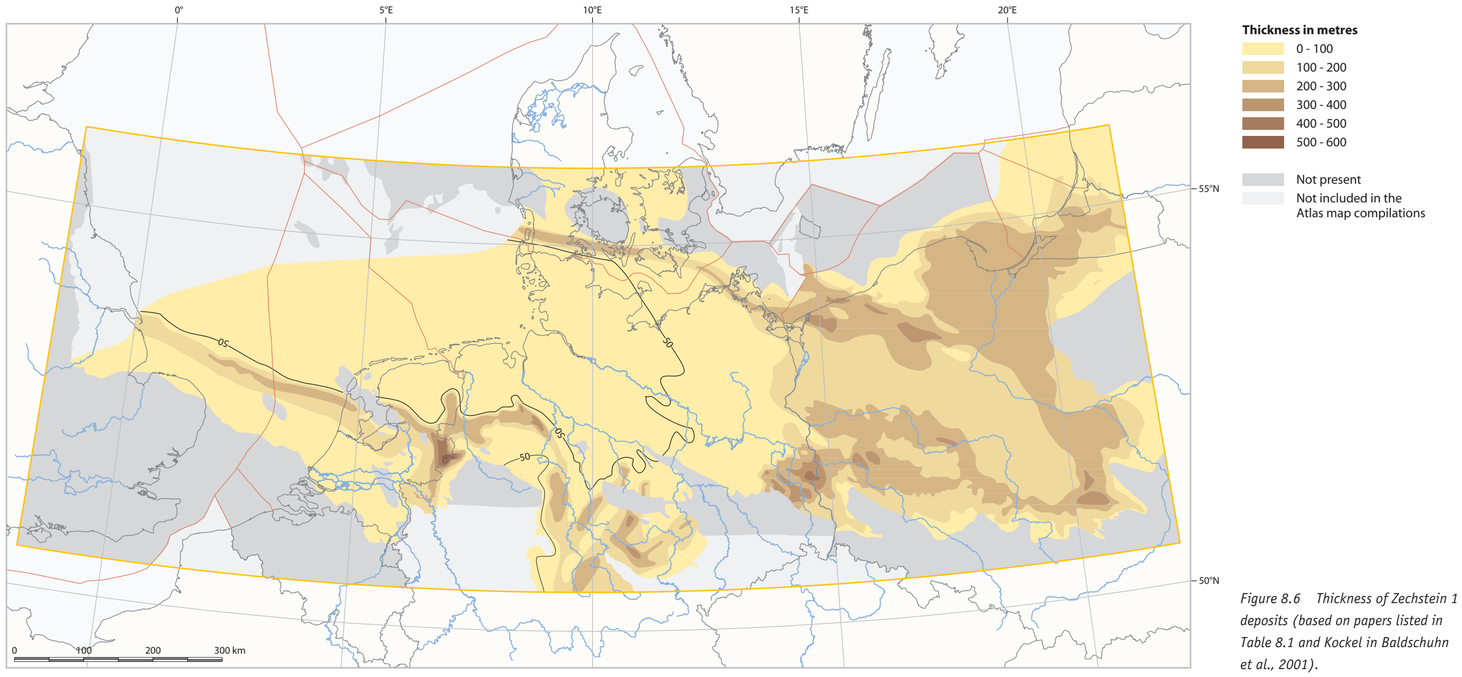

Figure 8.6 Thickness of Zechstein 1 deposits (based on papers listed in Table 8.1 and Kockel in Baldschuhn et al., 2001).

highs in the pre-Zechstein topography (as seen in the Harz Mountains: Paul, 1980). Zechstein reefs also have remarkably varied geometries (Paul, 1996, 2005). Fringing reefs have extensive flats and very steep (sometimes vertical) fore-reef slopes; patch-reefs formed archipelagos with nearly enclosed lagoons; conical pinnacle reefs built up seawards of both reef types (see Section 6). Microbial communities, bryozoans (mostly small, bushy and fenestrate forms) and encrusting foraminifers were the main reef builders. Early submarine cementation was an important factor in creating these rigid structures. In the centre of the basin, thin (<10 m) limestones and dolomites with mudstone and wackestone textures are intercalated with oncolithic packstones and stromatolites in the upper part of the Zechstein Limestone. Intrabasinal shoals are characterised by both thin (<1.5 m) condensed sequences (Peryt & Ważny, 1980; Peryt, 1981b) and more than 50 m-thick sections. The latter are often bioclastic accumulations, which are regarded as reef bodies (Dyjaczynski et al., 1997; Raczyński, 2000). Within these reef bodies, five Zechstein Limestone units can generally be recognised: (I) a basal breccia; (II) bioclastic grainstones with extraclasts; (III) bioclastic grainstones and packstones with abundant anhydrite; (IV) bioclastic wackestones-grainstones with intraclastic breccia and carbonate crusts and (V) stromatolitic-pisolithic carbonates (Dyjaczynski et al., 2001; Kiersnowski et al., 2010) (**Figures 8.10** & **8.11**). Units I to IV generally reflect subaqueous deposition whereas unit V originated in a very shallow-water or temporarily subaerial environment. Unit I is interpreted as a transgressive systems tract, units II to IV as a highstand systems tract, and unit V as a lowstand systems tract. 3D-seismic data reveal that the reef bodies have a very irregular shape and a sharp decrease in thickness corresponding to facies change at the reef margins (Dyjaczynski et al., 2001).

Paul (1996, 2005) estimated water depths during reef growth between 70 m on the seaward reefs and <20 m towards the shore. Early reef buildups were isolated; however, they gradually expanded and then merged (Smith, 1994). Most simple reefs are a few metres thick and 10 to 25 m wide, but where closely spaced reefs have merged to form larger complexes they can be more than 20 m thick and 120 m wide as seen in England (Smith, 1981a, 1989, 1995), and more than 120 m thick and 1000 m wide in the Thüringian Forest of central Germany (see Section 6). There are also reefs in the Dutch subsurface, although only a few wells have penetrated these Zechstein rocks (Visser, 1955).

Towards the basin margins, carbonate facies gradually pass into siliciclastic facies. The facies transitions are well documented along the southern flank in the Netherlands, Germany and Poland (see Section 5). The facies associations are quite variable; in the southern Netherlands and north-east Belgium, the carbonate passes gradually into fine-grained sandstones (Geluk et al., 1997). In southern Germany, there are several sub-basins that accumulated more than 100 m of grey and red laminated clays and marls, including some thin mudstone and wackestone beds with shelly fauna, which are coeval with basinward deposition of the Zechstein Limestone. Farther shoreward, there are extensive sandstones up to some hundred metres thick, which contain a marine fauna and glauconite (Dittrich, 2005). In Poland, carbonate lenses with brachiopod fauna occur within conglomeratic alluvial-fan complexes.

The Zechstein Limestone grades upwards into basinal-facies Lower Anhydrite deposits (Peryt & Piątkowski, 1977). In the marginal facies, the Zechstein Limestone is overlain by Upper Anhydrite deposits (e.g. Peryt & Kasprzyk, 1992). The upper part of the Zechstein Limestone in southern Germany consists of dolomites up to 80 m-thick with common anhydrite nodules.

The overlying Werra Anhydrite is divided into a lower and upper part, except in the UK and the Netherlands where there is only one massive Z1 anhydrite, which is locally more than 200 m thick. The Lower Anhydrite is clearly transgressive. Several cycles may be distinguished (Taylor, 1980; Richter-Bernburg, 1985; Steinhoff & Strohmenger, 1999; Becker & Bechstädt, 2006) in which the lowermost sediments have nodular anhydrites that may have formed in subaerial to shallow-water environments (**Table 8.3**). These are succeeded by bedded anhydrites, commonly lenticular at the base and often with pseudomorphs after selenitic gypsum, which may also have originated in shallow-water environments (**Table 8.3**). A distinct palaeogeographical zonation evolved during subsequent phases as expressed by varied development of the upper part of the sequences, and by the total thickness of the Lower Anhydrite. In sequences more than 150 m thick, there are massive anhydrites with pseudomorphs after selenitic gypsum and local breccias; laminated anhydrites are common in thin sequences (**Figure 8.12**). The thick sequences build sulphate platforms with slopes characterised by widespread graded bedding and massive slope-failure, as indicated by brecciation and contortion (Herrmann & Richter-Bernburg, 1955; Richter-Bernburg, 1955a, 1955b; Meier, 1975; Schlager & Bolz, 1977; Paul, 1987; Peryt et al., 1993). The thickness of the slope sequences is intermediate between that of the basinal areas (50 m or less) and sulphate platforms. The thick sequences of Z1 anhydrites usually occur on the broad margins of the sedimentary basin and were related to the slopes of the Zechstein Limestone carbonate platform or to zones that were elevated during the time of Zechstein Limestone deposition (Clark & Tallbacka, 1980; Richter-Bernburg, 1985; Paul, 1987; Peryt & Antonowicz, 1990). Fine-grained sabkhas accumulated to the landward side of the anhydrites.

The distribution of evaporite shoals and depressions was probably controlled by tectonics, as suggested by the linear or block-type pattern of the shoal or platform areas, and by major thickness variations combined with the constant lithofacies (**Figures 8.13** & **8.14**). The basins that remained after deposition of the Lower Anhydrite became the focus of halite formation (>200 m thick), whereas only thin halite sequences were deposited on the sulphate platforms.

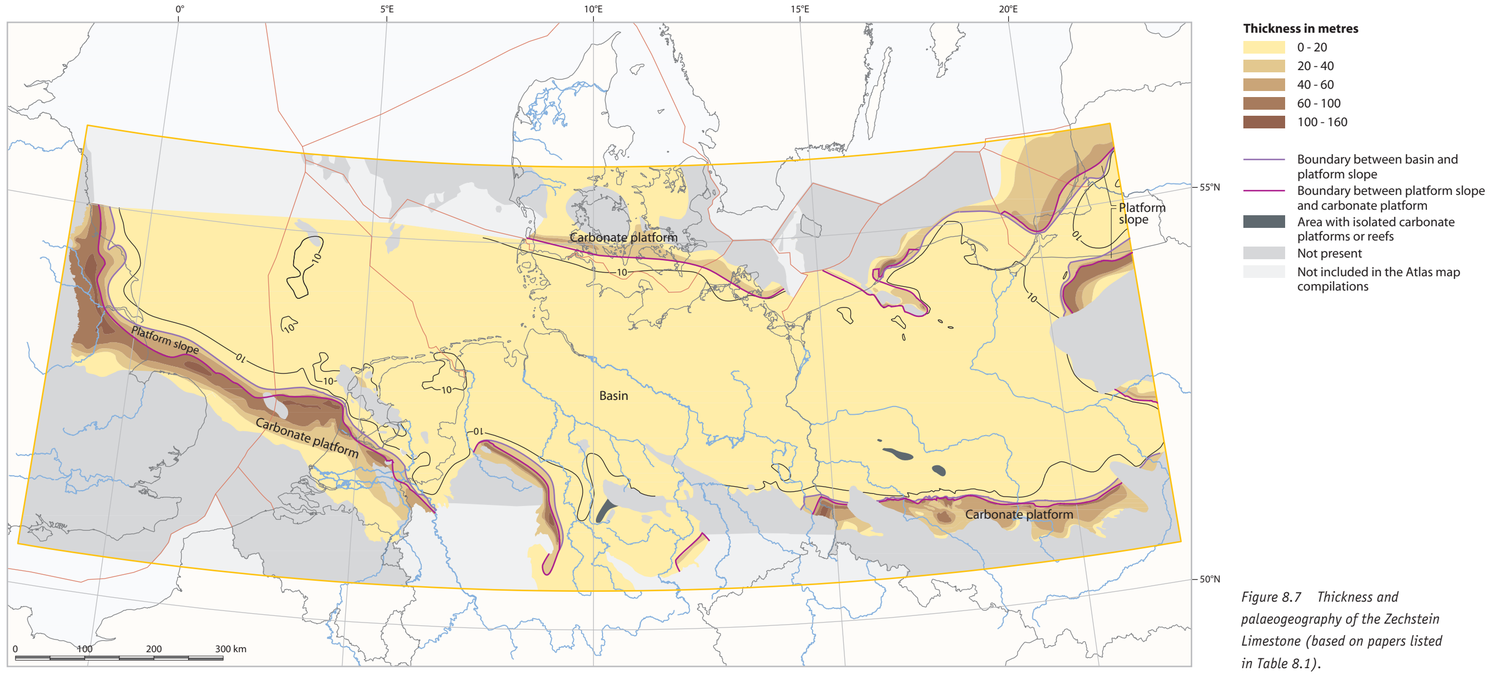

Figure 8.7 Thickness and palaeogeography of the Zechstein Limestone (based on papers listed in Table 8.1).

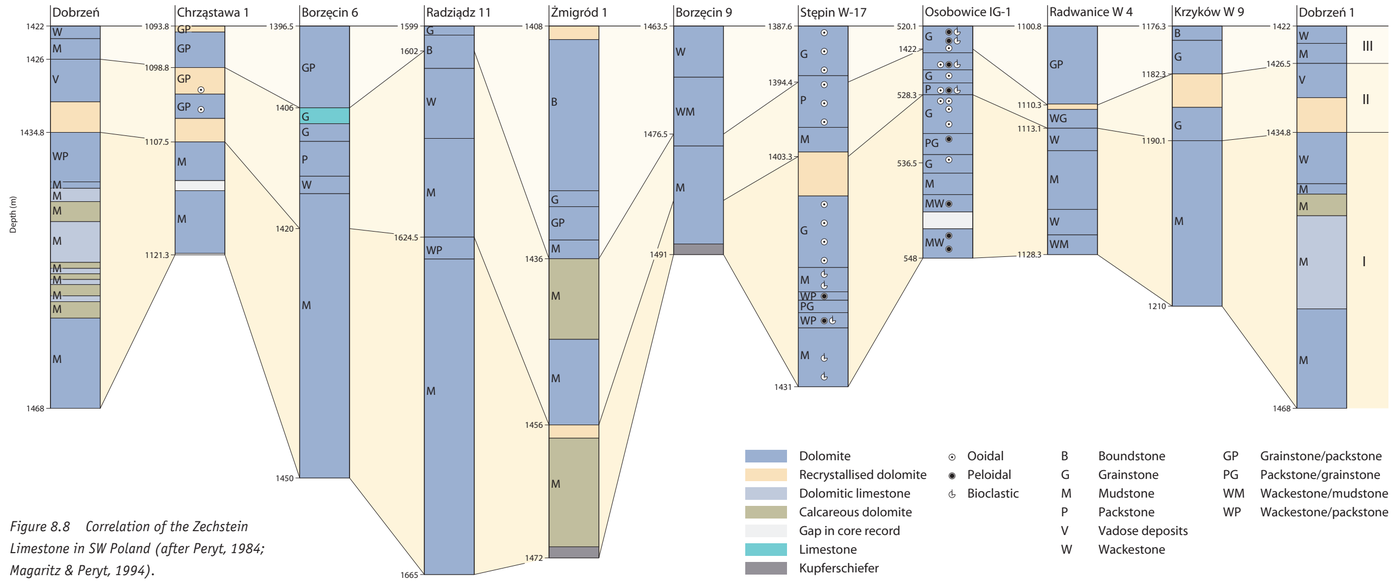

Figure 8.8 Correlation of the Zechstein Limestone in SW Poland (after Peryt, 1984; Magaritz & Peryt, 1994).

The thickness and character of the Oldest Halite (including potassium-magnesium salt) deposits are related to their palaeogeographical position (**Figure 8.15**). In the Netherlands and Germany, the Z1 halite is normally restricted to the peripheral sub-basins to the south of the main basin. Some of these basins have anhydrite intercalations in halite deposits up to several tens of metres thick (e.g. Peryt & Kovalevich, 1996) (**Figure 8.16**). In the southern North Sea and Denmark, halites are locally replaced by carbonates in the stratigraphic section (Middle Carbonate Member), which indicates the unstable, varied chemical conditions that occurred in the basin at that time. In Poland, the Oldest Halite is found in both the basin centre and in the former basins of the Lower Anhydrite within the marginal sulphate platform complex, where thick halite sequences may have originated in a deep-water setting. The halite sequences are clearly cyclic (e.g. Peryt et al., 2005) (**Figure 8.16**). In contrast, shallow-water halite deposits formed in the former shoal areas of the sulphate-platform system (Czapowski, 1987) (**Figure 8.17**; **Table 8.4**). Lenses of potassium-magnesium salts accumulated in salt lagoons in the area of the present-day eastern Netherlands and in the Werra-Fulda Sub-basin, where the potassium salts are now mined.

The sheet-like Upper Anhydrite is usually a few tens of metres thick. Basal mudstones with anhydrite nodules are overlain by bedded and laminated anhydrite with abundant pseudomorphs after selenite crystals. At the basin margins, interbeds of nodular anhydrite with dolomite are common, which probably formed in very shallow-water and subaerial depositional environments, whereas those in the basin centre were probably deposited under stable subaqueous conditions. A transgressive sequence is typical of the Upper Anhydrite.

Table 8.3 Lithologies of the Lower Anhydrite (after Peryt, 1994).

Lithology		Environmental interpretation
Nodular anhydrite		Polygenetic deposit formed at different times, often by early diagenetic growth of gypsum/anhydrite in a sabkha or by subaqueous gypsum crystallisation in shallow ponds
Massive sulphate	Massive sulphate with pseudomorphs after upright-growing gypsum crystals	Subaqueous shallow-water environment of fluctuating conditions, often with very high salinity (close to halite saturation)
	Clastic sulphate	Shallow-water origin. Fragmentation of autochthonous upright growing gypsum crystals by periodic high-energy events. Gypsum, sand and mud formed in a shallow coastal environment, thereafter resedimented
	Textureless anhydrite	Polygenetic group including all other massive anhydrites
Stratified sulphate	Bedded sulphate	Shallow-water environment
	Laminated anhydrite	Deep-water environment
Anhydrite breccia		Very shallow-water environment
Mudstone with anhydrite nodules and encrustations		Sabkha environment

The Upper Anhydrite has a distinctive palaeogeographical zonation consisting of four belts: a sabkha belt; a belt of interfingering continental and very shallow-water, lagoonal environments; a belt of predominantly lagoonal conditions; and finally a zone characterised by stable subaqueous conditions. Towards the southern basin margin, clay and sandy layers are increasingly intercalated within the sulphate before replacing it entirely. At the end of deposition of the Upper Anhydrite, sea level fell and much of the peripheral area became exposed. The early dewatering of gypsum deposits led to the intensive gypsum diapirism seen in the Harz Mountains, east of the Rhenish Massif, and in northern Hesse (Fulda 1929; Hemmann, 1972; Paul, 1987; Williams-Stroud & Paul, 1997). The preferred orientation of the ridges south of the Harz Mountains may be due to the palaeo-strain and stress-field of the early Zechstein. The diapirism was caused by inverse density stratification and differential loading. The diapirs are either 50 m-high elongate ridges with steep flanks that can be traced over several kilometres, or they are 30 m-high cupolas with a diameter of 50 m and near-vertical walls (Paul, 1987; Williams-Stroud & Paul, 1997). Slumping of the overlying Z2 Main Dolomite deposits on the ridge flanks indicates early movements of the gypsum before lithification of the carbonate mud and transition of the gypsum to anhydrite. The Main Dolomite has been pierced in places, such that the Werra Anhydrite is in direct contact with the Basal Anhydrite (A2). The gypsum diapirs probably occur in other areas, but they have either not been observed because of deep burial or they are obscured by dissolution processes such as karstification.

2.2.2 *Zechstein 2 (Z2)*

The Z2 (Stassfurt) Formation comprises a basal carbonate unit, the Main Dolomite (Ca2) followed by the Basal Anhydrite (A2), Older Halite (Na2), Older Potash (K2) and the thin, recessive, Screening Anhydrite (A2r). At the basin margins, the formation consists of anhydrite-bearing mudstones and local sandstones (Kulick & Richter-Bernburg, 1987; Wagner, 1994; Geluk et al., 1996, 1997). The formation is less than 50 m thick in basin-marginal areas and more than 1000 m in its central parts. In contrast to the overlying and underlying Zechstein cycles, a transgressive shale is absent in this cycle.

As in the case of the Zechstein Limestone, three depositional cycles that reflect high-amplitude sea-level fluctuations (~40-120 m each) can be identified in the Main Dolomite deposits (Peryt et al., 1989; Peryt & Dyjaczyński, 1991), possibly reflecting Milankovitch cyclicity (Strohmenger et al., 1998). The outer part of the basin was subaerially exposed and karstified prior to the Main Dolomite deposition (Peryt, 1989a; Strohmenger et al., 1996a) when sea level fell by about 100 to 150 m. The first sea-level rise (of about 70 m) led to the deposition of an early transgressive systems tract only on off-platform highs (Strohmenger et al., 1998) and lower parts of the platform slope (Peryt, 1992). This was followed by a sea-level fall and the karstification of carbonates before a further sea-level rise that resulted in a final flooding event that affected the platforms (maximum flooding and deposition of a late transgressive systems tract and early highstand systems tract).

The Main Dolomite marine basin was smaller than the earlier Zechstein Limestone sea, even during the maximum flooding event. Following the maximum transgression, a coastal oolitic barrier system developed and started to prograde. Platform-edge, mostly ooidal, sands formed a system of barriers in many parts of the basin, although the barriers often emerged due to sea-level fluctuations during formation of the Main Dolomite.

The platform facies (**Figure 8.18a**) is a complex of oolitic, peloidal, bioclastic and pisolitic packstones and grainstones, and finely laminated wackestones (Clark, 1986; Peryt, 1986b; Van der Baan, 1990; Strohmenger et al., 1996a, 1996b). Fourteen different subfacies can be distinguished (**Table 8.5**; Strohmenger et al., 1996a; Strohmenger & Strauss, 1996) based on water energy-related parameters such as grain and bedding types. The subfacies represent a wide range of depositional settings including sabkha, tidal flats, algal shoals, oolite shoals, lagoons and ooid bars (Strohmenger & Strauss, 1996). The Main Dolomite has a shallowing-upward sequence in the platform areas with mainly carbonate mudstones in the lower part and ooidal, peloidal, and ooidal-peloidal grainstones in the upper sequence.

The carbonate platforms pass landward into sabkha complexes (**Figure 8.18a**; Goodall et al., 1992; Peryt & Kasprzyk, 1992; Fijałkowska & Peryt, 1995); salinas have been found in the eastern Netherlands (NITG, 2000). Ooidal and pisoidal barriers often formed at the edge of the carbonate platform and small stromatolite reefs have also been found (Paul, 1980). Sea level fell at the end of deposition of the Main Dolomite and most of the peripheral area became exposed and karstified before it was partly flooded during the next transgression related to the Basal Anhydrite. During the lowstand, a younger carbonate platform formed, which constitutes a wedge attached to the slope of the PZ1 evaporite platform (Zdanowski, 2004).

Beyond the platform areas there are zones of slope and basin facies. In the vicinity of the carbonate platforms, the slope facies are mainly slump and slide deposits, debris flows and turbidites (Smith, 1970a; Clark & Tallbacka, 1980; Huttel, 1989; Amiri-Garoussi & Taylor, 1992; Peryt, 1992; Van de Sande et al., 1996) consisting of pale-coloured calcitic and dolomitic mudstones, which are more than 200 m thick in the eastern Netherlands (Van de Sande et al., 1996), Germany (Strohmenger et al., 1996a, 1996b) and western Poland (**Figure 8.18b**). The slope facies can be subdivided into ten subfacies consisting of an upper-slope facies (one subfacies), middle-slope facies (four subfacies) and lower-slope facies (five subfacies) (Strohmenger et al., 1996a; Strohmenger & Strauss, 1996). The basinal deposits have two subfacies (Strohmenger et al., 1996a; Strohmenger & Strauss, 1996), and consist of thin (1-2 m thick in Germany, 4 m thick in Poland) dark-coloured, bituminous, finely laminated carbonates, known as the Stinkschiefer and Stinkkalk (fetid limestone). These rocks have source-rock potential, with a total organic carbon (TOC) content of up to 1.2% (Lokhorst et al., 1998).

The thickness of the Main Dolomite is typically a few tens of metres in the platform area, although it can be up to 120 m thick in places. 3D-seismic data have revealed the complex outline of the platform, including isolated off-platform highs and intra-platform basins (Van de Sande et al., 1996). To a large extent, the facies distribution of the Main Dolomite was controlled by the palaeo-relief of the Z1 Anhydrite platform.

Table 8.4 Characteristic features of salt deposits from the Oldest Halite of Poland (after Czapowski, 1987; Czapowski et al., 1993). A – monomorphic halite, B – polymorphic halite, C – primary banded halite, D – secondary giant halite.

Depositional features	Salt sedimentary environments (with frequence of occurrence)			
	Open sea		Salt lagoon	
	Open deep salt basin	Shallow salt basin and shoal	Deep	Shallow
Lithology				
C-halite	Common	Rare	Common	Rare
D-halite	Lacking	Rare	Lacking	Rare
Salt rhythmite	Common	Rare	Rare	Rare or lacking
Complete salt sequences A+B+C	Common	Rare	Rare	Lacking
Dominant salt sequences	A+C, A+B+C	A+B, A+C, B+C, B	B+C, A+B, A+B+C	B+A, B+C, B
Terrigenous material	Lacking	Rare	Rare	Common
K-Mg salts	Rare	Rare	Common	Rare
Sedimentary structures				
'Internal lamination'	Common	Rare	Common	Rare
Fine sulfate lamination	Common	Rare	Common	Rare
Hopper halite	Rare	Common	Common	Rare
Chevron halite	Lacking	Rare	Lacking or rare	Common
Halite intraclasts	Rare	Common	Rare	Common
Raft halite	Rare	Rare	Common	Lacking or rare
Erosion/dissolution boundaries	Rare	Common	Rare	Common

Table 8.5 Sedimentology and subfacies types of the Main Dolomite (after Strohmenger & Strauss, 1996).

Facies	Subfacies	Sedimentary structure		Sedimentary texture	Components	Mineralogy	Porosity type	
Platform	Karst	Disturbed fabric solution/collapse breccia (contortion)		Disturbed	Ooids, coated grains, composite grains, peloids (calcite)	Dolomite fissures moldic	Vuggy	intraparticle
	Sabkha	Contortion crinkle bedding micro-teepees	(disturbed) (algal doming) nodular anhydrlte	Disturbed	Ooids, coated grains, composite grains, peloids	Anhydrite (calcite) dolomite	(Intraparticle) (moldic)	
	Transgressive deposit	Massive (cross-bedding)		Packstone/grainstone	(Ooids), coated grains, composite grains, (peloids), (fossils)[1], anhydrite clasts	Dolomite (calcite)	Intraparticle moldic	(interparticle) (vuggy)
	Beach deposit	Cross-bedding shingled-bedding	graded-bedding	Packstone/grainstone	(Ooids), coated grains, composite grains, (peloids), (fossils)[1]	Dolomite (calcite)	Intraparticle moldic	(interparticle) (vuggy)
	Tidal-flat	mm to cm-bedding graded-bedding fenestral fabric mud cracks	(cross-bedding)	Mudstone-wackestone/ packstone alternations	(Ooids), (coated grains), (composite grains), peloids	Dolomite (calcite)	Intraparticle moldic	
	Pelletal tidal-flat	Cross-bedding herring-bone cross-bedding	(fenestral fabric) (sheet cracks)	Packstone/grainstone	(Ooids), (coated grains), (composite grains), peloids	Dolomite (calcite)	Intraparticle moldic	
	Algal tidal-flat	Crinkle bedding algal doming fenestral fabric	micro-teepees	Mudstone/wackestone bindstone	(Coated grains), (composite grains), (peloids)	Dolomite anhydrite (calcite)	Intercrystalline[2]	
	Algal-laminated shoal	Crinkle bedding		Packstone/grainstone	(Ooids), coated grains, composite grains, peloids, (fossils)[1]	Dolomite (calcite)	Intraparticle moldic	
	Grainy shoal	Massive (cross-bedding)		Packstone/grainstone	(Ooids), coated grains, composite grains, (peloids), (fossils)[1]	Dolomite (calcite)	Intraparticle moldic	(interparticle) (vuggy)
	Ooid shoah	Massive (cross-bedding)		Packstone/grainstone	Ooids, coated grains, (composite grains), (peloids), (fossils)[1]	Dolomite (calcite)	Intraparticle moldic	(interparticle) (vuggy)
	Ooid bar	Cross-bedding (herring-bone cross-bedding)		Grainstone	Ooids, coated grains, (composite grains), (peloids), (fossils)[1]	Dolomite (calcite)	Intraparticle moldic	(interparticle) (vuggy)
	Ooid inter-bar	mm to cm-bedding wavy-bedding	cross-bedding	Packstone/wackestone	Ooids, coated grains, (composite grains), peloids	Dolomite (calcite)	Intraparticle moldic	
	Lagoon	mm to cm-bedding (massive)	(wavy-bedding) (flaser bedding)	Mudstone (wackestone)	(Coated grains), (composite grains), (peloids), (fossils)[1]	Dolomite (calcite)	Intercrystalline[2]	
	Reefal buildup	Crinkle bedding algal doming		Boundstone/packstone	(Coated grains), (composite grains), peloids, fossils	Dolomite (calcite)	Intercrystalline[2] (intraparticle)	(moldic) (fissures)
Upper slope	Open marine	wavy bedding flaser bedding (cross-bedding)	(massive)	Mudstone (wackestone)	((Coated grains)), ((composite grains)), (peloids), fossils	Calcite dolomite	Non-porous[2] intercrystalline[2]	
Middle slope	f1	mm-bedding microstylolitic bedding		Mudstone	(Fossils)[1]	Dolomite calcite	Intercrystalline[2] vuggy	non-porous[3]
	f2	Folding slumping	mm-bedding microstylolitic bedding	Mudstone	(Fossils)[1]	Dolomite calcite	Intercrystalline[2] vuggy	non-porous[3]
	e1	mm to cm-bedding		Mudstone	(Fossils)[1]	Dolomite calcite	Intercrystalline[2] vuggy	non-porous[3]
	e2	Pull-apart mm to cm-bedding	micro-thrusting	Mudstone	(Fossils)[1]	Dolomite calcite	Intercrystalline[2] vuggy	non-porous[3]
Lower slope	B1	Flaser bedding wavy bedding	(dm-bedding)	Mudstone	-	Dolomite calcite	Intercrystalline[2] non-porous[3]	
	B2	Drag-folding slumping cm-bedding		Mudstone	-	Dolomite calcite	Intercrystalline[2] non-porous[3]	
	B3	Massive		Mudstone	-	Dolomite calcite	Intercrystalline[2] non-porous[3]	
	D1	mm to cm (dm)-bedding		Mudstone	-	Dolomite calcite	Intercrystalline[2] non-porous[3]	
	D2	Boudinage slumping	contortion brecciation	Mudstone	-	Dolomite calcite	Intercrystalline[2] non-porous[3]	(vuggy)
Basin	A1	mm-bedding		Mudstone	-	Calcite (dolomite) anhydrite (shale)	Intercrystalline[2] non-porous[3]	
	A2	Folding mm-bedding		Mudstone	-	Anhydrite (dolomite) (calcite) (shale)	Intercrystalline[2] non-porous[3]	
Turbidite		Graded-bedding massive (cross-bedding)		Packstone/wackestone (grainstone)	Ooids, coated grains, composite grains, (peloids), (fossils)	Calcite dolomite	Intraparticle moldic	

( ) Rare/subordinate (( )) Very rare 1 Fossils possibly abundant in East Germany 2 Intercrystalline porosity if dolomite 3 Non-porous if calcite

The Basal Anhydrite of Poland is a thin sequence of stromatolitic anhydrites (a few tens of metres thick above the Main Dolomite platform and a few metres thick in the basin centre) that passes into massive anhydrite with pseudomorphs of selenite crystals (a few millimetres to 20 cm in size), which formed in shallow-water, salina environments, followed by bedded and then laminated anhydrite. Well-bedded anhydrites are seen at the base of the Basal Anhydrite in the Harz Mountains. There are thin (centimetre to several tens of centimetres thick) sporadic intercalations of halite in the anhydrite (e.g. Peryt et al., 1996). Individual laminae in the anhydrite in the basin centre can be correlated across distances up to 400 km (Richter-Bernburg, 1955a, 1985).

More rapid subsidence in some parts of the basin, marked by a transgressive sequence of the Basal Anhydrite, formed a persistent depression that became the depositional centre for the Older Halite (Na2) and Older Potash (K2) sediments, which are more than 1000 m thick in the basin centre (Zirngast, 1991); in the areas of the PZ1 evaporite platform, equivalent deposits are either absent or only several tens to about 100 m thick. The Older Halite sedimentary basin evolved from a relatively deep-water open salt basin with free brine exchange, to a system of shallow-water closed salinas fringed by coastal salt pans along the basin borders. Water depths were up to tens of metres at the end of the Na2 deposition in a salina to salt pan environment (Czapowski et al., 1990). By the beginning of the Older Halite deposition, water depths may have been up to 140 m in the peripheral part of the basin, and presumably deeper in its central part, although by the end of its deposition they were only tens of metres (Czapowski et al., 1990). There was a rapid transition from a deep-water to a shallow-water environment as the basin filled and the salt began to encroach on to the slope and then the top of the former Ca2 platform. In addition to rock-salt, potassium-magnesium salts (several tens of metres thick) are found mainly in the central part of the basin where they originated in salinas. The main basinal areas, the Silverpit and North German basins and the Polish Trough, filled with a thick Z2 Salt succession (>95% halite). The thickest rock-salts (>700 m thick) were deposited in the former Main Dolomite basin, whereas thin salts accumulated in the Main Dolomite platform areas. In the Netherlands, three stages of deposition can be identified within the salt, based on distinct polyhalite marker beds (Geluk, 1995, 2005; Geluk et al., 2000). During the first two stages, the inherited topography continued to influence the deposition of platform halites that graded northward into deeper-water salt complexes (intercalated halite, polyhalite and carnallite), whereas the third stage of salt deposition filled most of the remaining depressions in the basin. The upper part of the Z2 Salt includes a regionally extensive potassium-magnesium salt layer with sylvite and carnallite, known as the Stassfurt-Kaliflöz. The Older Halite deposits were regionally overlain by the Screening Anhydrite (A2r) (<2 m thick), which is interpreted to be the result of mixing of residual brines and new sea water that heralded the Z3 transgression (Peryt et al., 1996). The Z2 Salt and overlying units have been strongly deformed due to extensive salt movements, which complicate the reconstruction of their primary thickness and composition.

2.2.3 Zechstein 3 (Z3)

The Z3 (Leine) Formation is up to 500 m thick and comprises the Grey Salt Clay (T3), Platy Dolomite (Ca3), Main Anhydrite (A3) and Younger Halite (Na3). In the southern North Sea, the carbonate grades southwards into fluvial sandstones (Geluk et al., 1997).

The basal member of the formation, the Grey Salt Clay, is an important regional marker within the Zechstein with thicknesses between 1.5 and 10 m. The Grey Salt Clay is regarded as the lowest member of the PZ3 cycle and was deposited in a basin environment that passed in nearshore areas into carbonates of the Platy Dolomite (Ca3) and local siliciclastic deposits related to a marine transgression (Czapowski et al., 1991). In Germany, the Grey Salt Clay is found everywhere in the Zechstein succession of the SPB and is up to 8 m thick in Bavaria. The sequence partly consists of fluvial sands, which extend from the basin margins.

The Platy Dolomite consists of thin, dark-coloured limestones up to a few metres thick (**Figure 8.19**). The slope facies comprises up to 40-m thick laminated and bioturbated carbonate mudstones and silty dolomites. The platform facies (**Figure 8.19**) largely consists of grey microcrystalline dolomites and algal boundstones, thought to represent a mainly shallow, quiet-water, possibly lagoonal environment (Taylor, 1998). In the areas of southern Denmark and Poland, carbonate shelves were constructed mainly by microbial deposits (Gąsiewicz et al., 1987; Stemmerik & Frykman, 1989; Peryt, 1990; see Section 7). In southern Germany, Möller (1985) distinguished a Calcinema/ooid facies and a cyanophycean facies farther shoreward. Local oolitic and bioclastic grainstones were deposited in the area adjacent to the slope (Van Adrichem Boogaert & Burgers, 1983; Baird, 1993) and on the landward margin of the platform. An off-platform shoal has been found on the Groningen High.

A common feature of the Platy Dolomite is the recognition of only one shallowing-upward cycle and oolite shoals with lagoonal deposits between those shoals and the land (see Section 7). Wide carbonate shelves interfinger with the basin-centre sulphates that overlie the deep ramp facies; the interfingering is partly attributed to later diagenetic alteration. A detailed study in the Łeba Elevation of northern Poland suggested that the Platy Dolomite sequence was transgressive (Gąsiewicz, 1990) and that there was a sedimentary transition between the Platy Dolomite and Main Anhydrite in that area with no change in sedimentary regime (Gąsiewicz & Peryt, 1994)

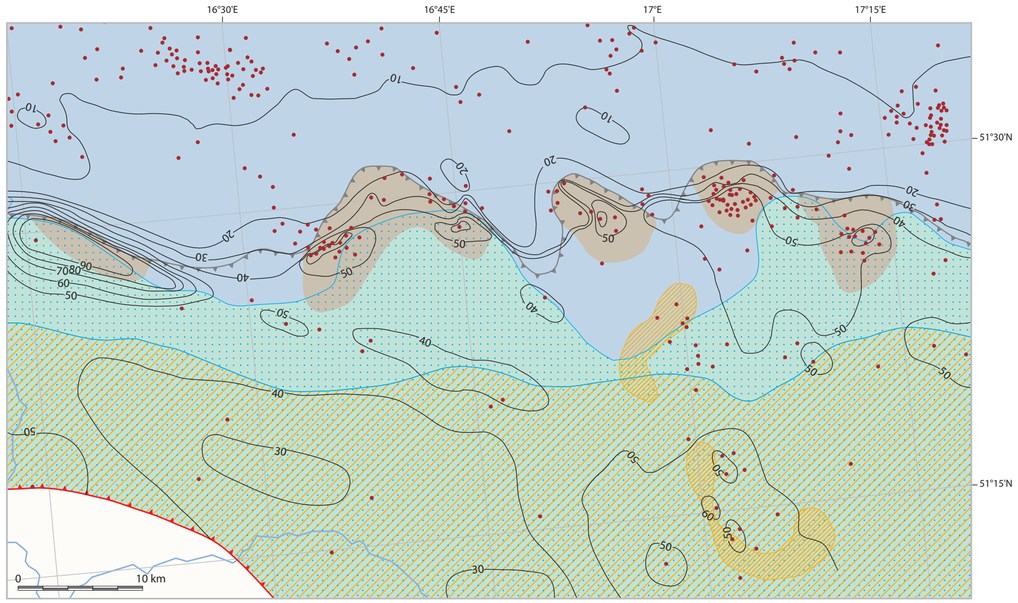

- Area of persistent marine deposition
- Area of dominant marine deposition with periodic subaerial exposure
- Reefs
- Area of periodic subaerial exposure – cycle I
- Area of periodic subaerial exposure – cycle II
- Area of carbonate sands related to shoals – subcycle II
- Area of carbonate sands related to shoals – subcycle III
- Edge of the carbonate platform of the subcycle III
- Present-day (erosional) limit of the Zechstein Limestone deposits
- 10 — Thickness of the Zechstein Limestone (metres)
- Borehole

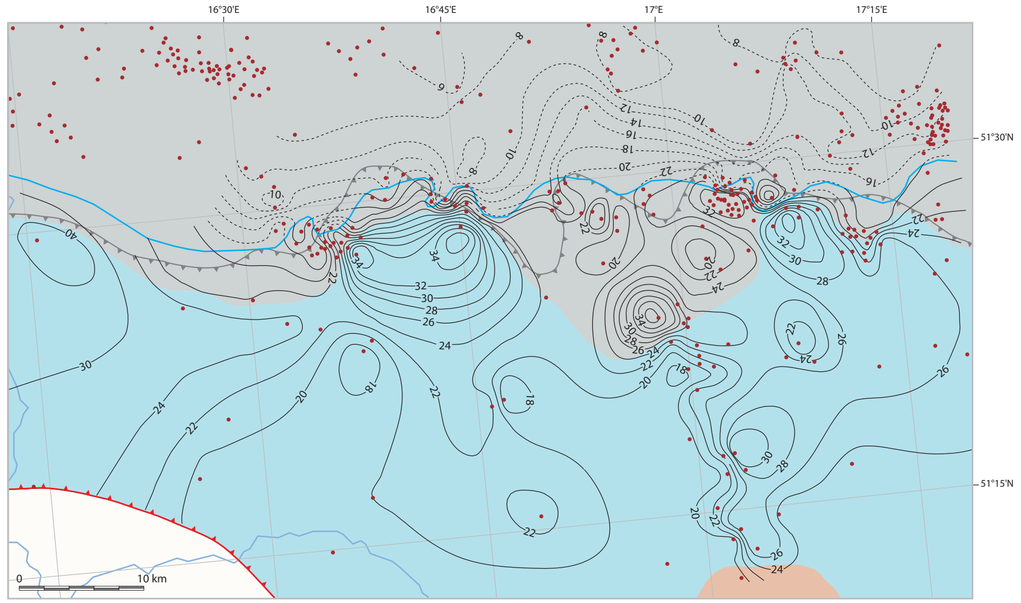

- Marine deposits
- Marine vadose deposits
- Sabkha deposits

} Mudstones and subordinate wackestones deposited at the end of subcycle I

- Northern limit of subcycle I deposits that can be differentiated from the subcycle II deposits (subcycles I and II can not be subdivided to the north of this limit)
- Edge of the carbonate platform of subcycle III
- Present-day (erosional) limit of the Zechstein Limestone deposits
- 10 — Thickness of subcycle I deposits (metres)
- Borehole

a.

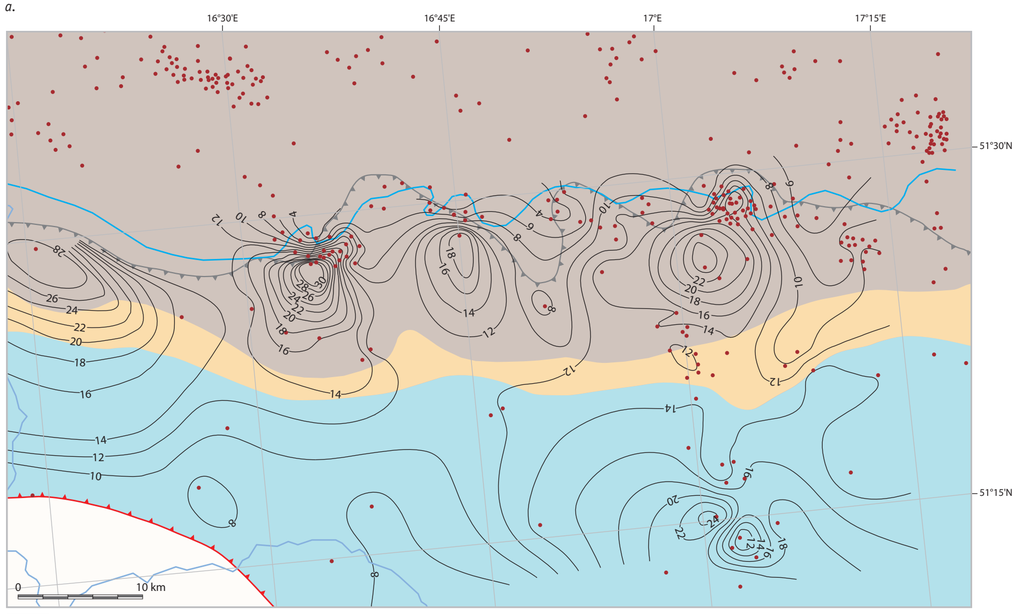

- Mudstones
- Wackestones and packstones
- Marine vadose deposits – grainstones
- Northern limit of subcycle I deposits that can be differentiated from the subcycle II deposits (subcycles I and II can not be subdivided to the north of this limit)
- Edge of the carbonate platform of subcycle III
- Present-day (erosional) limit of the Zechstein Limestone deposits
- 10 — Thickness of subcycle II deposits (metres)
- Borehole

c.

b.

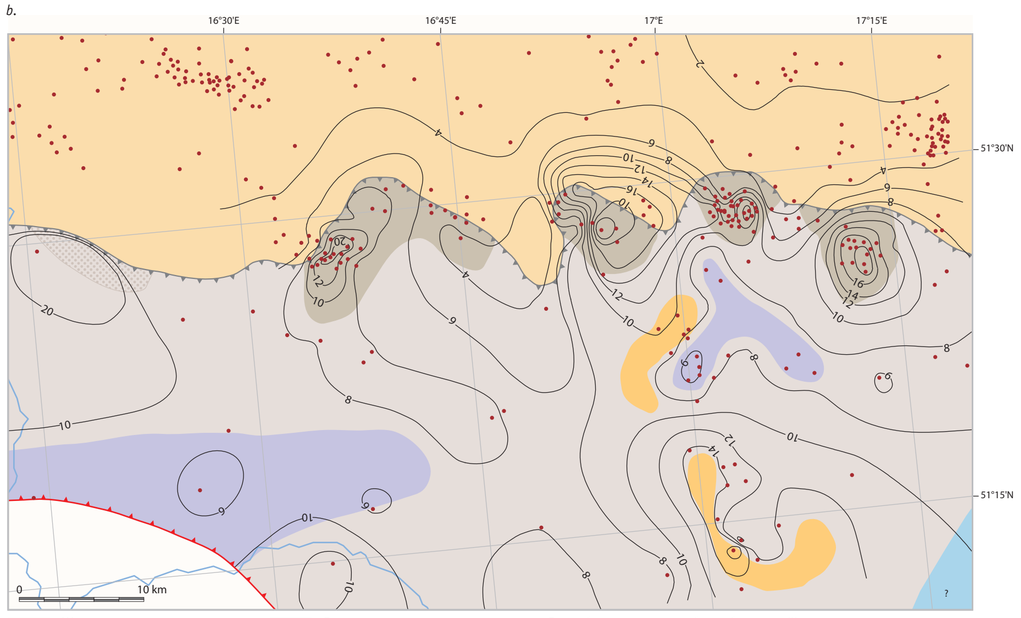

- Wackestones and packstones
- Reefs (recorded)
- Reefs (presumed)
- Wackestones and mudstones
- Packstones
- Grainstones
- Algal laminites
- Edge of the carbonate platform of subcycle III
- Present-day (erosional) limit of the Zechstein Limestone deposits
- 10 — Thickness of the subcycle III deposits (metres)
- Borehole

d.

Figure 8.9 Thickness and palaeogeography of the Zechstein Limestone in SW Poland (a) and its three subcycles: I (b), II (c) and III (d).

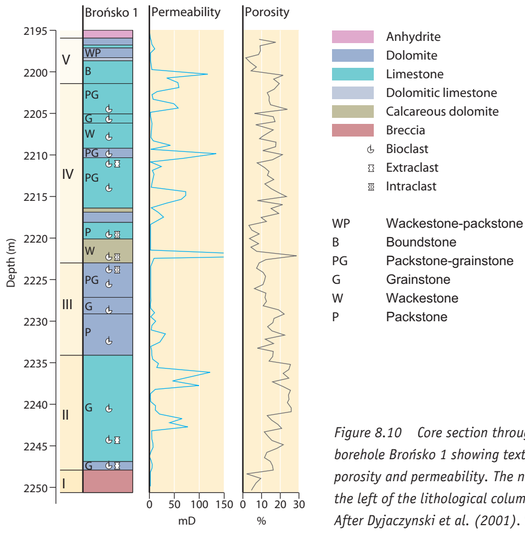

Figure 8.10 Core section through the Zechstein Limestone at borehole Brońsko 1 showing textures of carbonate rocks, measured porosity and permeability. The number of each unit is shown to the left of the lithological column (see text for description). After Dyjaczynski et al. (2001). See Figure 8.11 for location.

The Main Anhydrite (A3) in Germany and Poland is a transgressive sequence with nodular anhydrites at the base overlain by massive anhydrite, often with pseudomorphs after selenite crystals and, rarely, laminated anhydrite; anhydrite spherulites are found in the upper part of the sequence (Klapcinski, 1986). Some of the anhydrite units are laterally very extensive (**Figure 8.20**; Reimann & Richter, 1991). Elsewhere in the basin, for example in north-east England, the formation is highly varied; the anhydrites include nodular, lenticular, detrital-clastic, laminite, selenite-pseudomorphic and massive types. In the Netherlands, the Z3 Main Anhydrite was deposited only on the northern part of the Z3 carbonate platform, slope and basin. The anhydrite is up to 100 m thick and is a complex sequence (NITG, 2000). Movement of the underlying Z2 Salt caused the break-up of the unit into large slabs, known as rafts or floaters, which present major drilling hazards that could potentially cause the loss of drilling fluids or influx of high-pressured brines or gas. In the Sub-Hercynian Basin north of the Harz Mountains, Fulda (1929) named the Main Anhydrite diapirs that pierce the overlying Leine Salt the 'Anhydrit-Klippen' (anhydrite cliffs).

The Younger Halite (Na3) is mainly halite, but also includes potassium-magnesium salts in the middle part of a salt sequence in Germany and Poland, at its top in England, and in both the middle and top of the sequence in the Netherlands. The salts formed in isolated evaporite ponds, as indicated by variations in their mineralogy and bromine content (Bornemann et al., 2008). The salts that accumulated in the basin centre may be time-equivalent to the Main Anhydrite (A3) at the basin rim. The whole unit is probably of very shallow-water origin (Czapowski, 1993). In the Netherlands, the salts include up to 10 m-thick beds of the rare, and one of the most soluble salts, bischofite ($MgCl_26H_2O$), as well as kieserite, carnallite and sylvite (Coelewij et al., 1978). The Z3 Salt is up to 400 m thick.

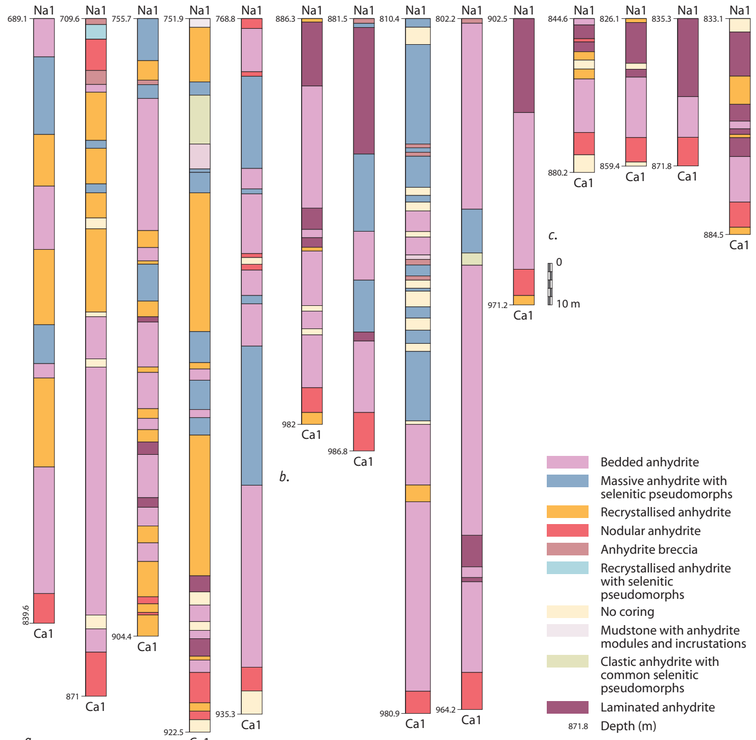

Figure 8.12 Sequences of the Lower Anhydrite in the Łeba sub-basin (northern Poland) (after Peryt, 1994): a. Thick sequences; b. thick and intermediate sequences; c. Thin sequences. See Figure 8.14a for locations of boreholes.

2.2.4 Zechstein 4 (Z4)

The upper part of the Zechstein sequence consists of salt, anhydrites and mudstones forming beds that are either dominated by a single lithology or as a mixture known as zuber. As mentioned previously, the upper part of the Zechstein in Poland is regarded as one series, therefore the Z4 elsewhere in the basin corresponds to the PZ4a in Poland (**Figure 8.21**). The following description accepts the conventional view.

The Z4 (Aller) Formation has a basal claystone, the Red Salt Clay (T4) (2 m thick) followed by the thin (0.5-2 m) Pegmatite Anhydrite (A4). These two units are widespread compared to the Youngest Halite

a.

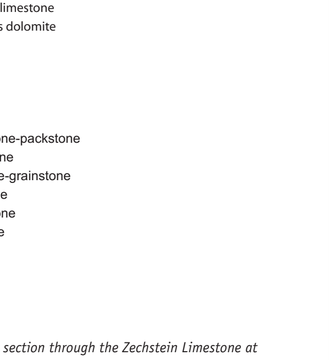

b.

c.

Figure 8.11 a. The Zechstein Limestone reefs in the Wolsztyn Ridge area (SW Poland); b. The Zechstein Limestone sequences in selected boreholes from the reef area; and c. Plot of porosity-permeability data for the Zechstein Limestone in the Kościan 14 borehole (after Dyjaczynski et al., 2001; Kiersnowski et al., 2010).

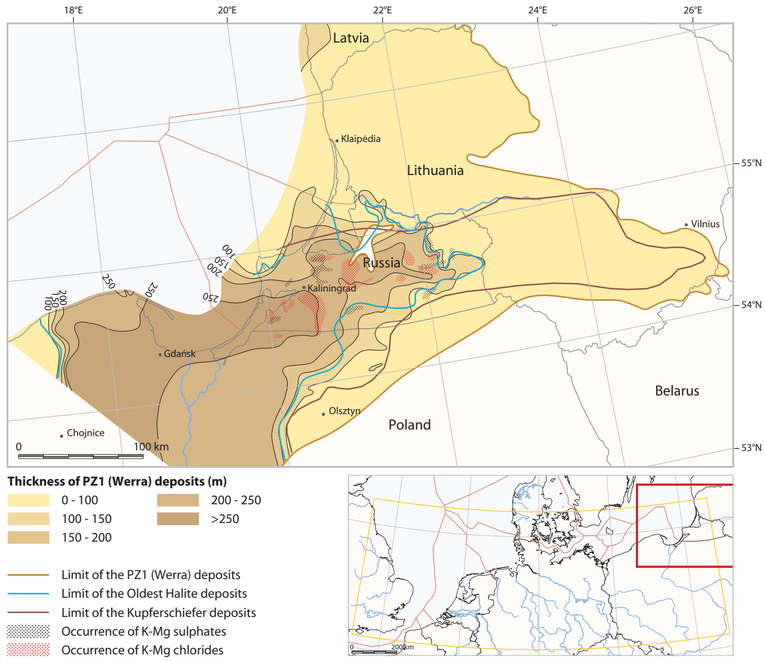

Figure 8.13 Occurrence of potassic salts in the Werra Peribaltic Basin (after Stolarczyk, 1972; Zagorodnykh, 1996).

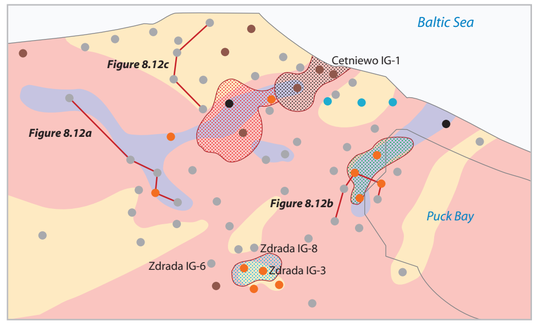

a.

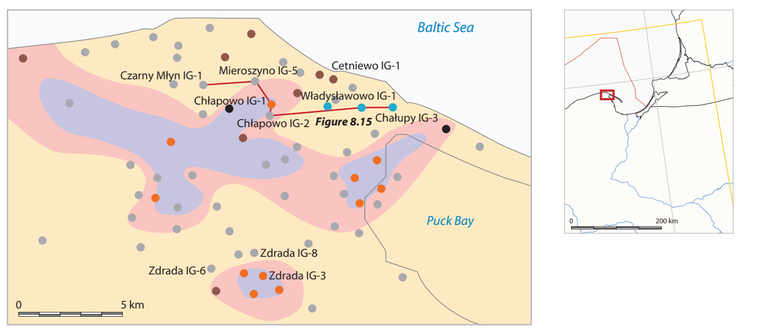

b.

Figure 8.14 a. Palaeogeography and occurrence of potassic salts in the Lower Anhydrite; and b. Oldest Halite, in the Puck Bay area (N Poland) (after Peryt et al., 2005).

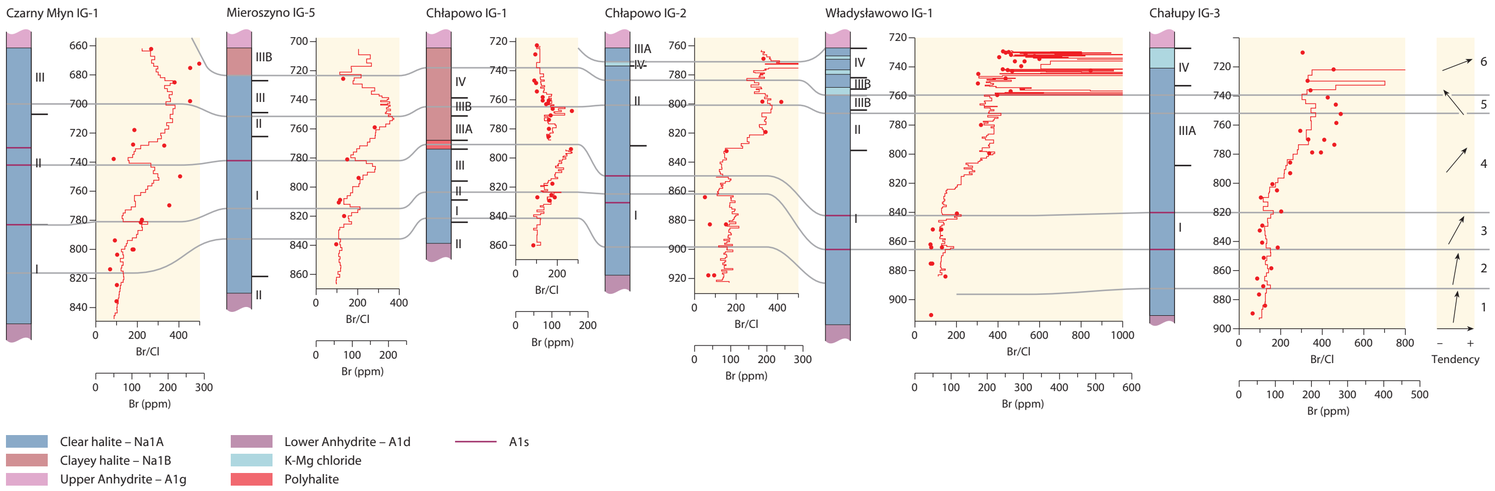

Figure 8.15 Geochemical correlation of the Oldest Halite sections in the Puck Bay area. See Figure 8.14b for locations. After Peryt et al. (2005).

(Na4), which consists of potassium-magnesium salts that are only found in great thickness in depocentres such as the North German Basin, the Polish Trough or as isolated remnants in half-grabens (Geluk, 1999a) where they are up to 150 m thick. Potassium-magnesium salts are found in the middle part of the salt sequence in the Netherlands, whereas the upper part consists of alternating halite and claystone. Around these salt basins, the formation comprises anhydritic claystones representing sabkha deposits and medium- to coarse-grained fluvial sandstones in the western offshore area. These sandstones are known as the Hewett Sandstone in the UK sector of the southern North Sea (Geluk et al., 1996).

The Z4 series originated in a diminishing marine basin. In southern Germany, the Z4 Anhydrite is the most laterally extensive marine unit of the Zechstein succession. In the south-western part of the SPB, fluvial sandy and muddy playa-lake deposits are time-equivalents of the salt-pan sediments of the main basin (Best, 1989).

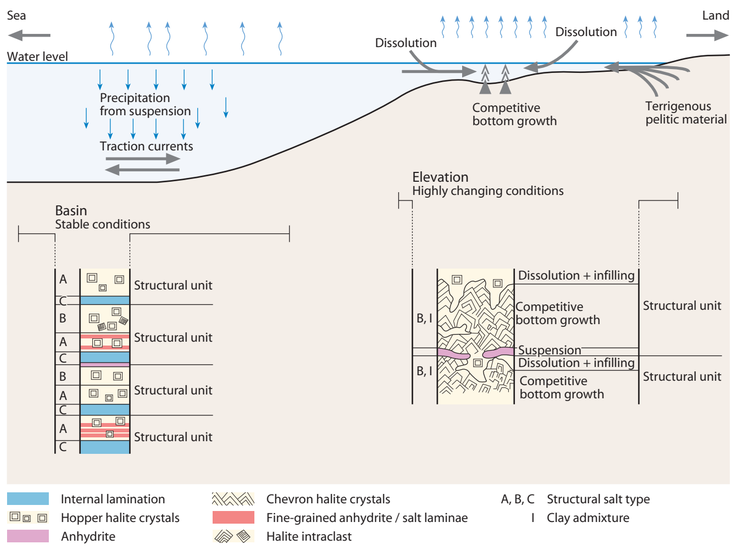

Figure 8.16 Scheme of origin of halite structural units in the Oldest Halite (after Czapowski, 1987).

2.2.5 Zechstein 5 (Z5) and younger cycles

A distinctive feature of the Z5 and younger cycles is that they were deposited in shrinking evaporite basins accompanied by simultaneous progradation of terrigenous deposits toward the basin centre. The high bromine content of the Z5 halites indicates that they formed in a marine environment. However, a subsequent rapid decrease in bromine concentrations in the Z6 halite reflects a change to a salt-lake environment, with no connection to the sea, accompanied by recycling of the salt (Kühn & Schwerdtner, 1959; Smith, 1971, 1974; Czapowski, 1990). In the Netherlands, the limited distribution of the Z5 (Ohre) Formation in the north-east, and offshore to the north-west, outlines the depocentres towards the end of Zechstein sedimentation. The formation comprises a several metres-thick basal claystone overlain by up to 15 m of halite. Younger Zechstein salts (Z6 and Z7) have been found in north-west Germany (Best, 1989) and Poland (Wagner, 1994), but their absence in the Netherlands is possibly because they were not deposited in this part of the SPB.

The Z7 cyclothem in Germany has two sedimentary cycles (Kulick & Paul, 1987), which also appear to be common in other parts of the basin (Käding, 2000). The Zechstein Upper Claystone Formation is widespread throughout the basin and disconformably overlies older Zechstein or Rotliegend rocks. Based on its palynology, the formation has been included in the Zechstein (Van Adrichem Boogaert & Kouwe, 1993) and is a sequence of red and grey anhydritic claystones and sandstones deposited in a lacustrine to mudflat setting with thicknesses that vary from 10 to 50 m.

Towards the end of the Permian, the connection with the Barents Sea was interrupted by major clastic influx in the area of the Viking-Central graben systems (Ziegler, 1990a). The basin initially evolved into an extensive sabkha environment with isolated salinas and later became an extensive inland playa lake in which the Lower Buntsandstein Subgroup was deposited (see Chapter 9) (Wagner & Peryt, 1997; Hug, 2004; Hug & Gaupp, 2006). During the late Zechstein, salt sedimentation increasingly retreated towards the centre of the basins (**Figures 8.21** & **8.22**). Tectonics, in combination with a lowering of the base level, resulted in downwarping of the central parts of the basin and uplift and minor unconformities on its margins (Geluk, 1999a). These mild tectonics (Tubantian II phase) appear to be contemporaneous with the Pfalzian tectonic phase observed in southern Germany and eastern France (Boigk & Schöneich, 1974). Zechstein evaporite sedimentation ended with progradation of the uppermost Z7 cycle, a sequence of fine-grained clastic facies formerly called the 'Bröckelschiefer'.

2.2.6 Synsedimentary tectonics

The general subsidence of the SPB, which often followed old tectonic trends manifested in the subsidence pattern characteristic of the Rotliegend, was accompanied by syndepositional tectonism. The effect of the tectonism is especially well expressed along the basinward margin of the A1-Ca2 platform (e.g. Strohmenger et al., 1998), although active faulting can also be seen elsewhere within the basin. This faulting initiated a system of horsts and grabens that respectively became the loci for deposition of thick sulphate and thick chloride deposits during the Werra cycle (e.g. Peryt, 1994). Although the faults were small-scale in amplitude, they had a significant impact on lithofacies development as the formation of evaporites is very sensitive to even small changes in the environment, such as minor fluctuations in water depth.

Small-scale faulting also affected sediment distribution during carbonate deposition (see e.g. Peryt & Dyjaczyński, 1991) whereas vertical movements of particular tectonic blocks also influenced the broader development of Zechstein sedimentation (e.g. Peryt, 1981a).

The palaeogeography and thickness variations of the Zechstein Limestone visually show little relationship to the tectonic framework. However, the facies and thicknesses of the evaporites of the subsequent Werra cycle, the Main Dolomite and the Stassfurt evaporites, suggest both regional and local tectonic control. There was a significant change at the end of the Stassfurt cycle when the palaeogeography and thickness of the Platy Dolomite varied from oblique to almost perpendicular to previous trends. As before, once evaporite deposition recommenced, the importance of the regional tectonic framework was restored especially in the shrinking Z4 basin where deposition was strongly influenced by subsidence in the axial part of the Zechstein Basin.

2.2.7 Reservoirs: sedimentary and diagenetic constraints

The reservoirs in the Zechstein Group are mainly carbonates. Most of the hydrocarbon fields are associated with platform or upper-slope facies with the best reservoirs in oolitic beds. The Zechstein carbonate reservoirs are complex due to their geometry, sedimentology and diagenesis. The geometry of the depositional environment is not only dependent on its position within the basin (e.g. platform, upper slope, lower slope), but also on small-scale factors such as the occurrence of isolated reefs or off-platform highs (Rasch et al., 1993; Strohmenger et al., 1993; Piske & Rasch, 1998; Piske & Karnin, 1999). On a smaller (field) scale, the distribution of oolite shoals on the platform may be important (e.g. Southwood & Hill, 1995). Another significant influence is the dynamic response of the whole system to sea-level fluctuations as outlined by Strohmenger & Strauss (1996) and Strohmenger et al. (1996a, 1996b). Diagenesis related to either meteoric or hypersaline fluids may create, enhance or destroy primary reservoir facies (e.g. Clark, 1980a, 1980b, 1986). These factors make it necessary to consider all aspects of the Zechstein carbonate during hydrocarbon exploration (e.g. Strohmenger et al., 1993; Van der Sande et al., 1996). In addition to reservoir complexity, the timing and nature of hydrocarbon charge are important and, depending on the local reservoir conditions (e.g. temperature and pressure), can lead to decomposition of hydrocarbon gases and the formation of hydrogen sulphide (see below).

Zechstein reservoirs are found in all carbonate units, although the Z2 Stassfurt Carbonate contains the largest number of fields. There are Z1 Carbonate reservoirs in Poland, especially in small bryozoan and algal reefs. Identical reef buildups have been found farther west (e.g. Füchtbauer, 1980), but despite their favourable reservoir characteristics they proved to be water-bearing either because there are no evaporite seals or there is a lack of charge. However, Z1 platform carbonates do form producing units in the Hewett and Q5-2 fields in the UK and the Netherlands, mainly from oolite bars. The Z2 (Stassfurt) Carbonate is an exploration target from the eastern Netherlands to Poland. The most prolific reservoirs have been found in the platform and upper-slope areas; the location of the fields coincides quite well with the outline of the Z2 Carbonate platform. Examples of gas-bearing Z3 Carbonate (Plattendolomite) are the P6 field (see Section 3.2) and the Alkmaar field (now converted into an underground gas-storage site; see Chapter 16) in the Netherlands (van Lith, 1983).

Clastic reservoirs are limited stratigraphically to the upper Zechstein (Z4/Z5) and geographically to the UK and Dutch sectors of the southern North Sea, where a number of Zechstein sandstone lobes have been identified (Geluk et al., 1996). Sandstones deposited in alluvial to playa settings are hydrocarbon-bearing in a few areas, the most important of which is the Hewett field in UK blocks 48/28, 29 and 52/5 (see Section 3.1) (Cooke-Yarborough, 1991; Cooke-Yarborough & Smith, 2003). The Hewett Sandstone, the

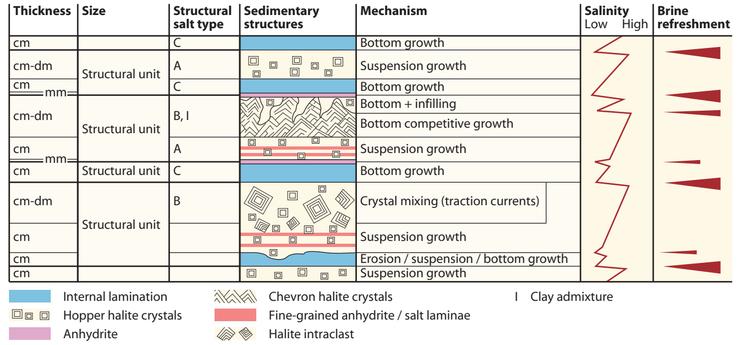

Figure 8.17 Position of halite structural units within an evaporitic basin (after Czapowski, 1987).

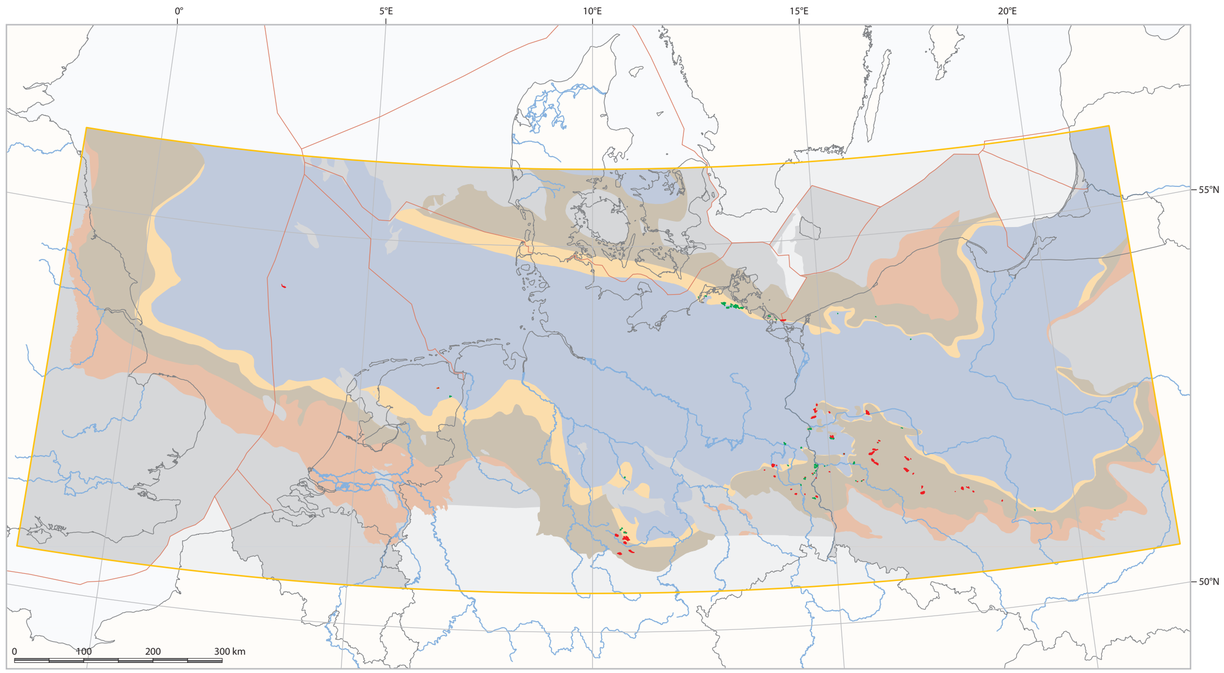

a.

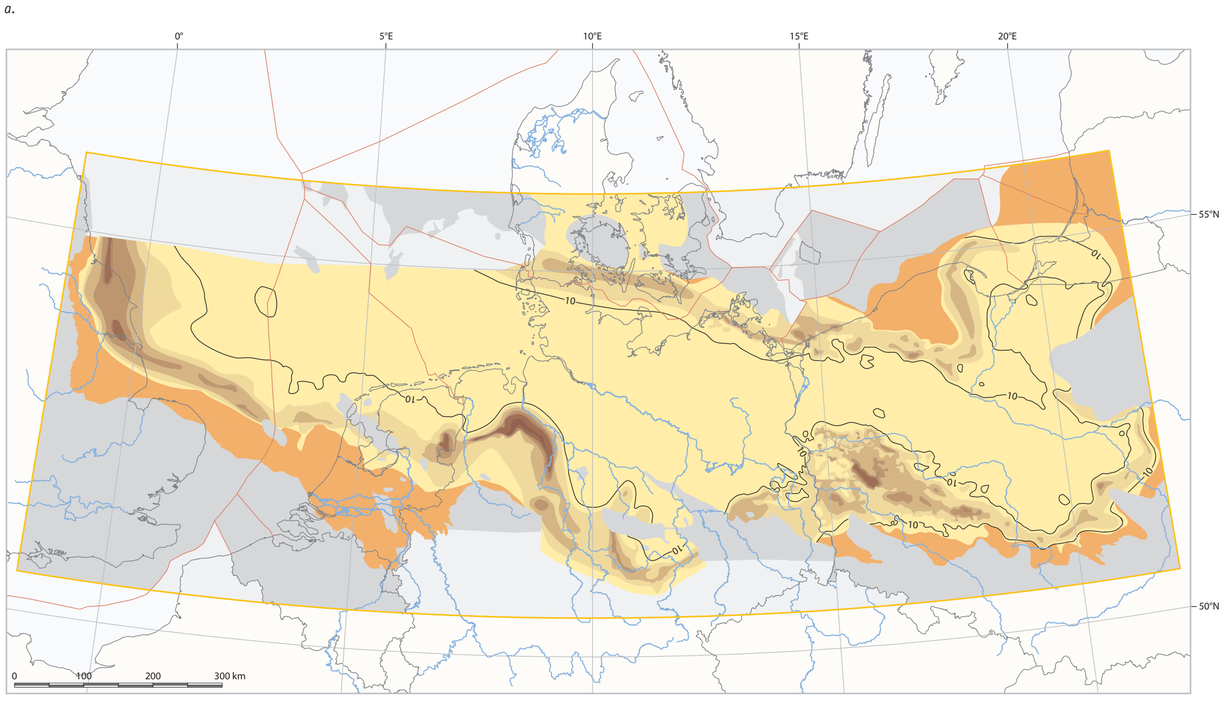

b.

Figure 8.18 Facies distribution of the Stassfurt Carbonates and equivalents. Fields with Zechstein reservoir; b. Thickness of the Stassfurt Carbonates and equivalents.

main gas-bearing reservoir in the field, is assigned to the Triassic in the UK stratigraphic scheme; however, in Dutch, German and Polish stratigraphy it is placed within the Zechstein (**Figure 8.23**).

The quality of Zechstein carbonate reservoirs is influenced by factors including diagenesis, facies, depositional environments and sea-level oscillations. The diagenesis of the Zechstein carbonates is complex (Clark, 1980a). In the case of the Zechstein Limestone, most diagenetic modifications occurred during subaerial exposure of the carbonate platforms when the deposits underwent cementation, vadose compaction, dissolution, and de-dolomitisation (see Section 8). Dolomites in the Zechstein Limestone may have formed due to mixing of sea and freshwater (Magaritz & Peryt, 1994). Some Zechstein Limestone sequences that are now fully dolomitised have undergone several stages of dolomitisation. The most important phase of dolomitisation was probably related to reflux processes during the deposition of the Lower Anhydrite when residual brines associated with sabkha and playa environments probably dolomitised the underlying deposits. These dolomites are characterised by a non-stoichiometric composition, poor ordering, and fabric selectivity in which the matrix is preferred. Primary porosity was considerably decreased during early diagenesis, especially on the carbonate platform where it was preserved mainly in the slightly cemented lime mudstones and wackestones of the lower part of the Zechstein Limestone carbonate platforms. Freshwater diagenesis created secondary moldic and vuggy porosity in the grainstones of the carbonate-platform area. The increase in temperature and pressure during burial was the main control on late diagenesis. In addition to dolomitisation, other significant processes that affected the deposits include processes of anhydritisation, pressure solution, and burial de-dolomitisation. The most important features of the porosity and permeability distribution were established when the Zechstein Limestone had been buried to depths of 600 to 900 m during the Early Triassic or soon after (Peryt, 1984).

The reservoir quality of the Main Dolomite is similarly controlled, mainly by early diagenetic processes. Subsequent multi-phase diagenetic changes resulted in modification, which although occasionally substantial, was not significant enough to change the reservoir properties (Strohmenger et al., 1998; see Section 9). The crucial diagenetic processes in the productive areas of the Main Dolomite are early meteoric cementation (which was of limited volumetric importance; Peryt, 1987b), dissolution, dolomitisation and replacement of carbonate by anhydrite, together with anhydrite cementation, de-dolomitisation (recorded in the slope facies) and halite cementation (Clark, 1980a; Depowski & Peryt, 1985; Peryt, 1987b; Strohmenger et al., 1998).

The platform-edge sands of the Main Dolomite often show evidence of very early cementation, mostly in a beach environment, and of vadose diagenesis including dissolution of ooids, which led to oomoldic porosity and solution compaction that formed the flattened ooids. Local meteoric water dissolved the unstable mineral suite (particularly aragonite) to create oomoldic porosity in the upper part of the Main Dolomite in the carbonate-platform area. Early leaching led to vuggy porosity, which was soon reduced by microbial deposits and subtidal, probably aragonitic, cements. As leaching did not form oomoldic porosity in the nearshore deposits, they were probably dolomitised by mixing mechanisms, whereas those in the basin were formed by reflux mechanisms (Peryt & Magaritz, 1990; Peryt & Scholle, 1996).

Increasing overburden pressure resulted in compaction that affected all grainstones in the carbonate-platform area. Progressive burial and increasing temperature caused gypsum to be replaced by anhydrite. This generated large quantities of water that, due to overpressuring, was injected into the Main Dolomite deposits; anhydrite began to replace the dolomite grains and periodically the cement. CO_2 was added to the pore fluids during moderate burial, probably as a result of thermal degradation of organic matter within the carbonates, which led to the congruent dissolution of dolomite. The phase of dolomite dissolution was marginally preceded by a phase of local calcitisation of dolomite and rarely of anhydrite. Again, the source of CO_2 was probably due to thermal degradation of organic matter. The de-dolomitisation was not complete and most of the previously preserved dolomite was subsequently dissolved. During late burial, when the production of CO_2 ceased, the pore waters again became saturated with respect to dolomite and there was some dolomite cementation and sporadic re-dolomitisation. An important difference between the reservoir quality of the shallow-water Main Dolomite carbonates at the platform edge and those in off-platform positions (Judersleben & Voigt, 1993) is that the former are characterised by low porosity and permeability, whereas the latter are good to very good reservoirs (Strohmenger et al., 1998).

Extensive diagenetic changes and complex diagenesis in the Platy Dolomite succession are related to the edge of carbonate platform. Tidal-flat and basinal areas underwent less differentiated diagenesis, but nevertheless the best developed reservoirs are found in the platform-edge sandy facies (Gasiewicz, 1990).

2.3 Hydrocarbon aspects

The Zechstein Group has played an important role in the exploration history of the SPB area. The earliest oil and gas discoveries were made in Zechstein rocks in the Thüringian Basin (oil was found in 1900; gas in 1932) and the first gas discovery in north-west Germany was also found in a Zechstein reservoir (Bentheim, 1938). In effect, the Zechstein rocks contain all the ingredients of a petroleum system: source rocks

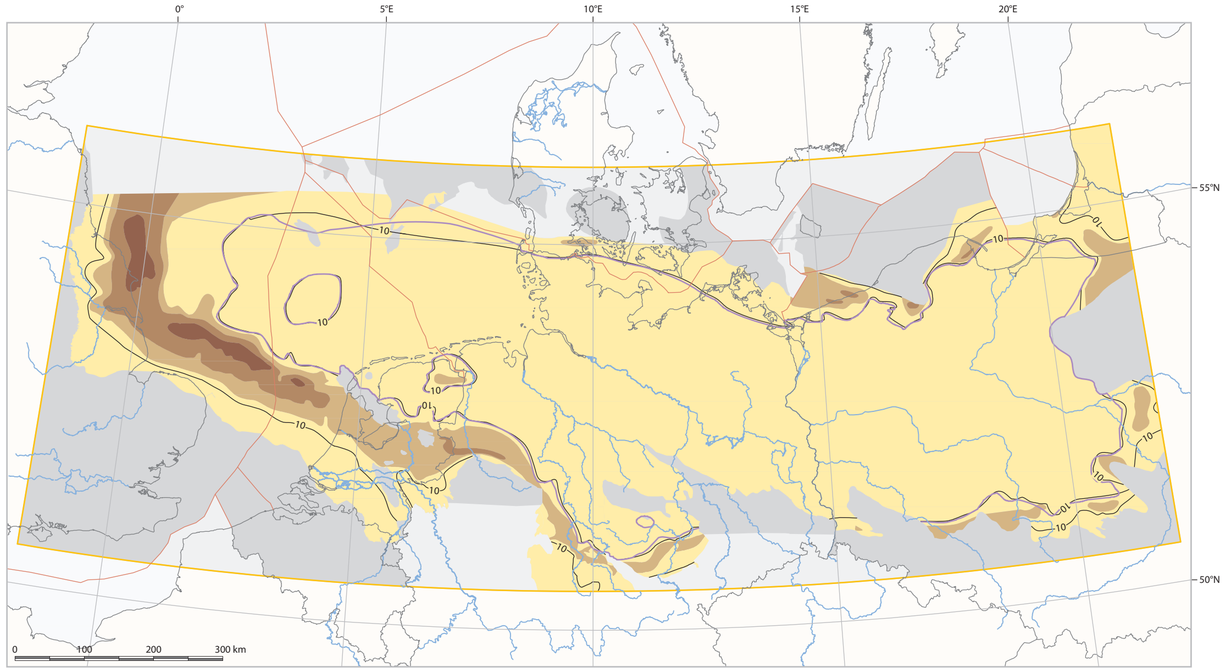

Figure 8.19 Thickness and palaeogeography of the Platy Dolomite Limestone deposits (based on papers listed in Table 8.1).

(Kupferschiefer, Z2 Carbonate), reservoirs (Z1, Z2 and Z3 carbonates, locally Z4/Z5 sandstones) and seals (anhydrite, salt). Zechstein hydrocarbon fields are found throughout the SPB area with most situated in the central and eastern areas. The total initial discovered hydrocarbon reserves are in excess of 600 bcm of gas and 2500 mmbbl of oil/condensate in 330 fields. Poland has by far the largest oil reserves, amounting up to 2200 mmbbl (expressed as Ultimate Recoverable (UR) Reserves) whereas most of the gas reserves are found in Germany (340 bcm; Plein 1994), the Netherlands (140 bcm; Geluk et al., 1997) and the UK (~100 bcm).

In the G16 field offshore of the Netherlands, the reservoir is formed by a Zechstein caprock and overlying Jurassic sediments on top of a salt diapir. When a salt diapir reaches the surface or an active aquifer, the soluble salts are dissolved. The insoluble components of the salt are left behind to form a caprock. The best developed caprock forms directly above the salt diapir and may locally include larger blocks of carbonate/anhydrite floating in the salt. The top seal of the G16 field is formed by Lower Cretaceous claystones (De Jager & Geluk, 2007).

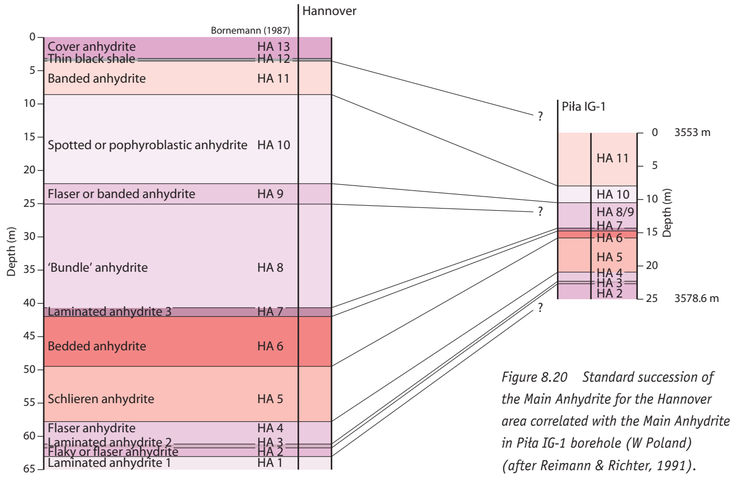

Figure 8.20 Standard succession of the Main Anhydrite for the Hannover area correlated with the Main Anhydrite in Piła IG-1 borehole (W Poland) (after Reimann & Richter, 1991).

In the UK sector of the southern North Sea, the Netherlands and north-west Germany, Carboniferous coals and Namurian shales form the gas source rock. In Poland, the Carboniferous source only applies to the Zechstein Limestone reservoirs (both the combined Rotliegend and Zechstein Limestone or, as in the Wolsztyn High area, only the Zechstein Limestone reefs). The play fairway generally extends over the Z1, Z2 and Z3 carbonate platforms where salt or anhydrite can provide a top seal. The Zechstein gas play in western Poland only works where the prolific Rotliegend sandstone reservoir is thin or absent. In central and eastern Germany and Poland, source rocks have been found in a facies of the Z2 Carbonate (Gerling et al., 1996a, 1996b; Karnin et al., 1996; Hindenberg, 1999; Kotarba & Wagner, 2007). Locally, Carboniferous source rocks had already reached gas maturity stage prior to the Permian. The Zechstein (Z1 Carbonate) belongs to the same petroleum system as the Rotliegend sandstones (with Carboniferous source rocks). Oil has been discovered (Auk, Argyll fields) in Zechstein carbonates (Brennand & Van Veen, 1975) on the flank of the Central Graben to the north of the Mid North Sea High.

Geochemical analyses show that the shales of the Kupferschiefer have excellent hydrocarbon potential, with TOC contents as high as 10.8 wt.% and thermal maturity of organic matter from about 0.6 to 0.9% Vr (Kotarba et al., 2006). However, only a small amount of hydrocarbons are generated and expelled from Kupferschiefer source rocks due to their limited thickness. At best, the Kupferschiefer shales are an additional source for some of the gases accumulated in Zechstein Limestone–Rotliegend reservoirs.

The oil that accumulated in the Main Dolomite in eastern Germany and Poland is autochthonous, and gas is partly syngenetic with the oil; the Main Dolomite therefore plays the role of both source rock and reservoir (Karnin et al., 1998). All oils were generated from type II kerogen in the middle and final phase of low-temperature thermogenic processes. Hydrocarbons were generated from the same organic matter in various sub-basins, with amounts depending on depth of burial (Kotarba et al., 2000a). The density of oil is 26 to 60°API, and the sulphur content is 0.08 to 1.67 wt.%. The saturated hydrocarbon fraction dominates the oil composition (51.5-99.2%) and the thermal maturity is 0.66 to 1.25% Vr (Kotarba et al., 2000a).

In Poland, most natural gases were generated from oil-prone type II kerogen. The basic part of the methane and higher gaseous hydrocarbons was produced in the early low-temperature phase of thermogenic processes (Kotarba et al., 2000b). The nitrogen in the Main Dolomite gas was generated mainly during the thermogenic stage of maturity of marine organic matter. The remaining gas that accumulated in the Zechstein is allochthonous, generated from type III kerogen at the high-temperature stage of thermogenic processes, with source rocks localised in deeper parts of the Zechstein and older Carboniferous strata (Kotarba et al., 2000b).

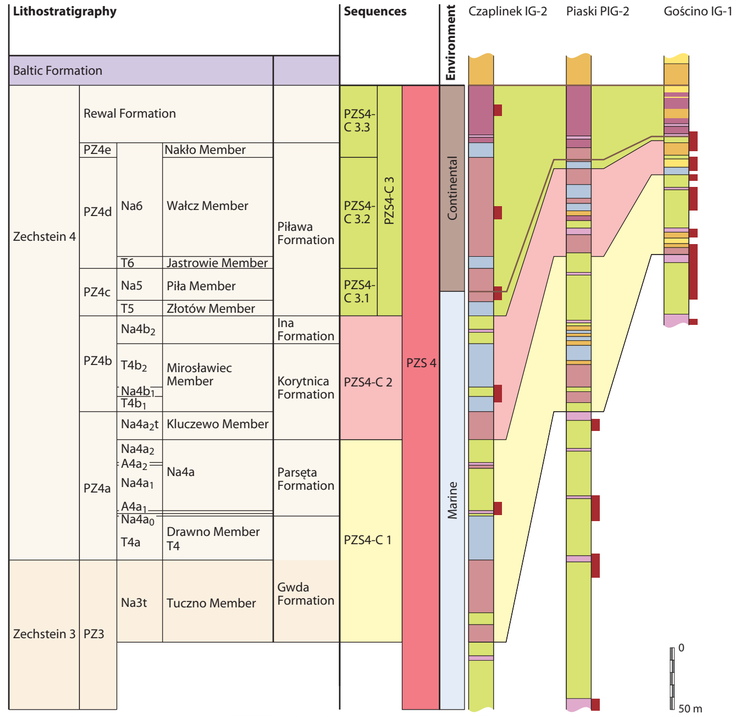

Figure 8.21 Correlation of climatic sequences in the PZ4 cycle, Polish Zechstein Basin (after Wagner & Peryt, 1997).

2.4 *Gas quality* (based on Lokhorst et al., 1998)

In the North Sea, the Netherlands and north-west Germany, the methane content of gas is usually more than 70%. Small areas with lower methane concentrations are often caused by thermochemical sulphate reduction (TSR), which is attributed to deep burial or the presence of volcanic intrusives. In Poland, methane contents are rather low and rarely exceed 65%. The wetness ratios in the north-east Netherlands and north-west Germany often exceed 200; towards the central Netherlands, C1/(C2+C3) ratios decrease to less than 50. The wet-gas compositions of the North Sea and Poland are similar.

In the North Sea, Netherlands and north-west Germany, the nitrogen content of gas is generally less than 10%, although there are exceptions such as the Valthermond field with 97% N_2. Higher N_2 concentrations are found, especially around the Bramsche-Vlotho-Uchte and Apeldorn intrusives. In Poland, nitrogen contents are always more than 10% and can be very high. At the Netherlands/north-west German border, CO_2 contents are more than 5% and these are also higher around the Bramsche-Vlotho-Uchte and Apeldorn intrusives. The development of thermochemical sulphate reduction (TSR) in this area has also generated CO_2. Elsewhere in the North Sea and the Netherlands, CO_2 contents are usually less than 5%. In Poland, CO_2 contents rarely exceed 2%.

Sour gases are only found in the Zechstein deposits of the SPBA area and are limited to carbonate reservoirs. TSR is believed to be the sulphide generating process, which leads to decomposition of hydrocarbons. The higher alkanes (ethane, propane and higher homologues) are normally reduced. The remaining gases have heavier carbon and hydrogen isotopes and so produce isotopically lighter CO_2. Finally, methane also decomposes as H_2S levels rise.

Mittag-Brendel (1994, in Lokhorst et al., 1998) has discussed the genesis of H_2S in the west German Zechstein natural gas deposits and its dependence on temperature, as well as the facies-structural formations of the Werra Anhydrite and the Stassfurt carbonates. These results suggest that TSR is a local phenomenon, which is strongly influenced by the reservoir temperature and other factors.

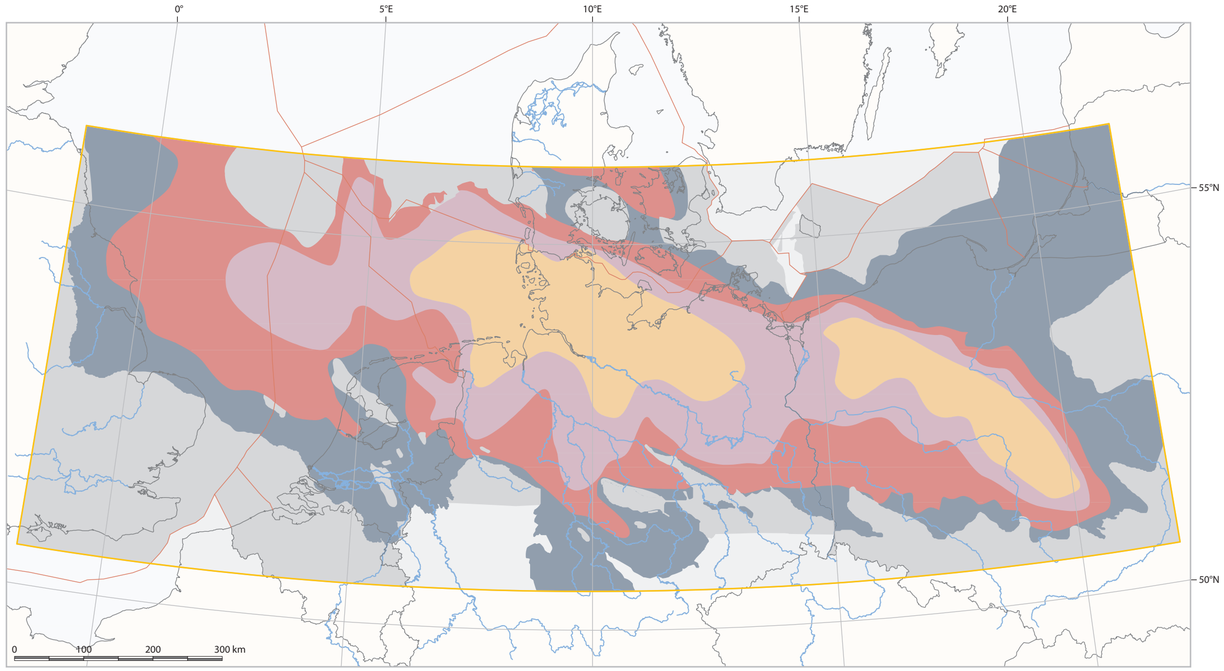

Figure 8.22 Distribution of the youngest Zechstein salts (after Best, 1989; Cameron et al., 1992; Geluk et al., 1997; Wagner in Dadlez et al., 1998; Glennie et al., 2003; Geluk, 2005).

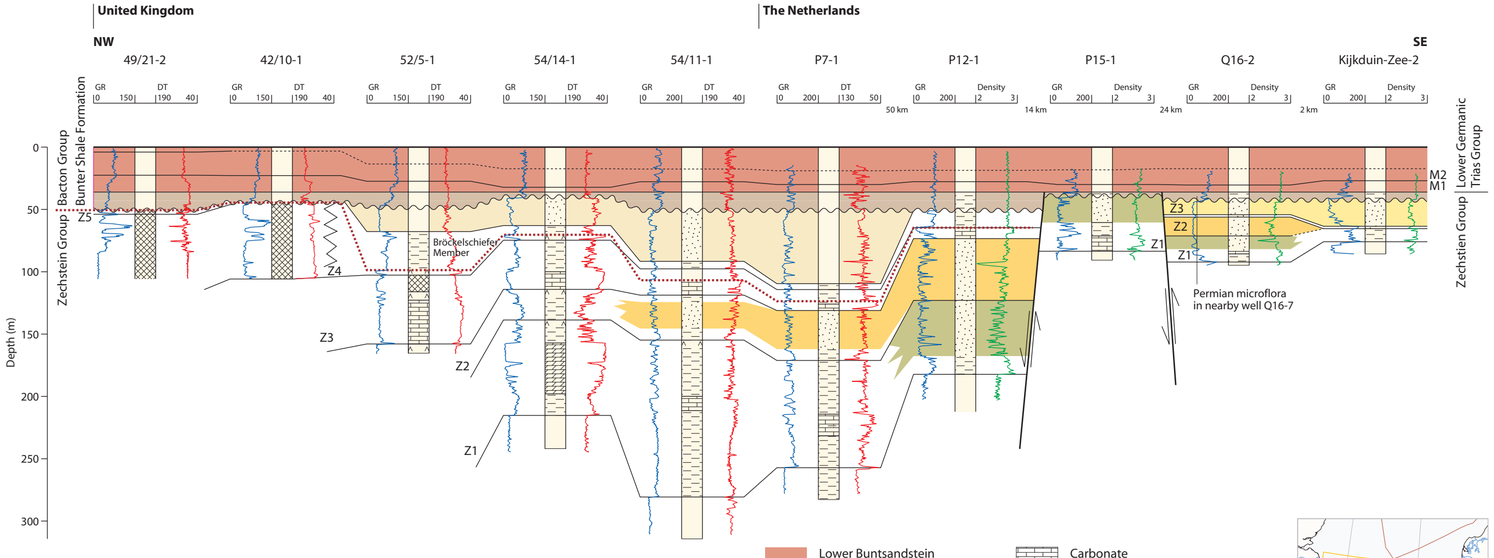

Figure 8.23 Stratigraphic well-correlation diagram of the uppermost Zechstein and lowermost Triassic in the southern North Sea area, based on gamma-ray and sonic logs. Note the onlap of the basal Zechstein strata towards the platform and the disconformable contact of the Zechstein Upper Claystone Formation with the underlying deposits. Well 52/5-1 is situated in the Hewett field. The reference level is the Dutch definition of the Lower Buntsandstein. The red dotted line represents the Zechstein-Bacton Group boundary according to the definition of Johnson et al. (1994). Note that it cuts across various Zechstein cycles. According to Johnson et al. (1994), the Hewett Sandstone belongs to the Bacton Group (Triassic), whereas in the Netherlands it belongs to the Zechstein. After Geluk (2005). The approximate position of the chronostratigraphic Permian-Triassic boundary based on palaeomagnetic work of Szurlies et al. (2003) has been indicated.

3 Hydrocarbon field examples

3.1 Hewett gasfield, offshore UK

The Hewett gasfield extends across UK blocks 48/28, 48/29, 48/30, 52/4 and 52/5 on the South Hewett shelf (**Figures 8.24** & **8.25**), approximately 25 km off the Norfolk coast. The field (*sensu stricto*) is the largest in a cluster that includes Big Dotty, Little Dotty, Della, Dawn and Delilah. The field was discovered in 1966 by well 48/29-1, started production in 1969, and is still producing. Data from the Hewett field are taken from Cooke-Yarborough (1991), Cooke-Yarborough & Smith (2003), Southwood & Hill (1995) and IHS Energy data. The field produces from three reservoirs: the Bunter Sandstone, Hewett Sandstone and the Zechsteinkalk. Although the Bunter Sandstone and Hewett Sandstone are considered to form part of the Triassic Bacton Group in the UK, in a basinwide context the latter unit forms part of the uppermost Zechstein as recognised by Geluk et al. (1996), Fisher & Mudge (1998) and Geluk (2005) (**Figure 8.23**). The Hewett field is unusual in that it is one of the few fields that produce from the Hewett Sandstone (apart from P11 in the Netherlands). The only other field in the western SPBA area where the Zechsteinkalk (or Z1 Carbonate) is gas-bearing is Q5-2 in the Dutch offshore sector (Geluk, 1999a). The gas volume (UR) of the Hewett Sandstone accumulation is 74 bcm, with a recovery factor exceeding 96%. The Zechsteinkalk gas volume UR is 12 bcm, with an estimated recovery factor of 50%.

The Hewett field is a fault-bounded 4-way dip closure situated above a basement high. The reservoirs occur in a north-west–south-east-trending anticline, bounded by faults on its north-east and south-west flanks (**Figure 8.24**). The source rock for the gas is formed by the Carboniferous Coal Measures directly underlying the structure. Zechstein evaporites seal the Zechsteinkalk accumulation. The Bunter Shale is the seal for the Hewett reservoir, whereas the ultimate top seal of the field is formed by the Röt evaporite (**Table 8.6**).

The Hewett Sandstone is limited in extent and is the erosional product of a phase of uplift of the London-Brabant Massif (Cooke-Yarborough & Smith, 2003). Some correlatable claystone barriers have been identified across the sandstone, which delineate the different reservoir zones. The reservoir pinches out directly to

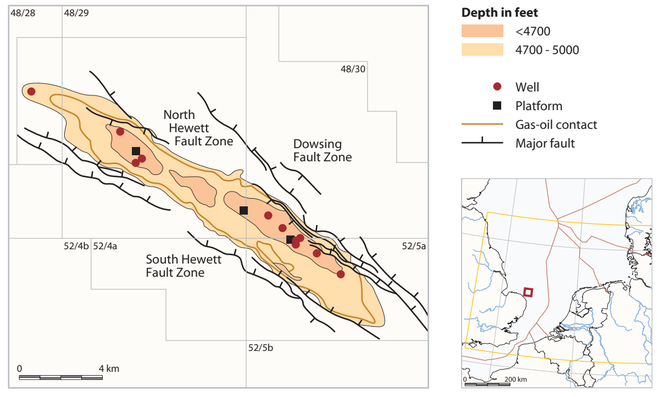

Figure 8.24 Depth to the top of the Zechsteinkalk in the Hewett field (after Southwood & Hill, 1995).

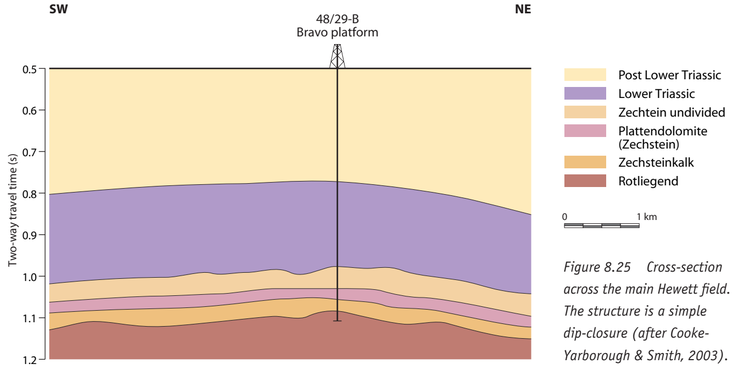

Figure 8.25 Cross-section across the main Hewett field. The structure is a simple dip-closure (after Cooke-Yarborough & Smith, 2003).

the north. The Zechsteinkalk reservoir is characterised by an extreme heterogeneous porosity distribution in the vertical and lateral sense (**Figure 8.26**). The field is situated close to the basinward edge of the Z1 Carbonate platform (Taylor, 1998) at the transition between lagoonal and foreshore environments (Southwood & Hill, 1995). The platform edge is approximately parallel to the strike of the Hewett field, which helps explain facies trends within the reservoir. The Zechsteinkalk is a sequence of interfingered tidal-flat muds and oolitic shoal-facies sediments (**Figure 8.27**). The depositional facies had only moderate differences in initial porosities, but later diagenetic processes (early leaching, dolomitisation, early carbonate and anhydrite cementation) have introduced considerable variation. Anhydrite cement is volumetrically the most important, clogging both pores and fractures in some reservoir intervals.

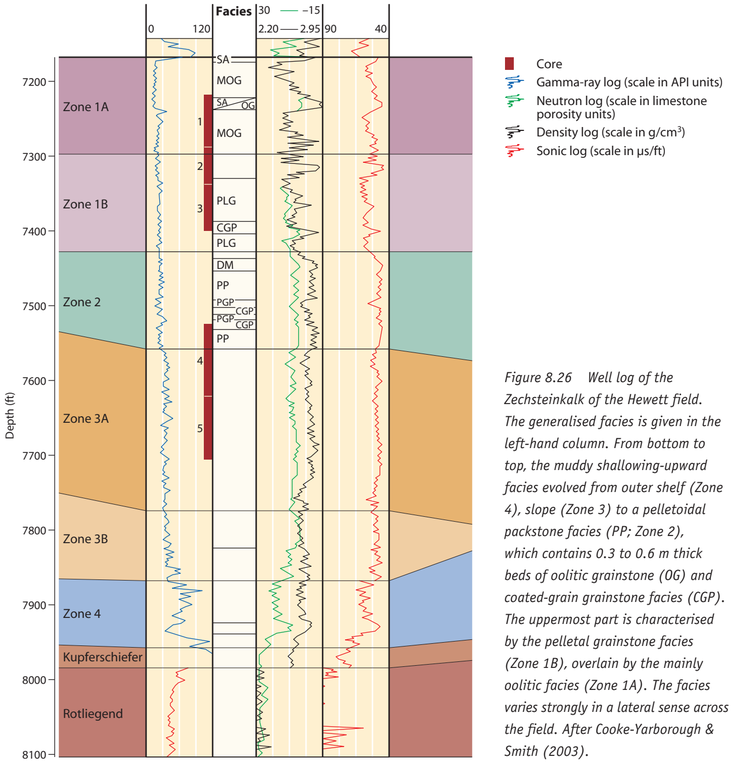

Figure 8.26 Well log of the Zechsteinkalk of the Hewett field. The generalised facies is given in the left-hand column. From bottom to top, the muddy shallowing-upward facies evolved from outer shelf (Zone 4), slope (Zone 3) to a pelletoidal packstone facies (PP; Zone 2), which contains 0.3 to 0.6 m thick beds of oolitic grainstone (OG) and coated-grain grainstone facies (CGP). The uppermost part is characterised by the pelletal grainstone facies (Zone 1B), overlain by the mainly oolitic facies (Zone 1A). The facies varies strongly in a lateral sense across the field. After Cooke-Yarborough & Smith (2003).

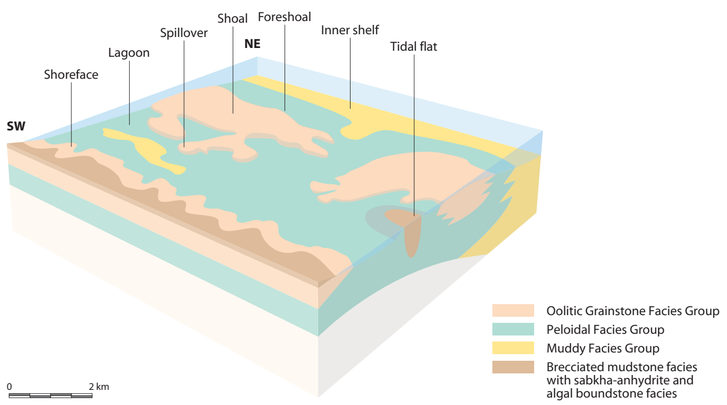

Figure 8.27 Schematic depositional model for Zones 1 and 2 (after Cooke-Yarborough & Smith, 2003).

Table 8.6 Properties of the Hewett field.

Reservoir	Zechsteinkalk	Hewett Sandstone
Lithology	Dolomite	Sandstone
Depth to top (m)	1370	1227
GWC/GOC.OWC (m)	1488	1344
Maximum column height (m)	118	117
Net reservoir thickness (m)	100	62
Net to gross ratio	Low and variable	0.87
Porosity (%)	6.5	23
Gas saturation (%)	60	80
Permeability (mD)	1000	1000
Fluid type	Gas	Gas
Gas composition	C1 93.5%, C2 + C3 3.8%, N_2 1.2%, CO_2 0.2%	C1 92.3%, C2 + C3 4.4%, N_2 2.3%, CO_2 0.02%
Initial pressure (bar)	150.2	139.6
Source rock	Westphalian Coal Measures	Westphalian Coal Measures
Seal	Zechstein evaporites	Bunter Shale and Röt evaporites

3.2 P6 gasfield, offshore Netherlands

The P6 gasfield is situated in the P6 Netherlands offshore block, approximately 60 km off the Dutch coast in the Broad Fourteens Basin. The field was discovered in 1968 by the well P6-1 (Mobil). The primary objective of the well (Rotliegend) was found to be dry; however, gas was discovered in the Main Buntsandstein Subgroup and the Z3 Carbonate. The field came into production in 1985. Several wells drilled the reservoir, but only a few turned out to be good producers (**Figure 8.28**). The ultimate recoverable volume of the Zechstein accumulation is about 2.8 bcm, with an estimated recovery of 45%. The setting of the Z3 Carbonate reservoir in the P6 field has been described by Van der Poel (1989) and unpublished Fugro data.

The P6 structure is a major fault-bounded, north-west–south-east-trending inversion anticline with an areal extent of 29 km^2. The sealing unit of the Zechstein Z3 Carbonate is formed by Zechstein evaporites. Westphalian Coal Measures are the source of the gas (**Table 8.7**).

Deposition of the Z3 Carbonate took place on an extensive carbonate ramp (Geluk, 1999a) on which a north-west–south-east-oriented oolitic shoal developed (Baird, 1993). The P6 field is situated at the transition of shoal and (lagoonal) back-shoal deposits, with the shoal facies having the best primary reservoir characteristics. The amount of pay zone varies from well to well. The reservoir is formed mainly by tight unfractured dolomite with a maximum thickness of 36 m, although some wells (P6-1, P6-B2 and P6-C2) found naturally fractured dolomite with variable quality. The Z3 Carbonate overlies the Grey Salt Clay, and

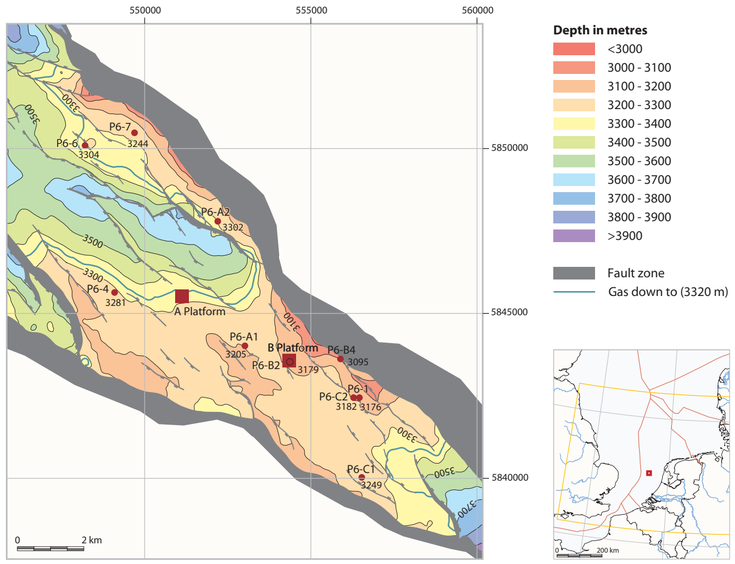

Figure 8.28 Depth to the top of the Z3 Carbonate in the P6 field, offshore Netherlands. Courtesy of Wintershall.

the Main Anhydrite rests on top of the unit. Four correlatable reservoir zones were identified by Van der Poel (1989; **Figure 8.29**). The lowermost Unit 1 is a dark grey to greyish black dolomite with minor intercalated anhydrite streaks grading upwards into Unit 2, which is characterised by argillaceous streaks and brecciated dolomites. Unit 2 is the thickest unit (>20 m) and in its upper part is mostly parallel bedded with purer, tan-coloured dolomites. Unit 3 shows an upward increase in shale content and Unit 4 consists of shaly dolomites with characteristic high gamma-ray readings. Sediment petrography (Van der Poel, 1989) shows that the units consist of medium-grained dolomite packstones, wackestones, boundstones and grainstones with algae, forams, shell fragments and pelloids. Porosity is vuggy, intercrystalline, intraparticle, moldic and fracture types. Porosities of up to 20% have been observed in the packstones/grainstones, whereas in other lithologies it is generally less than 5%. The diagenetic history comprises early and late leaching, late dolomitisation, anhydritisation and the formation of fractures during the late stages. Prediction of fracture and better-than-average vuggy matrix porosity distribution are critical for optimal field development.

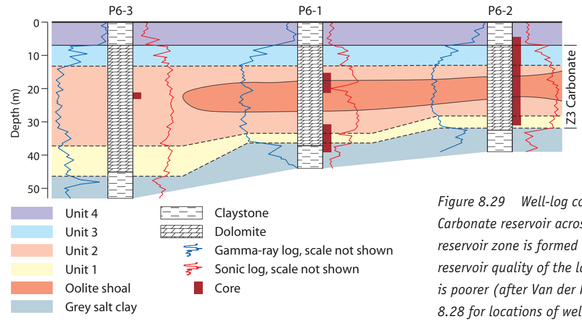

Figure 8.29 Well-log correlation of the Z3 Carbonate reservoir across the P6 field. The best reservoir zone is formed by an oolite shoal; the reservoir quality of the lagoonal and back shoal is poorer (after Van der Poel, 1989). See Figure 8.28 for locations of wells.

Table 8.7 Properties of the P6 field.

Reservoir	Z3 Carbonate
Lithology	Dolomite
Depth to top (m)	3204
GWC/GOC.OWC (m)	3320
Net reservoir thickness (m)	36
Porosity (%)	5
Gas saturation (%)	79
Permeability (mD)	1
Fluid type	Gas
Gas composition	C1 91.6%, C2 2.48%, C3 0.39%, N_2 1.54%, CO_2 3.22%
Initial pressure (bar)	365.4
Source rock	Westphalian Coal Measures
Seal	Zechstein evaporites

3.3 Schoonebeek gasfield, onshore Netherlands

The Schoonebeek gasfield underlies the giant Schoonebeek oilfield in the north-east Netherlands and straddles the border with Germany (**Figure 8.30**). The field was discovered by the well Schoonebeek-313 in 1957. The description of this field is based on proprietary NAM data, Clark (1980a), Van der Baan (1990) and IHS Energy. Gas volumes (UR) amount to 9.9 bcm.

The Schoonebeek gasfield is situated in the Lower Saxony Basin. The reservoir is formed by the Z2 Carbonate, which is sealed by Zechstein evaporites (**Figure 8.31**). The field is a complex fault/dip-closed structure in which fault closure determines its western limit (**Figure 8.30**). The source rocks are Westphalian coal seams (**Table 8.8**).

The Z2 Carbonate developed on the western flank of a Z1 Anhydrite platform, which was influenced by the underlying volcanics and a fault-bounded substratum (Van der Baan, 1990). The Z2 Carbonate reservoir consists of two facies, a slope facies in the west and a platform facies that built out over the slope in the eastern part of the field (**Figure 8.32**). Although the overall geometry of the Z2 Carbonate is a simple, sigmoidal shaped body, the internal architecture is much more complex. The thickness of the Z2 Carbonate varies considerably from 50 m on the platform area to 200 m on the middle slope, decreasing again westwards to 50 m in a lower slope/basin facies. Clark (1980a) identified four phases of carbonate deposition. The platform facies in the east is an alternating sequence of oolitic, pelletoidal, bioclastic and pisolitic carbonates. The oolitic complex has the best reservoir properties. The slope deposits are

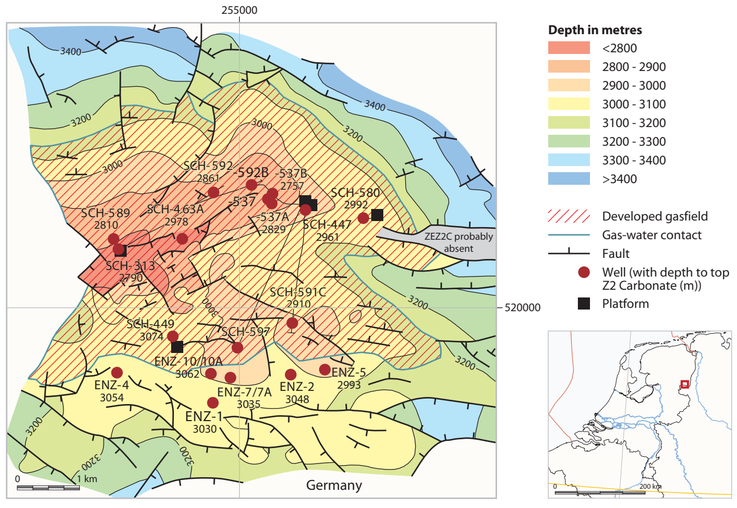

Figure 8.30 Depth-structure map of the top of the Z2 Carbonate in the Schoonebeek gasfield, eastern onshore Netherlands. The fields straddles the border with Germany. Courtesy of NAM.

dark-coloured, fine-grained, thinly-bedded turbiditic mudstones and intercalated slumps with low porosities. As a result, fracture networks are far more important for gas production on the slope than on the platform (Clark, 1980a). Permeability across the entire field comes mainly from an open-fracture system that is most pronounced in the tighter slope area.

Table 8.8 Properties of the Schoonebeek gasfield.

Reservoir	Z2 Carbonate
Lithology	Dolomite
Depth to top (m)	2790
GWC/GOC.OWC (m)	3145
Maximum column height (m)	355
Net reservoir thickness (m)	200
Net to gross ratio	Variable
Porosity (%)	2-13
Gas saturation (%)	40-50
Fluid type	Gas
Gas composition	C1 88.2%, C2 0.4%, N_2 5.1%, CO_2 6.1%, H_2S 60-2800 ppm
Initial pressure (bar)	303.4
Source rock	Westphalian Coal Measures
Seal	Zechstein evaporites

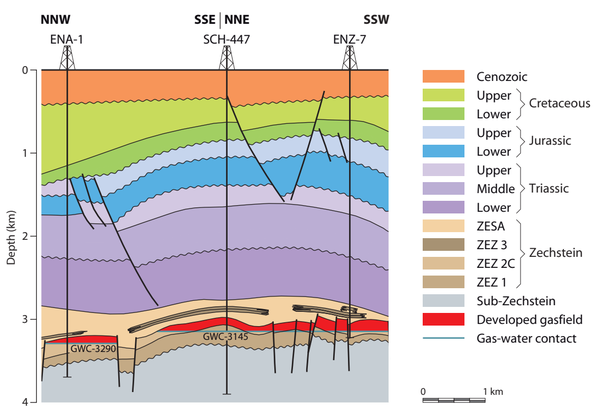

Figure 8.31 Cross-section across the Schoonebeek gasfield. See Figure 8.30 for locations of Schoonebeek and ENZ wells.

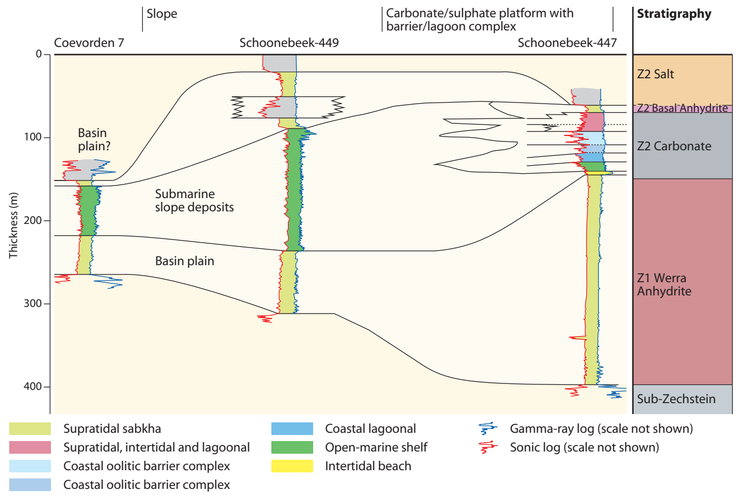

Figure 8.32 Well-log correlation across the reservoir zone of the Schoonebeek gasfield. Note that in the eastern part of the field (Schoonebeek-447) shallow-water platform carbonates prevail, giving way to a thick wedge of muddier slope deposits (Schoonebeek-449) before passing into basinal carbonates (Coevorden-7) beyond the field towards the west. The reference level is the reconstructed bathymetrical position at the end of Z2 Carbonate deposition. After Clark (1980a). See Figure 8.30 for locations of the Schoonebeek wells.

3.4 *Barnówko-Mostno-Buszewo (BMB) oil and gasfield, onshore Poland*

The Barnówko-Mostno-Buszewo (BMB) field is situated about 80 km south of Szczecin in western Poland in the area of Dębno Lubuskie (Gorzów Wielkopolski District). It is the largest oil accumulation in Poland (32.5 km^2) and was discovered by three exploratory wells drilled between 1992 and 1994 at sites that were thought to be three separate structures: the Mostno gaspool, the Barnówko gas accumulation at the top of the Main Dolomite and oil accumulation at its base, and the Buszewo oilpool (Mamczur & Czekański, 2000; **Figure 8.33**). The recovery factors are 0.6 and 0.2 for the gas and oil accumulations respectively. The oil and gas reserves are 64.4 × 10^6 t of oil and condensate (10.14 × 10^6 tm recoverable) and 29.4 bcm of gas (9.87 bcm recoverable; Górski & Trela, 1997). The field description is based on Mamczur et al. (1997), Górski & Trela (1997), Pikulski (1998), Górski et al. (1999), Kotarba et al. (2000a, 2000b), Mamczur & Czekański (2000) and Protas (2000).

Hydcarbons in the BMB field are both structurally (faults) and stratigraphically trapped (outlines of carbonate platform). The reservoir is capped by Basal Anhydrite (A2) deposits overlain by the Older Halite (Na2), which forms the top seal for the accumulation (**Figure 8.34**). The source rock of the BMB accumulations, which is the same as the reservoir (Main Dolomite), is characterised by TOC contents of 0.01 to 0.94% (average 0.27%). The kerogen is algal organic matter (mostly type II, sometimes with an admixture of type III). The maturity, expressed in vitrinite reflectance, is 1.05 to 1.23% Ro.

The Main Dolomite (Ca2) forms part of a carbonate platform that developed on the Werra sulphate platform at the north-western margin of the Fore-Sudetic Monocline. The thickness of the reservoir (dolomites, peloidal and ooidal grainstones in Barnówko and Mostno, and recrystallised rocks with relics of oncoids and oncoidal-intraclastic grainstones in Buszewo) varies from 33 to 83.5 m. The palaeo-relief was largely controlled by the inherited topography of the Wolsztyn High, an elevated block with no upper Rotliegend deposits. The Main Dolomite profile in the BMB region is clearly tripartite in the Buszewo region (predominantly lagoonal area; **Figure 8.35**). The three sequences are designated as Horizon A (the lowest), B and C. The subdivision is less clear towards the west; in the Mostno area there is a carbonate barrier that makes it more difficult to distinguish the three depositional-diagenetic sequences (**Figures 8.36** to **8.39**).

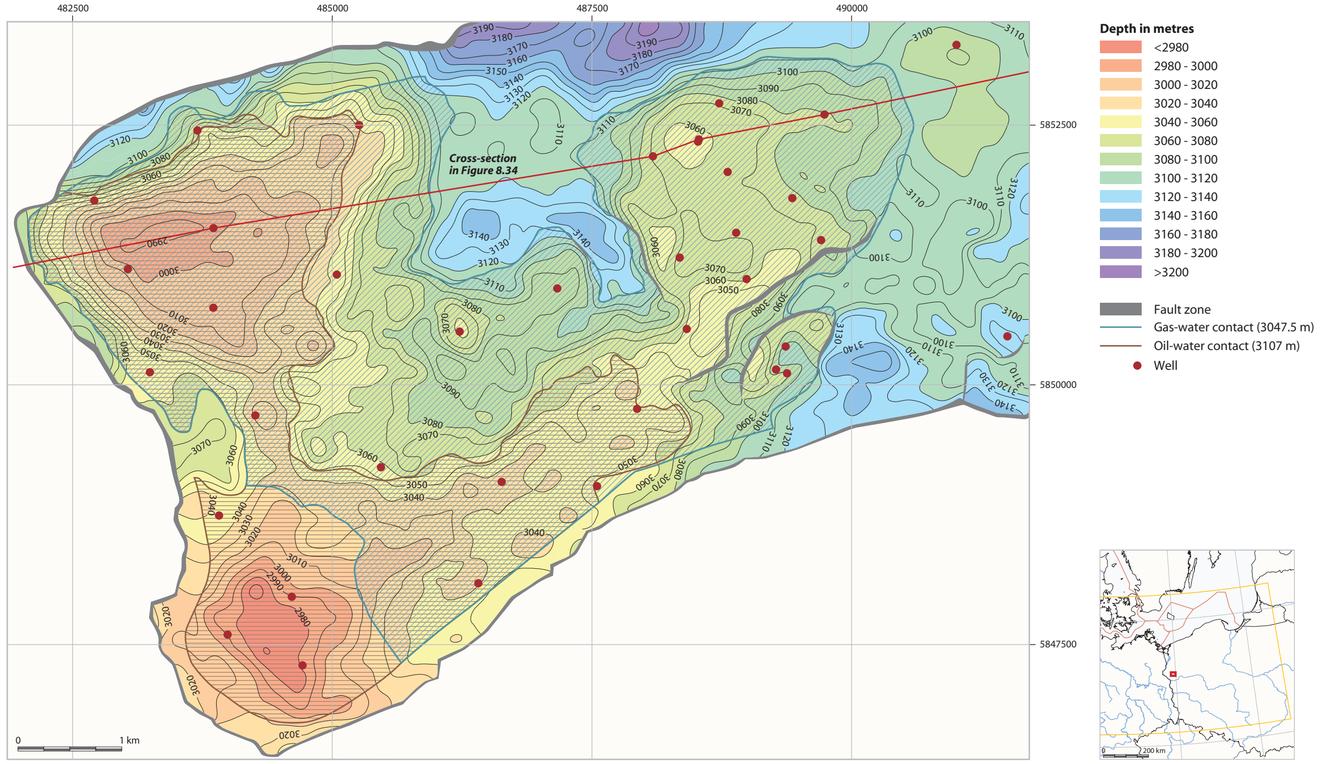

Figure 8.33 Depth-structure map to the top of the Main Dolomite in the Barnówko-Mostno-Buszewo field (Liberska et al., 1998, unpublished).

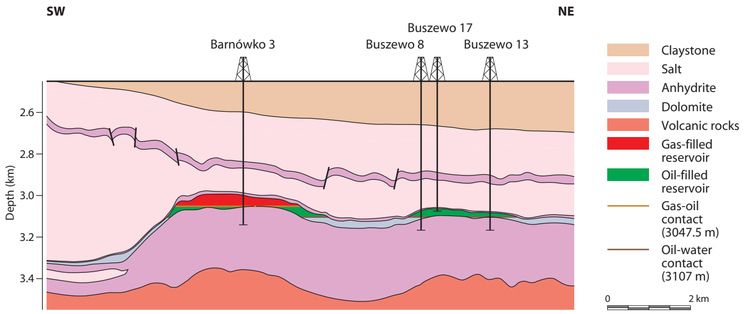

Figure 8.34 Schematic cross-section through the BMB reservoir. Courtesy of POGC. See Figure 8.33 for location.

Horizons A and B are both characterised by primary porosity, whereas Horizon A was subject to carbonate dissolution, secondary sulphate cementation and aggradational neomorphism (**Figure 8.36**). Horizon C underwent strong vadose modifications and is characterised by good secondary reservoir properties, although increased sulphate impregnation in its upper part reduces its reservoir properties (Protas, 2000). Porosities vary from 4 to 27% (the weighted average for the reservoir series varies from 9.6% in Buszewo 2 to 19.5% in Barnówko 2), the highest values are typically found in Horizon B. For example, in Buszewo 1 the average porosity for Horizon B is approximately three times greater than in Horizons A or C (Pikulski, 1998). Permeabilities are up to 28 mD (**Table 8.9**); the reservoir gradient is 0.178 MPa/10 m. The crude oil below the gas-bearing layer is a light oil (API 45°) with a density of 0.798 g/cm^3 and gas-oil ratio of 746 m^3/m^3. The crude oil in the lower part of the hydrocarbon column in the Buszewo area is of a heavy type (API 39°) with a density of 0.828 g/cm^3 and gas-oil ratio of 253 m^3/m^3.

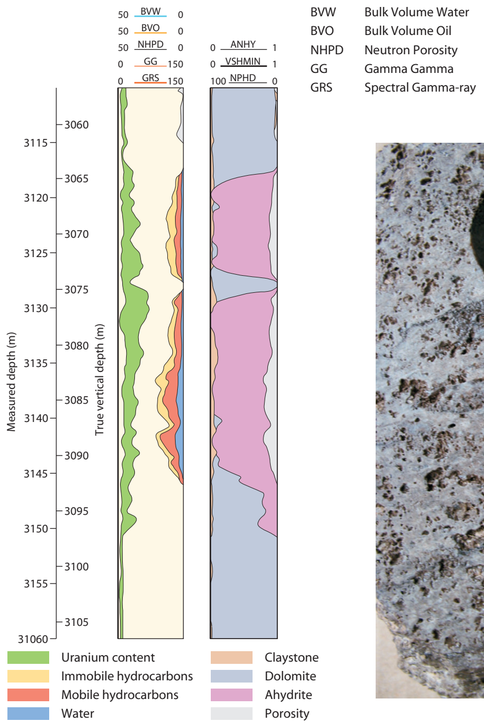

Figure 8.35 Composite log of the Buszewo 7 well. Courtesy of POGC. Based on various geophysical-log properties.

BVW	Bulk Volume Water
BVO	Bulk Volume Oil
NHPD	Neutron Porosity
GG	Gamma Gamma
GRS	Spectral Gamma-ray

Figure 8.36 Core showing small cavities throughout the rock. Mostno 8k well; depth 3134.7 m. Photomicrograph by K. Chłódek.

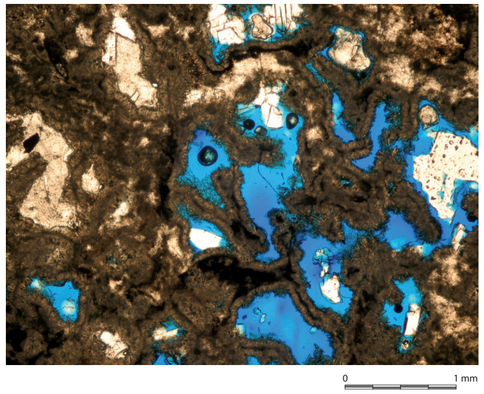

Figure 8.37 Recrystallised allochem grainstone (blue – porosity, white – anhydrite and isolated pores not filled by resin); Mostno 8k well; depth 3134.75 m. Photomicrograph by K. Chłódek.

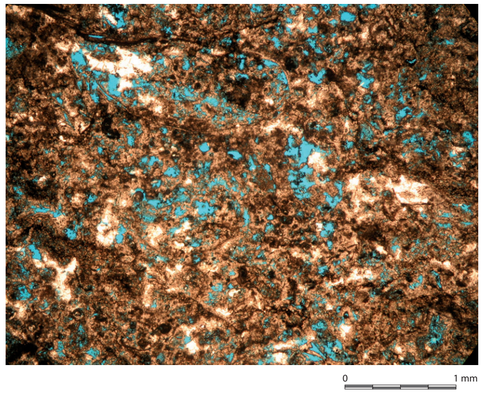

Figure 8.38 Recrystallised allochem packstone/grainstone, with ghosts of bivalves. Porosity reaches 20%. Mostno 8k well; depth 3137.6 m. Photomicrograph by K. Chłódek.

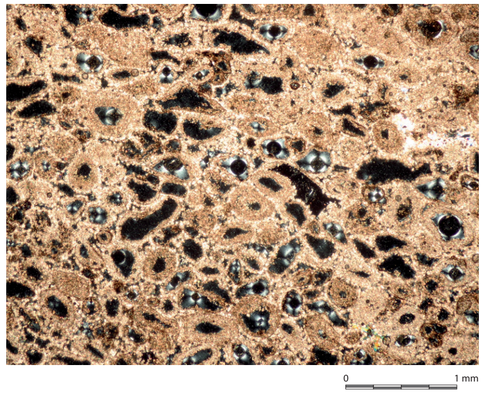

Figure 8.39 Ooidal grainstone; ooids often dissolved, sparite between allochems. Elongated ooids and pores indicate compaction. Barnówko 12 well; depth 3113.95 m. Photomicrograph by K. Chłódek.

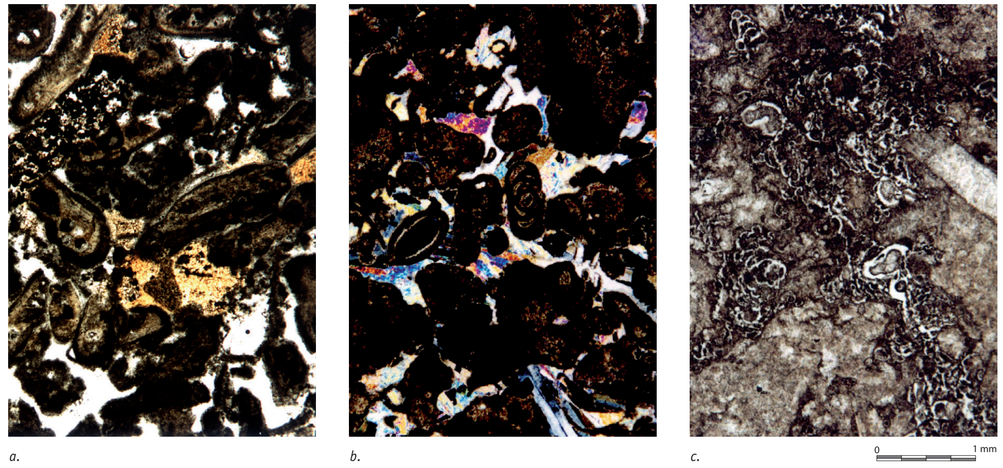

Figure 8.40 a. Bryozoan grainstone with extraclasts; the white areas are pores and anhydrite; the light brown areas are clay minerals and iron compounds. Brońsko 1 well; depth 2241.4 m; b. Bioclastic-intraclastic packstone-grainstone with sulphates replacing carbonate cements; black areas are pores. Brońsko 1 well; depth 2231.8 m; c. Bioclastic wackestone with encrusting foraminifers. Brońsko 1 well; depth 2206.45 m. Photomicrographs by K. Chłodek.

Table 8.9 Properties of the Barnówko-Mostno-Buszewo fields.

Reservoir	Main Dolomite (Ca2)
Lithology	Dolomite
Depth to top (m)	2982
GWC/GOC.OWC (m)	OWC 3107; GOC 3047.5
Net reservoir thickness (m)	33-83.5
Porosity (%)	4-27
Gas saturation (%)	88
Oil saturation	78
Permeability (mD)	11-28
Fluid type	Oil and gas
Gas composition	C1 35%, C2 3.9%, C3+ 4.8%, N_2 52.6%, CO_2 0.4%, H_2S 3.3 %
Oil gravity	0.736-0.826 (API 39°-59.6°)
Initial pressure (bar)	553
Temperature (°C)	117
Source rock	Main Dolomite (Ca2)
Seal	Stassfurt Series (Z2), anhydrite

3.5 Kościan and Brońsko gasfields, onshore Poland

The Kościan and Brońsko gasfields are located in south-west Poland, approximately 40 km south-west of Poznań. Production is from stacked reservoirs in the Zechstein Limestone. The Kościan field was discovered in 1975 when the Kościan 1 well encountered gas in porous bioclastic packstones (6.5 m thick) of the Zechstein Limestone (Głowacki, 1993; **Figures 8.40** & **8.44**). Further drilling failed to find hydrocarbons and the field was very quickly exploited (22.4 mln m^3; Karnkowski, 1999b; Dyjaczyński, 2000). In 1995, following a 3D-seismic study, the Kościan 6 well discovered a new gasfield (Kościan-South) and the same methodology made it possible to find a series of gasfields (including Brońsko) in the Zechstein Limestone of the region (**Figure 8.11**; Dyjaczynski et al., 2001). Small gasfields were also found in the Main Dolomite, capped by the Basal Anhydrite. The Brońsko field was discovered in 1998 by the Kokorzyn 1 well, which encountered 64.5 m of reefal Zechstein Limestone (**Figure 8.43**). A subsequent 15 wells also drilled the Zechstein Limestone reef complex. The field descriptions are based on data from Dyjaczyński (2000), Górski et al. (2000), Mamczur & Czekański (2000), Dyjaczynski et al. (2001) and unpublished POGC data.

Gas in the Kościan and Brońsko gasfields is stratigraphically trapped. Upper Anhydrite deposits form the sealing unit (**Figures 8.42** & **8.44**) and Carboniferous type III shales are the most important source rocks. However, in the Kościan Main Dolomite field, the reservoir is also a source rock.

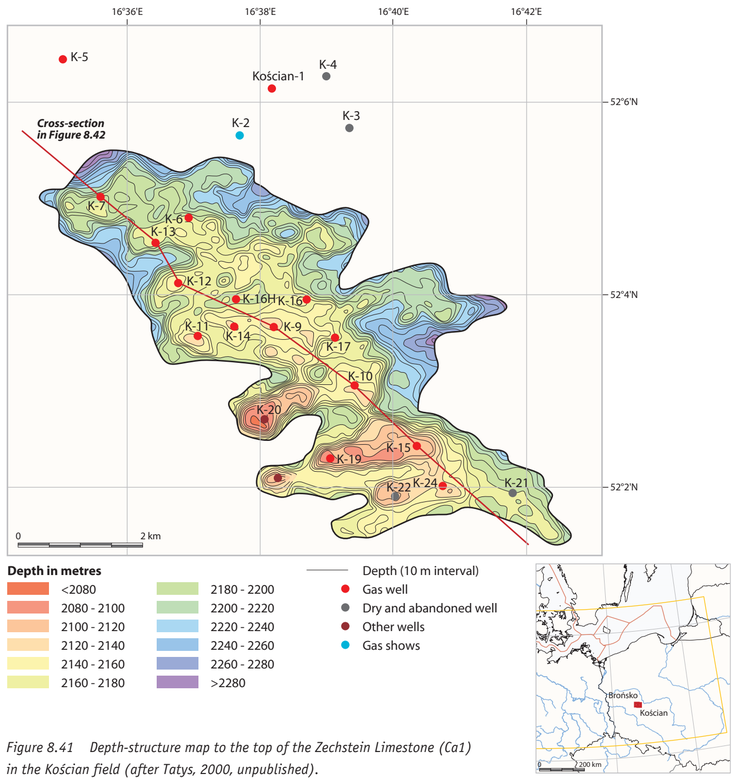

Figure 8.41 Depth-structure map to the top of the Zechstein Limestone (Ca1) in the Kościan field (after Tatys, 2000, unpublished).

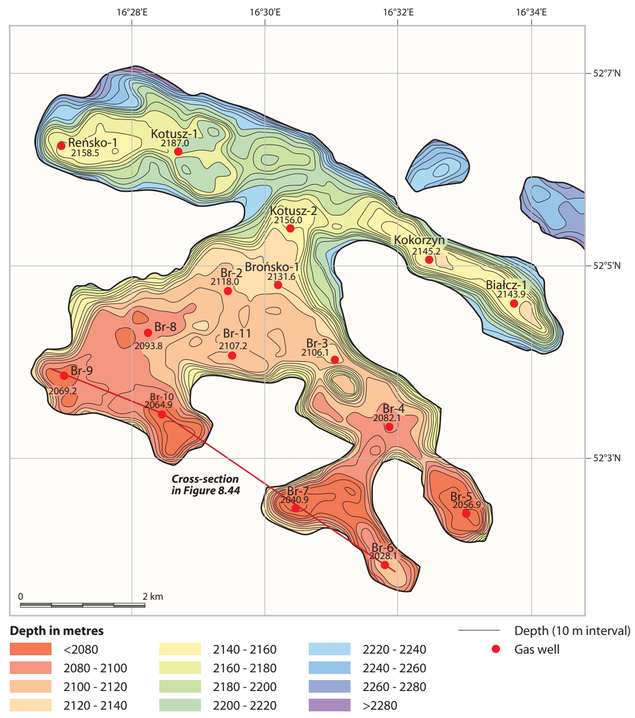

Figure 8.43 Depth-structure map to the top of the Zechstein Limestone (Ca1) in the Brońsko field (after Jakiel & Radecki, 2003, unpublished).

Table 8.10 Properties of the Kościan and Brońsko fields.

Reservoir	Zechstein Limestone (Brońsko)	Main Dolomite (Kościan)	Zechstein Limestone (Kościan)
Lithology	Limestone and dolomite	Limestone and dolomite	Limestone and dolomite
Depth to top (m)	2030	2006	2092
GWC/GOC.OWC (m)	~2150	2036.5-2111.5	2207.5
Maximum column height (m)	87	8-37	56.1
Net reservoir thickness (m)	19-91	5.7-24.8	27.7
Porosity (%)	9.7-19.6	13-15.4%	13.6-16.6
Gas saturation (%)	86	60-86	88
Permeability (mD)	40-69	5.1-24.9	17.4-86.6
Fluid type	Gas	Gas	Gas
Gas composition	C1 74.7%, C2 1.0%, C3 0.09%, N_2 23.8%, CO_2 0.3%,	C1 11.6-60%, C2 1.3-2.6%, C3+ 0.7-6.2%, N_2 36-87%, CO_2 0.5-1%, H_2S 0.48-1.14%	C1 80.5%, C2 0.7%, N_2 18%, CO_2 0.5%, He 0.1%
Initial pressure (bar)	246	259-268	247
Temperature (°C)	92	82-88	94
Source rock	Carboniferous shale	Main Dolomite	Carboniferous shale
Seal	Upper Anhydrite	Basal Anhydrite	Upper Anhydrite

3.6 LMG oil and gasfields, onshore Poland

LMG consists of three oil and gasfields: Lubiatów, Międzychód and Grotów. These fields are situated about 75 km west of Poznań in western Poland, in the northern part of the Fore-Sudetic area (**Figure 8.45**). They occur within the Gorzów-Wielkopolski-Międzychód concession area. Following a 3D-seismic study, the fields were discovered by wells Grotów 1 and Lubiatów 1, both in 2003. The field descriptions are based on proprietary POGC data.

The Grotów oilfield has a very irregular shape characterised by monoclinal dip towards the north-west (**Figure 8.45**). In the southern part of the field, the Main Dolomite deposits are found at a depth of 3115 m adjacent to a zone with poor reservoir properties that separates the Grotów and Międzychód fields. Towards the north and north-east, the Main Dolomite reaches a depth of 3282 m. The thickest sequence (up to 41.8 m) is to the north-west of the Grotów 2 well near the platform edge; elsewhere,

The Zechstein Limestone reservoir can be subdivided into five units: (i) breccia; (ii) bioclastic grainstones with extraclasts, (iii) bioclastic grainstones and packstones with abundant anhydrite; (iv) bioclastic wackestones-grainstones with intraclastic breccia and carbonate crusts and (v) stromatolitic-pisolithic carbonates (**Figures 8.10** & **8.11b**). The persistence of the units suggests that the areas of reef development had similar depositional histories. The Zechstein Limestone in the reefs shows variable diagenetic alteration including dolomitisation and de-dolomitisation, multiphase carbonate (calcite and dolomite) and/or anhydrite cementation and anhydritisation (Jasionowski et al., 2000; Sylwestrzak, 2000; see Section 8). The good lateral correlation of anhydritised zones is evidence of their syndepositional origin. They may have formed in a sabkha environment during periods of sea-level fall that affected the marginal Zechstein Limestone carbonate platform. Alternatively, the anhydrite zones may record the brine-level stands that occurred during the punctual lowering of water level related to the lowstand at the end of Zechstein Limestone deposition. Due to extreme changes in permeability (0.1-3000 mD; range of all measured samples), there is a need for acidising the reservoir. Although there is no clear correlation between porosity and permeability, both parameters show similar trends and the decrease of poro-perm values is commonly related to anhydrite cementation and dolomitisation. The uppermost unit of the Zechstein Limestone usually shows decreased porosity and permeability (**Table 8.10**, **Figures 8.11a** & **c**).

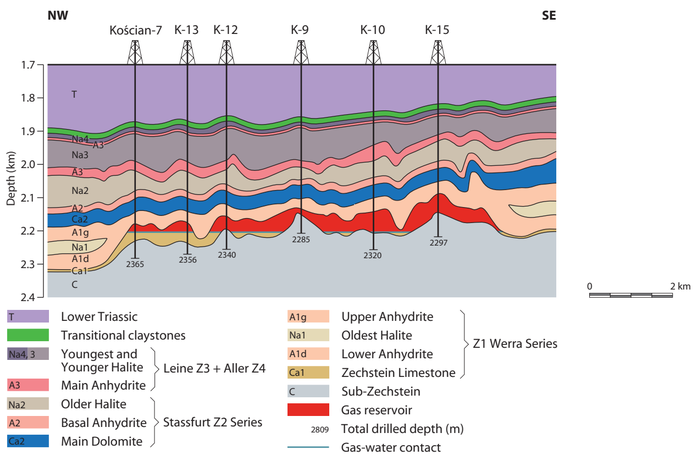

Figure 8.42 Cross-section through the Kościan field (after Dąbrowska-Żurawik in Dyjaczyński, 2000). See Figure 8.41 for location.

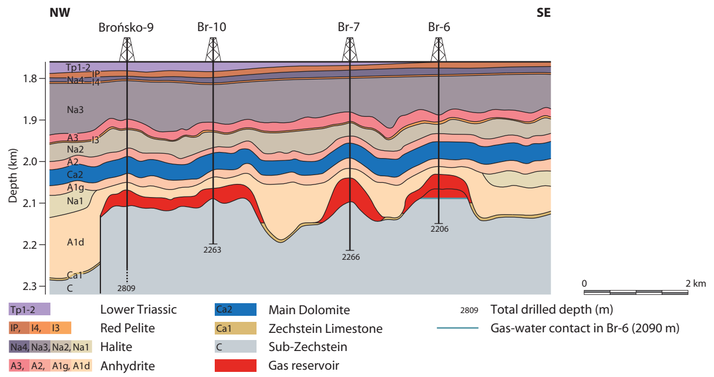

Figure 8.44 Cross-section through the Brońsko field (after Jakiel & Radecki, 2003, unpublished). See Figure 8.43 for location.

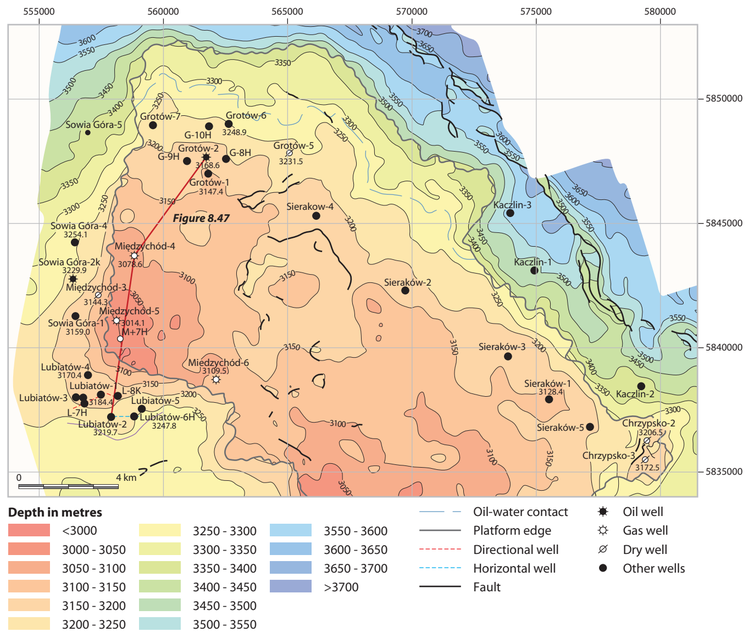

Figure 8.45 Depth-structure map to the top of the Main Dolomite in the LMG area (courtesy of POGC). See Figure 1.4 for locations of LMG fields.

it is characterised by a thickness of 25 to 30 m in the central part, decreasing to 10 to 15 m towards the field margin. The average effective thickness is 21.5 m. The Lubiatów oilfield also has a very irregular, elongated form, its axis trending west-north-west, and is characterised by monoclinal dip towards the south-west (**Figures 8.45** & **8.46**). In the northern part of the field, the Main Dolomite is found at a depth of 3150 m, and towards the south and south-west is at a depth of 3250 m. The thickest sequence (~80 m) is found towards the platform, north-east of wells Lubiatów 1 and 2, and elsewhere is typically 50 m thick in the central part, decreasing to between 10 and 15 m towards the basin and the field boundary. The average effective thickness is 32.4 m. As is clear from the description above, the reservoirs in the LMG field are stratigraphically trapped. In both fields, the seal consists of PZ2 (Stassfurt) evaporites: Basal Anhydrite (3.5-8.5 m in Grotów and 4-20 m in Lubiatów) and Older Halite (40-110 m in Grotów and >300 m in Lubiatów). The source rocks are microbial-algal deposits within the Main Dolomite strata of the region (**Table 8.11**), which constitute 15 to 44% of the total thickness at Grotów and more than 50% of the total thickness at Lubiatów. The original TOC content is calculated to be 1.0 to 5.0 wt.%. Conditions in the area are excellent for the preservation of organic matter and the development of reservoir rocks (Kotarba & Wagner, 2007).

The Grotów field is located within the Main Dolomite carbonate-platform facies. The sulphur content is 0.15% and oil contains 3.7 vol.% of paraffin. Saturated hydrocarbons constitute 94.4% and aromatic hydrocarbons 4.8%. The accompanying gas contains 48.6 vol.% of hydrocarbons. The Main Dolomite reservoir of the Lubiatów oilfield occurs within a transitional zone between the carbonate platform and the basin (**Figures 8.46** to **8.48**; Section 9). There are two concepts regarding the origin of the Main Dolomite in the field. The first assumes that it was a lowstand platform attached to the proper Main Dolomite platform (cf. Zdanowski, 2004) and the second assumes that the Lubiatów deposits are slope and toe-of-slope sediments (Jaworowski & Mikołajewski, 2007). The entire Main Dolomite of the Lubiatów oilfield is oil-saturated. The sulphur content is 0.11%. Saturated hydrocarbons constitute 93.8% and aromatic hydrocarbons 5%. The accompanying gas has a hydrocarbon volume of 54%.

Table 8.11 Properties of the LMG fields.

Reservoir	Grotów (Main Dolomite)	Lubiatów (Main Dolomite)
Lithology	Dolomite	Dolomite, minor limestone
Depth to top (m)	3115	3150
GWC/GOC.OWC (m)	3282	The entire Main Dolomite is oil-saturated
Maximum column height (m)	41.8	46.8
Net reservoir thickness (m)	21.5	32.4
Porosity (%)	10.3	17.4
Gas saturation (%)	89	90
Oil saturation	80	90
Permeability (mD)	0.25	9.97
Fluid type	Oil and gas	Oil
Gas composition	C1 33.7%, C2 6.6%, N_2 48.1%, CO_2 0.5%, H_2S 2.8%	C1 36.7%, C2 6.85%, N_2 37.5%, CO_2 0.6%, H_2S 7.85%
Oil gravity	0.804 (API 43.7)	0.811 (API 42.3)
Initial pressure (bar)	426	429.7
Temperature (°C)	126	127
Source rock	Main Dolomite	Main Dolomite
Seal	Basal Anhydrite and Older Halite	Basal Anhydrite and Older Halite

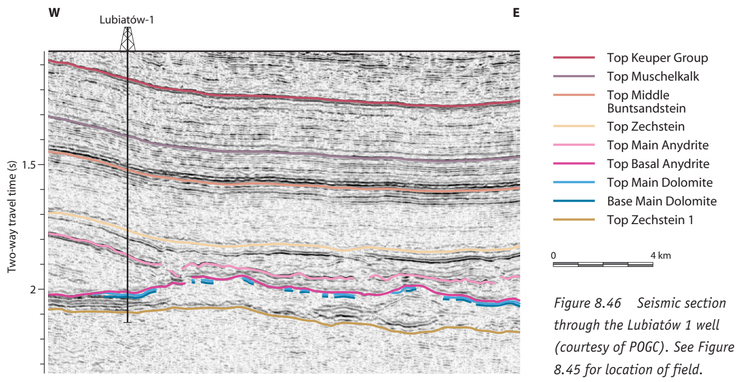

Figure 8.46 Seismic section through the Lubiatów 1 well (courtesy of POGC). See Figure 8.45 for location of field.

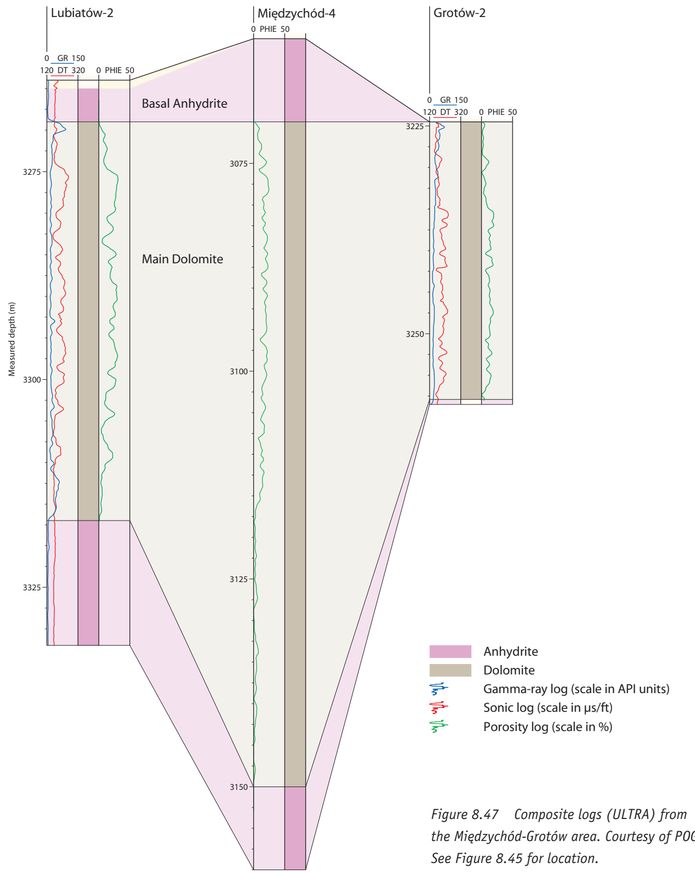

Figure 8.47 Composite logs (ULTRA) from the Międzychód-Grotów area. Courtesy of POGC. See Figure 8.45 for location.

4 Lithuania and Latvia – the easternmost part of the Southern Permian Basin (Valentinas Kadunas: Institute of Geology and Geography, Vilnius, and Paweł Raczyński: University of Wrocław)

The Zechstein deposits of Lithuania, Latvia and the Kaliningrad Region (Russian Federation) lie at the north-easternmost part of the Southern Permian Basin (**Figure 8.48**). During the Zechstein, this area formed the Baltic Gulf, which had a restricted connection with the main part of the basin due to elevation of the Mazury High. The Zechstein section is generally similar to that of Germany and Poland, although local variations are related to its basin-marginal position (**Figure 8.49**). The area is within the East European Platform, beyond the zone of Variscan deformation. The Zechstein deposits usually overlie Silurian, Devonian and Lower Carboniferous sedimentary rocks, with Lower Permian deposits of the Perloja Series found only along the Polish border. Siliciclastic deposits equivalent to the Border Conglomerate/Weissliegend are known from several boreholes. The Zechstein section is clearly condensed, with evaporite horizons commonly thin or absent, although some carbonate units are thicker than those in more basinward locations.

The Z1 Kupferschiefer equivalent (Sasnava Series) is usually 0.4 to 1.7 m thick (maximum 15 m) and is found only in the central part of the Baltic Bay where it consists of calcareous, sandy and bituminous shales. There are local increases in metal concentrations (mainly of copper, lead and zinc), but these are not economically important. The Zechstein Limestone deposits are included in the Naujoji Akmené Series, which has three main facies: basinal, reefal and shelf. The thickest (exceeding 80 m) sediments are found where the reef facies forms a narrow belt rimming the shelf. The reefs are built largely by bryozoans accompanied by a rich assemblage of brachiopods and bivalves. The shelf deposits are the most widespread facies and are a sequence of up to 30 m-thick limestones, dolomitic limestones and marly limestones with common tempestite layers. Due to their very shallow depositional depth, the sediments were sensitive to

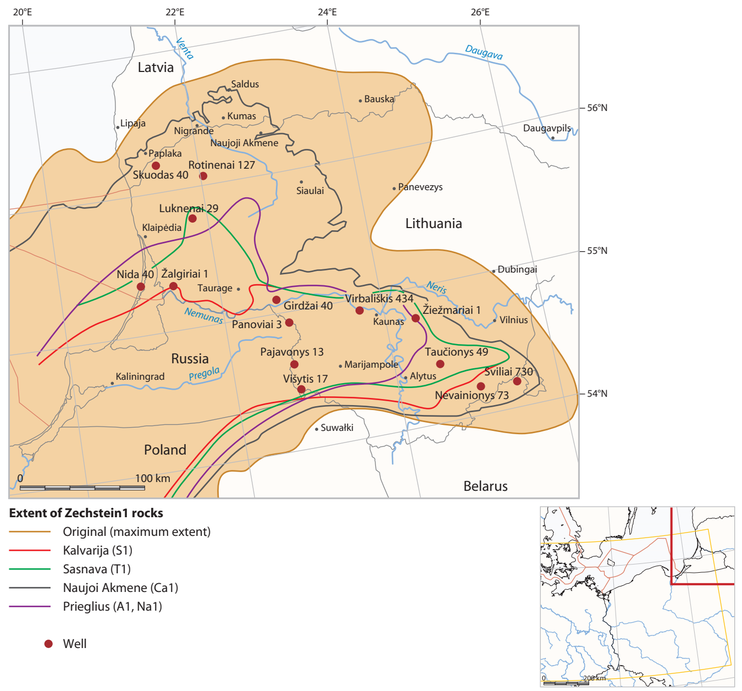

Figure 8.48 The distribution of Upper Permian (Zechstein Z1) formations in the eastern part of the Southern Permian Basin (after Kadunas, 2001).

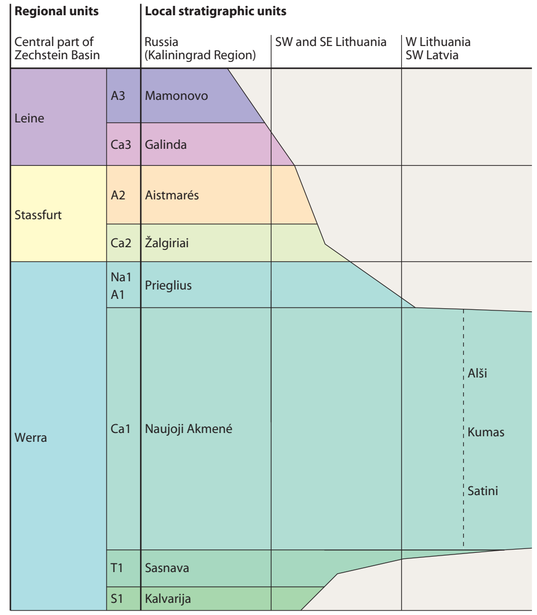

Figure 8.49 Stratigraphic correlation of the Permian sediments in Latvia, Lithuania, Russia and the central part of the Southern Permian Basin.

minor fluctuations in sea level during deposition. The Werra evaporites are included in the Prieglius Series. These are mostly gypsum, anhydrite and local halites with thicknesses exceeding 250 m. The equivalent of the Z2 Stassfurt cyclothem consists of two series; the Žalgiriai (carbonate) and Aistmarés (sulphate) series. The dolomites and limestones of the Zalgiriai Series are usually 5 to 7 m thick (maximum 26 m; Kadunas, 2001). Detailed correlation in north-east Poland (Gąsiewicz & Peryt, 1989a) indicated that most carbonates in north-east Poland, Lithuania and Russia, which were previously included in the Main Dolomite, should be assigned to the Platy Dolomite; this scheme is followed in this chapter. Anhydrites dominate the Aistmares Series (15-20 m thick), but become clay-rich at the margins. Clay-rich halite has also been found in several boreholes.

Limestones and dolomites of the Galinda Series (4-7 m thick) are equivalent to the Z3 Leine cyclothem (Kadunus, 2001). These are overlain in a restricted area by up to 25-m thick anhydritic-clayey deposits of the Sventapilis (Mamonovo) Series. The Zechstein is overlain by Triassic claystones or, where eroded, by Jurassic mudstones, sandstones or claystones. Along the Lithuanian-Latvian border, Zechstein Limestone deposits are overlain by Pleistocene glacial sediments. Karst phenomena developed locally; the sinkholes are mostly filled by Cenozoic deposits, although Jurassic megaspores have also been found, possibly indicating polygenic karst phenomena in the area. The economic importance of the Zechstein deposits is mostly related to limestones, which have been exploited since the 17th century from outcrops along the Lithuanian-Latvian border; the limestones are now used in the cement industry. Projects aimed at exploiting the rock-salt in south-west Lithuania are in the initial phase of development.

5 North-Sudetic Basin: nearshore carbonate and siliciclastic deposits (Paweł Raczyński: University of Wrocław)

The North-Sudetic Basin (**Figure 8.50**) is located at the southern, nearshore edge of the Zechstein Basin. It is a complex tectonic structure that formed after the Cretaceous. Zechstein deposits within the basin overlie conglomerates and sandstones of the upper Rotliegend, which mostly consist of fluvial and fan deposits. Aeolian sediments are found only in the northern part of the trough. Marine fossils (bivalves and brachiopods) are found locally in the uppermost siliciclastic deposits (**Figures 8.51** & **8.52**).

The Zechstein section is condensed and formed mainly by deposits of the PZ1 and PZ3 cyclothems (**Table 8.12**). Most evaporite units are absent (**Figure 8.53**) as are the Kupferschiefer deposits (**Figure 8.54**). Instead, in the lowest part of the PZ1 cyclothem, the Zechstein Limestone passes downward into facies

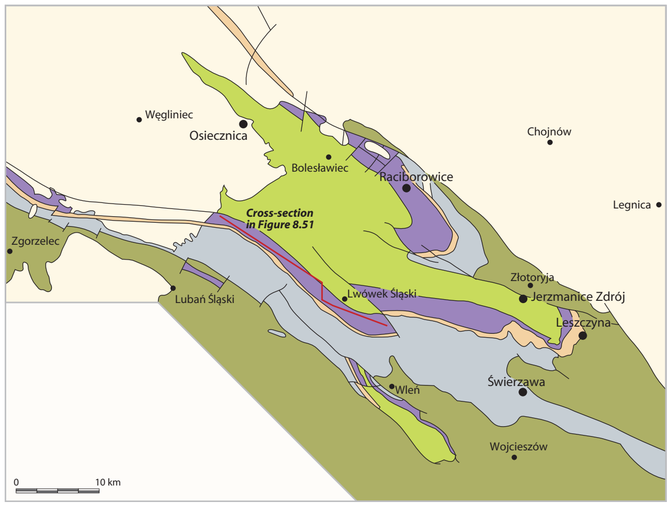

Figure 8.50 Geology of the North-Sudetic Basin.

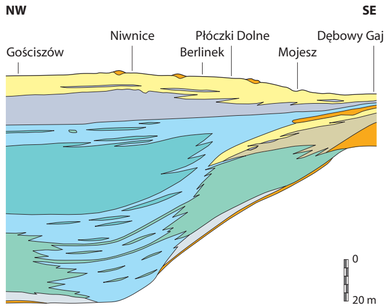

Figure 8.51 The carbonate-siliciclastic Zechstein succession with anhydrite (A1g) in the southern part of the North-Sudetic Basin. See Figure 8.50 for location.

similar to those that characterise the shallow-water sediments of the Kupferschiefer in the Fore-Sudetic area. These rocks often contain the remains of continental flora in addition to marine bivalves, inarticulate brachiopods and *Lingula*. Towards the south-east, the Zechstein Limestone passes into sandy deposits with marine fossils. The copper mineralisation in the lower part of the Zechstein Limestone is not found in most nearshore parts of the basin. In the major part of the trough, the copper-bearing unit is underlain by Rote Fäule deposits.

The Zechstein Limestone is usually 20 to 40 m thick. Tempestite deposits form a major part of the succession, which represents the nearshore part of the carbonate platform. The tempestites in the lower part are distal (**Figures 8.55** & **8.56**), whereas those higher in the succession are proximal (**Figure 8.57**). There are also lagoonal and ooidal barrier deposits, especially in the upper part of the Zechstein Limestone. The rich fossil assemblage (**Figure 8.58**) includes more than 120 species representing all major groups and indicates a predominantly marine depositional environment. Due to the shallow-water sedimentary environment, relative sea-level fluctuations are very clearly recognised. In a generally transgressive facies sequence, it is possible to distinguish at least three cycles that are separated by subaerial erosion surfaces at the basin margins (Śliwiński, 1988).

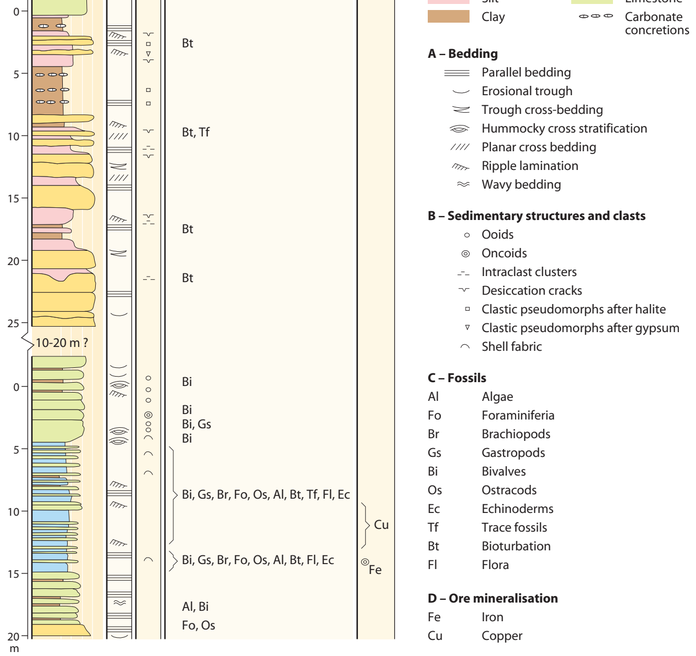

Figure 8.52 Simplified profile of the Zechstein rocks in the eastern part of the North Sudetic Basin.

Table 8.12 Stratigraphic subdivision of the Upper Permian in the North Sudetic Basin.

	Scupin (1931)	Peryt (1978a)		Raczyński (1996)		
Zo3	Oberer Zechsteinsandstein	Buntsandstein		Sandy-muddy-clayey series	Upper Zechstein	PZt
Zo2	Plattendolomit mit *Schizodus rotundatus*	Platy Dolomite Ca3	Leine Z3	Platy Dolomite Septarian shales		PZ3
Zo1	Unterer Zechsteinsandstein	Detrital Series	Werra Z1	Upper Zechstein (lower) sandstones		PZ1
Zm	Dolomitische Kalke mit Letten	Zechstein Limestone Ca1		Middle Zechstein limestones and shales	Middle Zechstein	Ca1
Zu	Gervillienschichten			Lead-bearing marls	Lower Zechstein	
	Kupfermergel			Copper-bearing marls		
	Zweischalermergel			Patchy Marls		
	Basalkalke	Basal Limestone		Basal Limestone		
	Zechsteinkonglomerat		Rotliegend	Basal Conglomerate		S1
	Rotliegendes			Rotliegend		

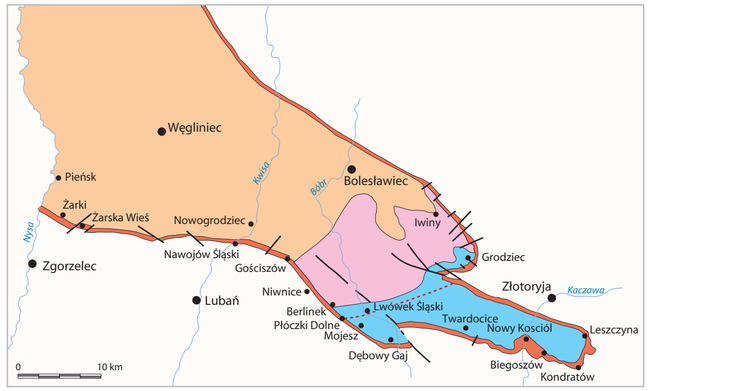

Figure 8.53 Siliciclastic and anhydrite facies in the upper Werra (Z1) succession in the North-Sudetic Basin.

The Zechstein Limestone passes upwards into sandy and clayey deposits. In the north-western part of the trough, these are accompanied by anhydrites of the Upper Anhydrite (**Figure 8.53**). Their equivalents in the south-east of the trough are sandy-clayey deposits with beds of sandy casts after halite and gypsum crystals (**Figures 8.58** & **8.59**). Tracks of terrestrial tetrapods are also preserved in these horizons (**Figure 8.60**).

The PZ1 deposits are overlain by the Platy Dolomite (Ca3); there is no clear evidence of erosion prior to their deposition (Peryt, 1978a). The sediments are a sequence of nearshore carbonate-platform, mostly lagoonal and barrier deposits, with fossils that indicate restricted ecological conditions. The abundant accumulations of calcareous algae, bivalves and gastropod remains are not taxonomically diversified.

The Platy Dolomite is overlain by heterolithic deposits of the Permian to Triassic transitional series (**Figure 8.61**). In the absence of clear criteria, it is difficult to place the Zechstein-Buntsandstein boundary. The absence of higher Zechstein units suggests that it may be diachronous in the North-Sudetic Basin unequivocally.

6 Zechstein reefs in Germany (Josef Paul: University of Goettingen, retired)

Carbonate buildups are described from the Zechstein 1 Werra cycle in England (Smith, 1981a, 1981b; Tucker & Hollingworth, 1986; Hollingworth & Tucker, 1987; Hollingworth & Pettigrew, 1988), the Netherlands (Geluk, 2005), Denmark (Stemmerik & Frykman, 1989), Germany and Poland (Peryt, 1978b; Dyjaczynski et al.,

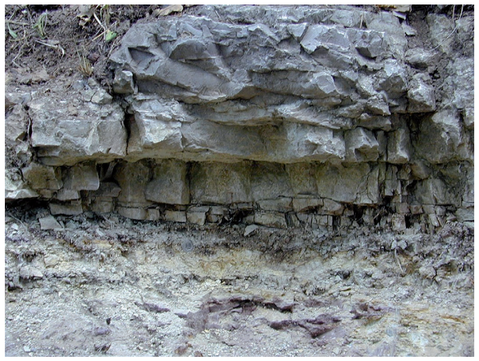

Figure 8.54 The lower boundary of the Zechstein Limestone. The outcrop height is 0.3 m.

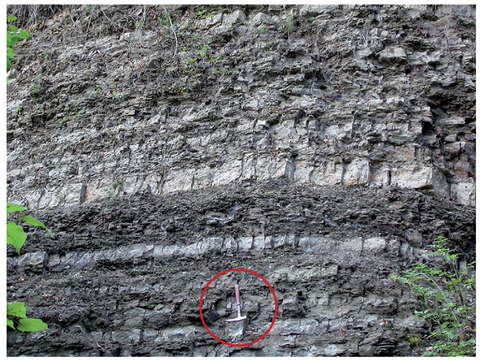

Figure 8.55 Distal tempestites in the lower part of the Zechstein Limestone.

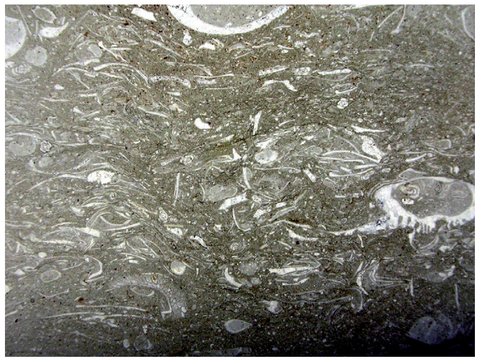

Figure 8.56 Bioclastic packstone, distal tempestite in the Zechstein Limestone. Sample length 2.5 cm.

Figure 8.57 Hummocky cross-stratified beds of the Zechstein Limestone.

Figure 8.58 Shell of bivalve Aviculopinna prisca *(Geinitz) preserved in growth position.*

Figure 8.59 Sandstone casts after halite crystals. Sample length, 12 cm.

2001). In Germany, the reefs are exposed or have been penetrated by boreholes in the Harz Mountains (Herrmann, 1957; Paul, 1980), Thüringia (Brauch, 1923; Mägdefrau, 1937; Kerkmann, 1969; Paul, 1995; Paul & Huckriede, 2004), the Emsland (Füchtbauer, 1980), Hesse (Becker, 2002), and the Baltic Sea areas (Zagora & Zagora, 1997). Metazoan reef-builders are absent in the Zechstein reefs. However, these buildups meet all definitions of reefs in that they were formed by depositional and biological processes, they built significant topographic highs, were wave resistant, and influenced adjacent areas. The diversity of the fauna was higher than in the surrounding area and facies belts were zoned. Micro-organisms were the frame-builders of the reefs. They all flourished during the Werra cycle.

6.1 Pre-requisites of reef growth

Reefs grew at the margins of the Zechstein Basin, but also on intrabasinal highs. In general, they developed preferentially on elevations of the inherited pre-Zechstein relief, such as cliffs of Devonian or Carboniferous greywackes or Rotliegend volcanoes. The pre-conditions for the growth of substantial Zechstein reefs are: a slightly subsiding sea floor, medium to high wave or current activities, and normal marine to hypersaline waters. Reefs are absent in deep water and at the mouth of larger permanent or ephemeral rivers, because the growth of microbial mats is inhibited by deposition of mud.

6.2 Reef types

The good exposure of the reefs in eastern Thüringia has helped to interpret the various reef-types (**Figures 8.62** & **8.63**). In this area, the overlying sulphates were dissolved only during the Pleistocene, leaving the outlines of reef-carbonates largely unaffected by erosion and with a shape closely corresponding to their internal structure. There are fringing or barrier reefs, patch-reefs and isolated pinnacle reefs at an increasing distance from the coast (**Figure 8.63**). The barrier reefs ran parallel to the coast or they lined passages; partly atoll-like patch-reefs were about 10 to 20 m thick near the coast and up to 120 m high in deeper waters. Isolated pinnacle reefs formed on elevations away from the coast and were relatively high compared to their width. Patch-reefs may have coalesced to cover an area of up to one km^2 (**Figure 8.64**). Fringing reefs reached lengths up to 5 km. Towards the sea, there was a steep fore-reef slope with an angle of 35° to nearly vertical (**Figure 8.65**); the strata dip radially from the reef-centre (Paul, 1980). Reef-derived carbonate sand can be traced up to a kilometre seaward of the reef belt. A narrow reef-crest is linked with the surprisingly smooth reef-flat consisting mainly of laminated microbial mats. In the field, the reefs resemble table mountains. The less spectacular back-reefs often contain thin clayey or marly layers that are intercalated with the reef carbonates.

6.3 Bathymetry

The well-preserved reefs of eastern Thüringia were not affected by later tectonic displacements (**Figure 8.66**). The present dips of reef-flats (~3° on patch-reefs, fringing and pinnacle reefs) form a plain dipping very gently towards the basin centre. These dips can be rotated back using the extensive reef-flats as the zero-line for the former sea level, which shows that the reefs grew on a slightly inclined sea floor dipping at about 1° towards the centre of the Thüringian Basin. As the reef-flats are controlled by sea level, it is possible to calculate the exact water depth of the reef area at the time that reef growth ended (**Figure 8.67**). Water depths vary between 20 m nearshore and 70 m at the seaward reefs. The shoreline can be reconstructed by extrapolation of sea level and the pre-Zechstein surface up to the point that they converge. The reefs formed about 1 to 2 km from the coast. By extrapolation, it is also possible to calculate the water depth near the centre of the Thüringian Basin. On the basis that the dip of the strata is approximately the same, a water depth of about 200 m may have been reached.

6.4 Reef-builders and reef-organisms

The reefs are built by micro-organisms, most likely cyanobacteria, which form mats or stromatolitic crusts at the sediment surface. Laminar or concentric crusts are the most typical features of the reefs. The thickness of single laminae may vary between 50 and 500 µm. Pervasive dolomitisation has destroyed all microscopic tissue such that no direct evidence of the microbial origin has been preserved. However, they are thought to be phototrophic organisms, as suggested by the growth pattern of uneven or inclined surfaces (Paul, 1980). The sides and roofs of synsedimentary reef caves are also draped with mats that may have been produced by chemotrophic organisms.

The large number of fossils found in the region has attracted geologists ever since the early days of geology (King, 1848; Geinitz, 1861; Rübenstrunk, 1913; Mägdefrau, 1937; Kerkmann, 1969; Pattison et al., 1973; Hollingworth & Pettigrew, 1988; Ernst, 2001). Bryozoans, brachiopods, bivalves, gastropods, cephalopods, echinoderms, ostracods, encrusting foraminifera and calcareous algae are all described from various reef localities. Bryozoans are the most common species, such that Zechstein reefs are sometimes designated as bryozoan reefs. The frequency and diversity of the reefal fauna are high in comparison with off-reef communities. The distribution of fossils is irregular; in places they are clustered. Biodiversity is highest at the reef-crest, followed by upper fore-reef slopes, whereas there is a restricted number of species in back-reefs. The outer, isolated pinnacle reefs have a higher biodiversity than reefs near the shoreline. Different species are loosely associated with the various reef environments, for example fenestellids prefer the reef-crest and upper fore-reef slope environment, whereas branching bryozoans such as *Acanthocladia* are distributed over the entire reef. However, stratigraphic level is a more important factor in their distribution (see section on reef evolution). Detailed information about the reef fauna is given by Kerkmann (1969) and Hollingworth & Pettigrew (1988).

6.5 Facies

The extensive reef-flat at, or just below, sea level consists of horizontal, roughly bedded packstones to wackestones and bindstones composed of laminar encrustations with a limited number of gastropods and bivalves. Thrombolites, laminar mats and oncoids are common components that are produced by microbes. A distinct reef-crest separates the flat from the fore-reef front. The reef-crest is composed of packstones to floatstones with fossils that are often found *in situ*; biodiversity is highest on the crests. The amount of detritus is higher at the upper fore-reef front, with typical allochthonous unrounded and unsorted blocks of variable size; the largest blocks are some metres in diameter. Grain sizes generally vary from a few millimetres up to 20 cm. On vertical slopes, the fans of *Fenestella* are positioned nearly parallel to bedding planes. The lower fore-slope and talus apron consist of grainstones with grain sizes of about

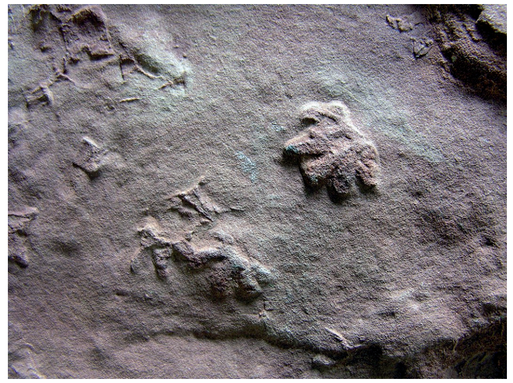

Figure 8.60 Tracks of terrestrial tetrapods. Sample length is 10 cm.

Figure 8.61 Heterolithic Permian-Triassic transitional series.

0.2 to 0.5 mm. These well-sorted reef sands border the reefs, forming spits at lee sides, and are found up to one kilometre away from producing reefs. The grain size of sediments from inter-reef areas depends on their distance from the reefs and the topography. Some passages perpendicular to the shore are lined with reefs (**Figure 8.63**). These passages acted as current channels and transported large siliciclastic gravels (-2 cm ∅) from the land to the sea. They are incorporated into the reef carbonates.

Stromatolitic crusts show a wealth of growth forms, which can be attributed to different levels of energy: plane mats grew in quiet water, columnar stromatolites in intermediate, and domal stromatolites in high-energy environments. Oncoids and thrombolites formed at the reef-flat. Generally, the northern front of the reefs is always the high-energy side as storms and trade winds came from a northerly direction (Paul, 1980). Peryt (1986b, 1986c) emphasised the importance of early cementation for the rigidity and wave resistance of the reefs. Füchtbauer (1980) estimated the gross composition of the Schale reef in the Emsland area to be 45% stromatolites, 10% bryozoans, 5% other fossils, 25% matrix and 15% cement.

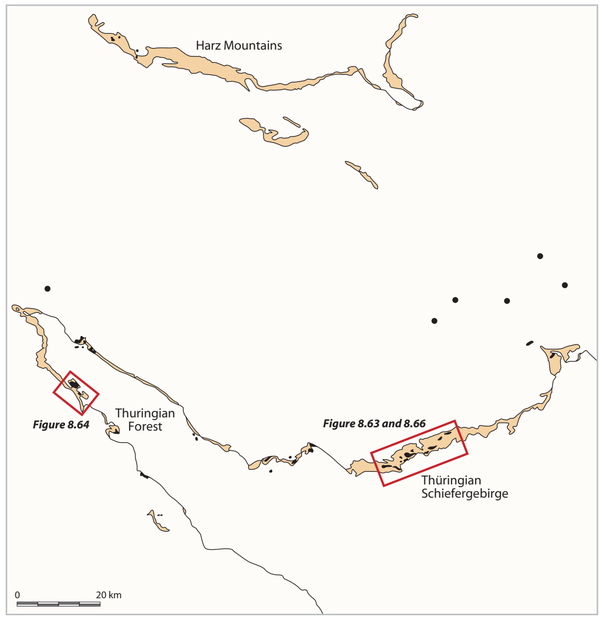

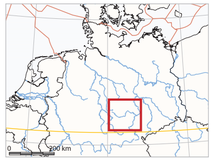

Figure 8.62 Zechstein outcrops in central Germany and exposed or drilled reefs.

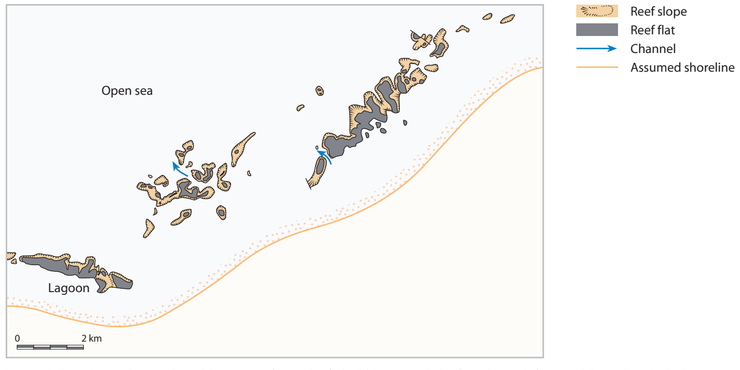

Figure 8.63 Pinnacle, patch and barrier reefs north of the Thüringian Schiefergebirge (after Paul & Huckriede, 2004). See Figure 8.62 for location.

6.6 Reef evolution

Reefal growth started at the second cycle of the Zechstein Limestone, both in England, where there are two cycles, and in Germany, where there are three. The base of the reefs consists of wackestones and floatstones composed of crinoids, bryozoans, brachiopods, bivalves and coated grains (**Figure 8.68**). A second unit is built of bindstones formed by irregularly layered microbial mats. Crinoids disappear with the onset of the bindstones. Towards the top, bryozoans, brachiopods and other fauna progressively decline and finally become absent one after the other. At the top, only microbial communities such as stromatolitic crusts or oncoids have survived. These reductions in biodiversity may have been due to increasing salinity. A sharp sea-level fall led to subaerial exposure and formation of cavities by dissolution or sabkha conditions (Füchtbauer, 1980). The extensive reef-flats appear at a late stage of reef evolution. Both aggradation and progradation of the reefs can be observed in most cases (**Figure 8.64**).

A renewed transgression of more-or-less normal marine sea water enabled a second phase of reef growth. The second generation formed on top of the former reef-flat, but did not reach the dimensions of the first reef phase. In the UK and Germany, there are only reef knolls or small patch-reefs. The new transgression brought back normal marine fauna such as bryozoans and brachiopods. In Thüringia, this reef-phase is only a few metres thick in contrast to the 100 m of the first generation, whereas in Emsland the second phase is about 25 m thick. In England, there is more or less the same pattern of reef evolution. Smith (1980) assumed that the last phase (the recovery of the reefs) should be time-equivalent with the precipitation of the Z1 Anhydrite, although the faunal record does not support this assumption.

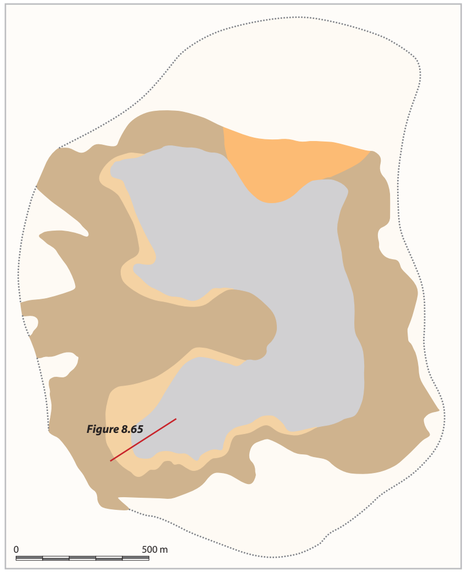

Figure 8.64 Facies zonation of the Altenstein reef, west of the Thüringian Forest (after Pretzer & Stadler, 1994). See Figure 8.62 for location.

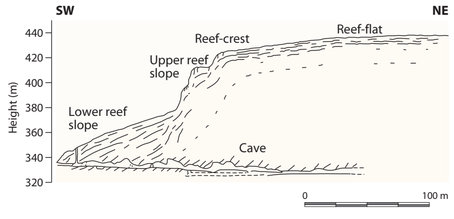

Figure 8.65 Schematic section showing progradation and aggradation of the Altenstein reef, west of the Thüringian Forest (after Pretzer & Stadler, 1994). See Figure 8.64 for location.

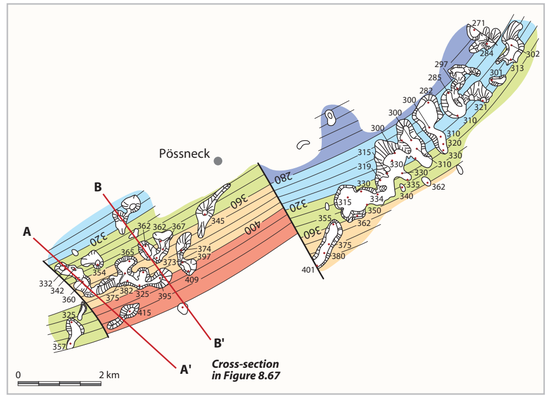

Figure 8.66 Position of reef-flats in eastern Thüringia (height above recent sea level).

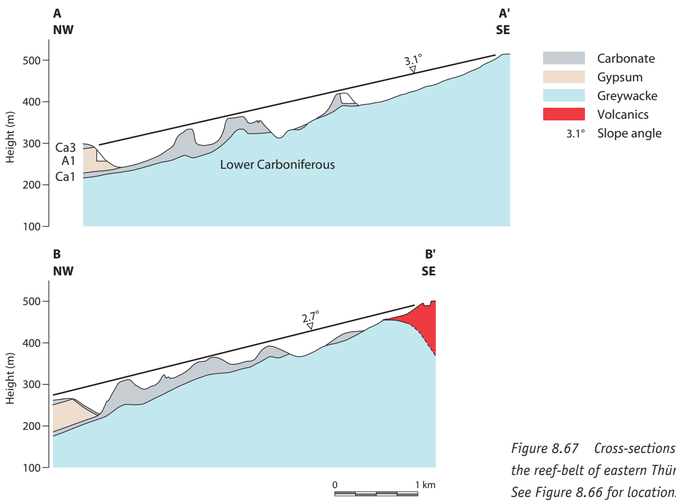

Figure 8.67 Cross-sections through the reef-belt of eastern Thüringia. See Figure 8.66 for locations.

6.7 Duration of reef growth and productivity

The duration of the seven Zechstein cycles is estimated to be less than 3 Ma; the first cycle may have been the longest. It is assumed that the small-scale cycles mentioned above are Milankovich Cycles of 100 ka. On the basis of this assumption, reef growth would have lasted less than 200 ka.

Productive areas of the reefs are restricted mainly to the reef-flat and reef-crest. Calculations of the amount of produced carbonates and the productive area indicate a growth rate of some millimetres per year, a rate comparable with modern coral reefs.

6.8 Diagenesis

The reefs consist of dolomite towards the back-reef, whereas they are mainly composed of calcite on the seaward side. This distribution points to early dolomitisation caused by reflux of brines from sabkhas and salinas and descending brines released by the dewatering of the overlying gypsum deposits. The dolomite has a stoichiometric composition. These brines also led to anhydritisation, which reduced the original porosity. Total or partial recalcitisation may have taken place during burial or even later by dissolution of sulphates (Clark, 1980b; Peryt, 1987b). Corresponding to this general distribution, reef-cores, back-reefs and reefs near the coast consist mainly of dolomite, whereas fore-reef-slopes and isolated seaward pinnacle reefs are calcitised. Füchtbauer (1980) measured the porosities of calcite sections at the Schale reef to be 2 to 5% whereas dolomites have porosities of 4 to 12%.

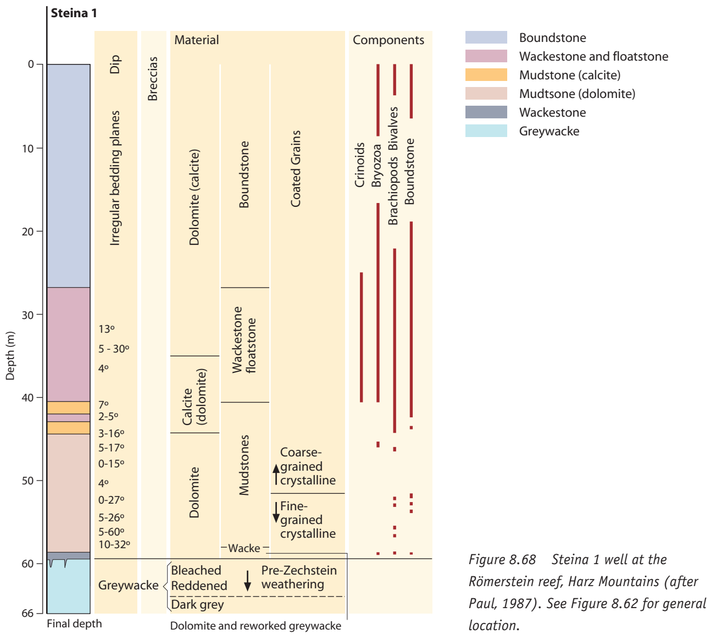

Figure 8.68 Steina 1 well at the Römerstein reef, Harz Mountains (after Paul, 1987). See Figure 8.62 for general location.

7 Platy Dolomite (Ca3) carbonate platform in northern Poland

(Andrzej Gąsiewicz: PGI)

During deposition of the third Zechstein cycle, the basin periphery was formed by numerous carbonate platforms (Kiersnowski et al., 1995). In the area of present-day northern Poland, where the Platy Dolomite developed (**Figure 8.72**), the carbonate platform was attached to the land and rimmed by an arched and narrow oolitic barrier (Gąsiewicz, 1990). The whole carbonate sequence was deposited on the almost flat surface of the second Zechstein evaporite cycle, but in more basinward locations it is separated from the previous cycle by the siliciclastics and sulphates of the Grey Pelite (T3) (Czapowski et al., 1991). To the north, the Platy Dolomite is unconformably overlain by the Triassic Buntsandstein Group; however, basinward it is in sedimentary continuity with the overlying sulphates of the Main Anhydrite (A3) (Gąsiewicz & Peryt, 1994).

The Platy Dolomite rocks are mainly dolomites, limestones and anhydrites. The most common carbonate mineralogy is microcrystalline to finely crystalline replacive and fabric-preserved dolomite crystals (up to 20 µm in size). The dolomites have $\delta^{18}O$ values from 7.4 to –4.6‰ and $\delta^{13}C$ from 6.4 to –6.7‰ indicating that the dolomitisation mechanism was early diagenetic evaporative reflux (Peryt & Scholle, 1996). Local de-dolomitisation has affected the sequence, especially in the lower part of the Platy Dolomite sequence (Gąsiewicz, 1986). The sulphate content varies up to 30% of the rock volume in places. Other minerals include common halite crystals and trace amounts of amorphous organic matter (up to 0.2% TOC). Macrofossil material is common, but of low diversity except in the lower part of the sequence. The most common fossils are bivalves, foraminifera, and ostracods; gastropods, brachiopods, bryozoans and algae are rare. Sedimentary structures within the carbonate-platform deposits indicate that the sequence originated in a variety of peritidal environments and a predominantly arid climate, with a tendency towards increased dryness and periodic small-scale freshwater influxes. The most characteristic structures are common fenestrae, sulphate granules and nodules (often arranged in distinct horizons), local truncation surfaces, contorted layers and tuft laminae, whereas mud cracks, palisade structures, graded bedding, vadolites, intraclasts and cross-bedding are rarely seen.

The depositional sequence is characterised by various shallow-water carbonate microfacies (Gąsiewicz & Peryt, 1989b; Gąsiewicz, 1990). They are: (1) thin bioclastic wackestones, packstones, and rudstones, all more common shoreward; (2) thicker grained peloidal wackestones and packstones; (3) relatively thick oolitic wackestones, packstones, and grainstones, which developed more seaward and built up a carbonate sandy barrier; (4) microbialites (*sensu* Burne & Moore, 1987), which include biolaminoids, stromatolite-like forms or stromatolitoids and stratiform stromatolites, and (5) mudstones. The main depositional units of the Platy Dolomite series are differently laminated rocks classified as microbialites (Gąsiewicz et al., 1987; Brehm et al., 2002). The microbialites built most of the carbonate platform (**Figure 8.69**) and are intercalated shoreward and basinward (**Figure 8.70**) with common non-microbialite facies. The most characteristic subfacies are generally poorly laminated biolaminoids (*sensu* Gerdes & Krumbein, 1987) (**Figure 8.71**), which are up to 30 m thick locally. The other microbialites form rather thin, flat and discontinuous layers (up to about 1-2 m thick). The distinct flat stromatolites are most prominent, especially where they are well developed at the beginning and end of the Platy Dolomite succession (Gąsiewicz et al., 1987). Beyond the carbonate-platform area, the Platy Dolomite deposits are much thinner (up to 5-8 m thick) and here they developed as dark-coloured, muddy or clayey carbonates with numerous bioclasts typical of a deeper basin.

The unit thickness varies substantially and increases basinward, reaching up to 43 m in the carbonate-platform margin zone (**Figure 8.72**). It is possible to distinguish several palaeogeographical zones in the platform area. However, the two predominant zones are a proximal sabkha environment coupled with a carbonate tidal flat (with ponds and tidal channels), and a distal environment that developed as a narrow, mobile barrier system. The barrier belt of predominantly ooidal sands was separated from the rest of the basin by a small lagoon. Carbonate sabkha-type sediments passed seaward into variably biolaminated intertidal-flat deposits then into lagoonal complexes with a sulphate admixture. The shallow-water lagoon separated a coastal sabkha and tidal-flat domain from the carbonate-platform margin system represented by ooidal sands (Gąsiewicz, 1990). The sabkha and tidal-flat deposits are a monotonous succession of various microbialite subfacies that have filamentous (**Figure 8.73**) and coccoid (**Figure 8.74**) microfossils, which are interpreted as the remains of cyanobacteria (Maliński et al., 2009). The microbialites formed (Gąsiewicz et al., 1987) under restricted microenvironments on the sabkha plain, usually in various peritidal settings (from uppermost subtidal to supratidal), with subaerial exposure and accretion protected by a barrier system (**Figure 8.72**). The sandy belt is in the upper Platy Dolomite sequence and represents an area of shoals with limited tidal flats indicated by interfingering of microbialite and carbonate sandsheets (**Figure 8.70**). Together these formed a barrier system developed in the subtidal to supratidal zone and differentiated into numerous small sub-environments. The barrier system records high-energy conditions with intervals of calmer sedimentary regimes reflected mainly by microbialite intercalations. There are up to four or five upward-thinning oolite-microbialite cycles in this platform zone (Gąsiewicz, 1985).

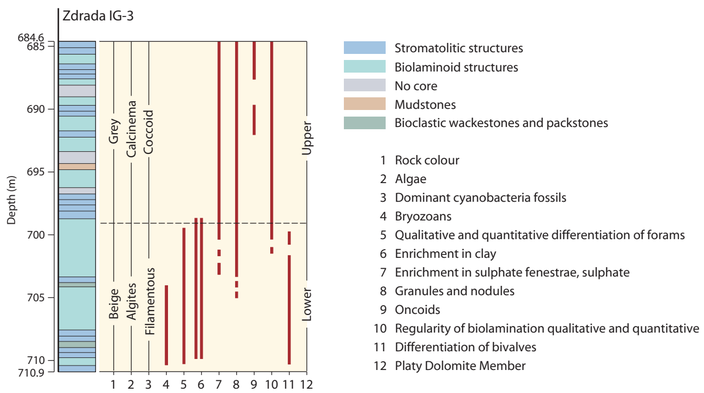

Figure 8.69 Facies composition of the Platy Dolomite inner platform zone in the Zdrada IG-3 well. See Figure 8.72 for location.

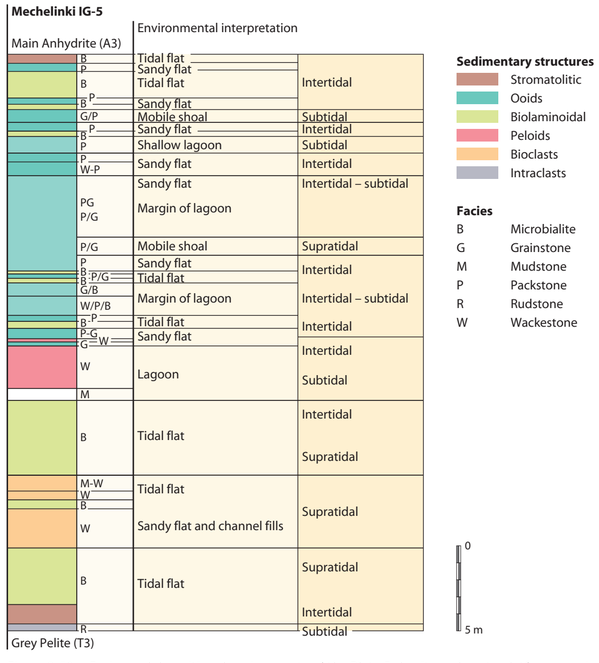

Figure 8.70 Facies and depositional environments of the Platy Dolomite carbonate platform margin in the Mechelinki IG-5 well. See Figure 8.72 for location.

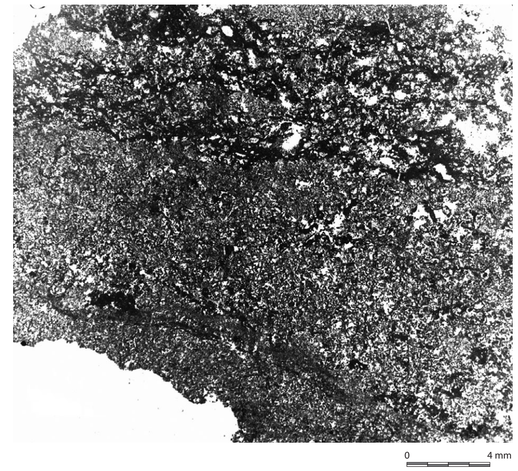

Figure 8.71 Thin section showing biolaminoid with poorly developed organic laminations (dark) and frequent fenestrae. Swarzewo IG-7 well.

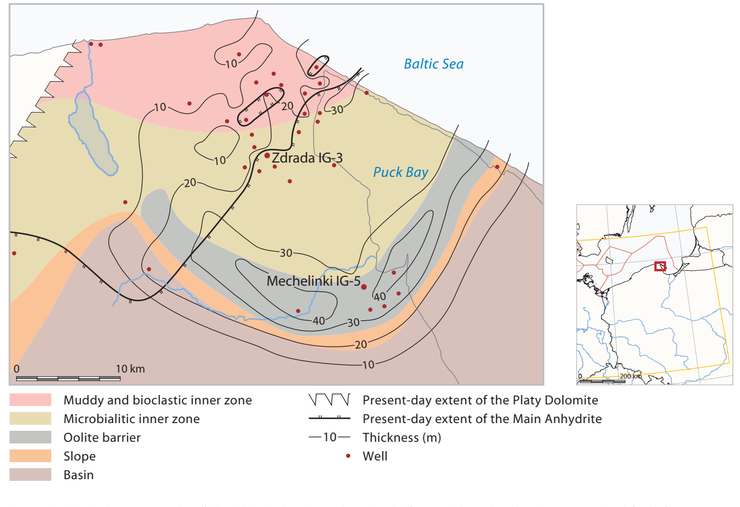

Figure 8.72 Palaeogeography of the Platy Dolomite carbonate platform in the Łeba Elevation area (modified after Gąsiewicz & Peryt, 1989b).

Macro- and microscopic studies allow the Platy Dolomite section to be subdivided into lower and upper parts (**Figure 8.69**). The lower part is more diverse in microfacies composition, fauna and flora and also has higher carbonate-mud contents and bioclastic intercalations. The upper part is more monotonous with a strongly impoverished low-diversity faunal content and has numerous stromatolite intercalations and evaporite structures; the sequence thickens basinward (with a maximum at the barrier belt). In the carbonate-platform margin area, the upper part of the Platy Dolomite is distinctly marked by the development of carbonate-sand complexes. This bipartition is related to a regional change in the sedimentary regime, from a carbonate ramp gently inclined seaward that developed during the early interval of Platy Dolomite deposition, to a rimmed-carbonate platform developed during deposition of the upper Platy Dolomite (Gąsiewicz, 1990).

There are no oil or gas accumulations in the Platy Dolomite sequence of the Łeba Elevation. The inner platform deposits have very low porosities due to intensive cementation processes. There is limited secondary porosity in the carbonate-sand bodies of the platform margin as a result of local meteoric-water activity.

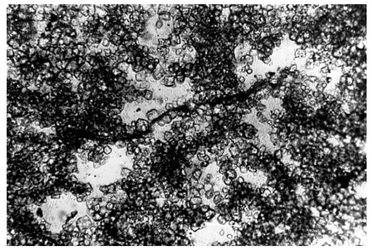

Figure 8.73 Thin section showing biolaminoid with preserved microfossil in fenestral carbonate lamina interpreted as the remains of filamentous cyanobacteria encrusted by fine-grained dolomite crystals. Puck IG-2 well.

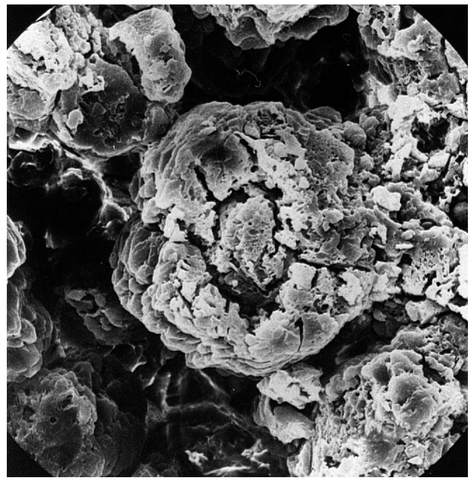

Figure 8.74 Scanning electron micrograph (SEM) of biolaminoid with fine-scale microfossils interpreted as the remains of coccoid cyanobacteria. Władysławowo IG-2 well.

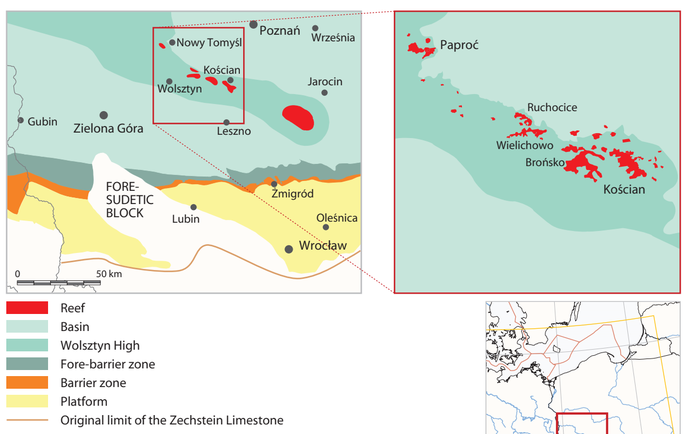

Figure 8.75 Palaeogeography during deposition of the Zechstein Limestone (Ca1) in SW Poland and locations of the Zechstein Limestone reefs within the Wolsztyn High area (after Dyjaczynski et al., 2001).

8 Diagenesis of the Zechstein Limestone (Ca1) carbonates on the Wolsztyn High (south-west Poland) (Marek Jasionowski: PGI)

Permian marine sedimentation on the Wolsztyn High (**Figure 8.75**) started with shallow-water carbonates of the Zechstein Limestone (Ca1). These carbonates are up to 90.5 m thick and formed isolated carbonate platforms several kilometres across (sometimes called 'isolated reefs'). Today they are buried at depths of 2000 to 2500 m and are overlain by evaporites of the Lower and/or Upper Anhydrite (a few tens of metres thick) followed by other Zechstein strata and subsequently by Mesozoic and Cenozoic deposits (Dyjaczynski et al., 2001).

The Zechstein Limestone deposits on the Wolsztyn High are mainly of bioclastic facies. Individual sections have variable thicknesses and slightly different successions, in which the most important facies are bioclastic grainstones and packstones, usually dominated by bryozoan skeletons. Other biota include foraminifera, crinoids, molluscs and brachiopods. Reefal framestones or boundstones are only found locally; microbialites and sabkha deposits occur in the upper parts of some sections.

Zechstein Limestone carbonates represent the full range from pure calcite to pure dolomite, although they are usually a mixture of dolomite and calcite with considerable anhydrite content. Diagenetic alteration is variable in its intensity and spatial distribution, but dolomitisation plays the most important role. Other significant diagenetic processes include calcite cementation of synsedimentary, meteoric and burial origin, dolomite and anhydrite cementation, recrystalisation and de-dolomitisation (see **Figures 8.76** to **8.83**).

Early marine diagenesis is widespread within the bioclastic and reefal facies. Synsedimentary cementation with fibrous calcite rims and botryoidal aragonite fans (**Figures 8.76** & **8.77**) has reduced primary porosity to a varied degree.

The next most important diagenetic process is dolomitisation, which took place in different diagenetic environments as indicated by petrography and oxygen-isotopic signatures. Most dolomites are the result of replacement, but dolomite cements are also very common (**Figures 8.76** to **8.81**). Dolomitisation is both fabric-preserving and fabric-destructive. The dolomites occupy a very wide range of $\delta^{18}O$ values in regions of both low and high-temperature origin (**Figure 8.84**). Crypto- to microcrystalline dolomites with heavy oxygen-isotopic signatures ($\delta^{18}O$ close to 0‰ or higher, up to +2‰ PDB) are typical of sabkha deposits (**Figure 8.84**). Some dolomitised bioclastic grainstones with well-preserved primary fabric may be isotopically heavy because of seepage reflux of evaporated water at relatively low temperatures. The rest of the dolomites exhibit a very wide range of $\delta^{18}O$ values (from +2 to −9‰ PDB), with the saddle dolomite being the lightest isotopically (**Figure 8.84**). Many samples fall in the overlap between low and high-temperature dolomite (−6 to −2‰ PDB) (Allan & Wiggins, 1993), so it is difficult to determine their origin unequivocally, although they probably formed in a deeper, higher temperature environment. The carbon-isotope signature of almost all dolomite samples typical of Permian marine carbonates ($\delta^{13}C$ from +2 to +8‰, average c. +4‰ PDB) (**Figure 8.84**) suggests that there was no significant shift in carbon-isotopic composition due to diagenesis and that the source of the carbonate ion was the Zechstein Limestone itself (with or without a contribution from Zechstein marine water).

Burial calcite cementation and replacement (de-dolomitisation) postdates dolomitisation (**Figures 8.80**, **8.82** & **8.83**). Only a small fraction of the $\delta^{18}O$ values in calcitic components is found within the range of Permian marine carbonates. Most samples are depleted in heavy oxygen isotopes (**Figure 8.84a**); however, the highest $\delta^{18}O$ values were measured in evidently diagenetic products, including calcite mosaic, which is probably at least partly de-dolomite in origin (**Figure 8.84a**). The fluids from which they formed must be relatively enriched in heavy oxygen isotopes and/or have low temperatures. On the other hand, the extremely low $\delta^{18}O$ values (−13‰ PDB in poikilotopic cement and euhedral calcite mosaic with relics of dolomitised bioclasts) may be the result of the high-temperature effect under burial conditions. In some cases, the lighter oxygen content may be related to an inflow of meteoric water, as is likely in the case of the grainstones with blocky calcite cements that show positive correlation of $\delta^{18}O$ and $\delta^{13}C$.

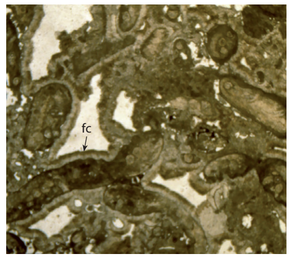

Figure 8.76 Completely dolomitised (fabric-preserving dolomitisation) bryozoan grainstone with fibrous cement rims (fc). Preserved high primary intergranular porosity. Paproć 21 well.

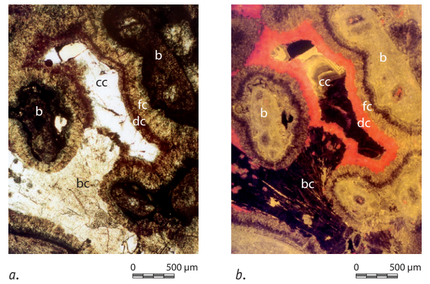

a. *b.*

Figure 8.77 Bryozoan (b) grainstone. Porosity infilled with marine fibrous isopachous (fc) and botryoidal (bc) (originally aragonite) calcite cements followed by isopachous dolomite cement (dc). The last cement generation is coarse-grained crystalline burial calcite (cc): a. Parallel polars; b. CL. Kościan 10 well.

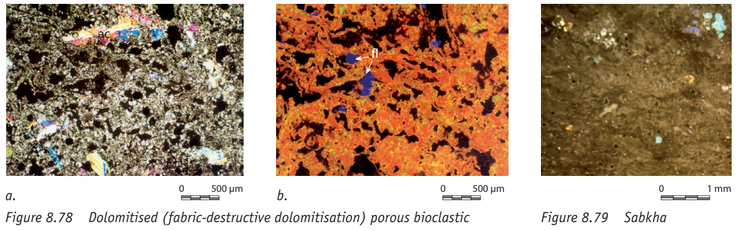

a. *b.*

Figure 8.78 Dolomitised (fabric-destructive dolomitisation) porous bioclastic grainstone with dolomite cement (dc), anhydrite cement (ac) and fluorite (fl): a. cross polars; b. CL. Paproć 21 well.

Figure 8.79 Sabkha dolomicrite (crossed polars) with anhydrite. Kościan 9 well.

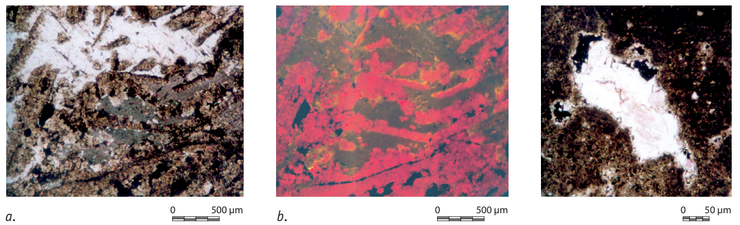

a. *b.*

Figure 8.80 Poikilotopic calcite cement in dolomitised bioclastic grainstone: a. crossed polars; b. CL. Paproć 29 well.

Figure 8.81 Saddle dolomite crystal in void within sabkha dolomicrite (crossed polars). Kościan 10 well.

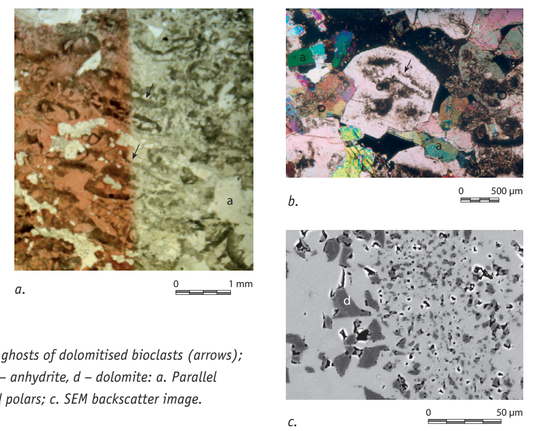

a. *b.* *c.*

Figure 8.82 Calcite mosaic with ghosts of dolomitised bioclasts (arrows); originally bryozoan grainstone, a – anhydrite, d – dolomite: a. Parallel (stained with alizarin); b. crossed polars; c. SEM backscatter image. Paproć 29 well.

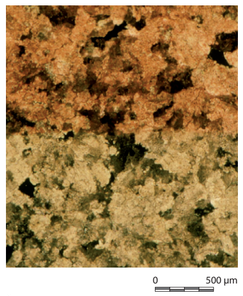

a.

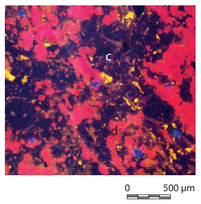

b.

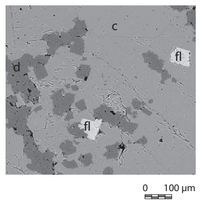

c.

Figure 8.83 Calcite mosaic (?de-dolomite): a. Parallel (stained with alizarin); b. crossed polars; c. SEM backscattering image (c – calcite, d – dolomite, fl – fluorite). Paproć 2 well.

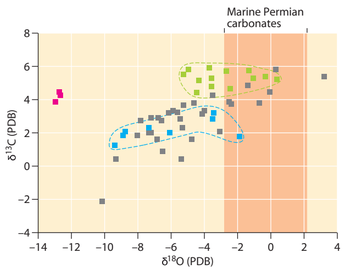

a.

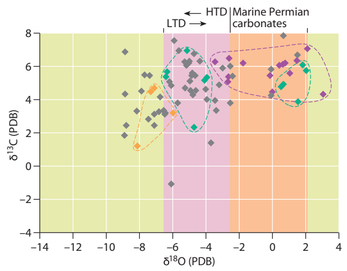

b.

Figure 8.84 Isotopic compositions of: a. Ca1 calcites; and b. dolomites from the Wolsztyn High. $\delta^{13}C$ values are typical of Permian marine carbonates and range from ca. –2 to +6‰ Pee Dee Belemnite (PDB) (average +2.74‰) in calcite and from –1‰ to +8‰ PDB in dolomite (average +4.81‰). $\delta^{18}O$ values are from ca. +3‰ to –13‰ PDB in calcite (average –5.1‰) and from +3‰ to –9‰ PDB in dolomite (average ca. –4‰). Calcite mosaic (?de-dolomite) exhibits rather high $\delta^{18}O$ and so originated in relatively heavy water and/or low temperature. Poikilotopic calcite cement/mosaic precipitated at high temperature. Other calcites seem to show some meteoric influence as is evidenced by positive correlation of $\delta^{18}O$ and $\delta^{13}C$. Sabkha dolomicrites precipitated in water with high $\delta^{18}O$ (e.g. if we assume a temperature of 40°C, the $\delta^{18}O$ of water would be close to 0‰ SMOW, which corresponds with a slightly evaporated Permian marine water). If the remaining dolomites are low-temperature precipitates, the $\delta^{18}O$ content of dolomitisation water appears to be in most cases unrealistically low. The better explanation seems to be a high-temperature origin for these dolomites, which is supported by the presence of saddle dolomite.

9 Diagenesis of the Main Dolomite (Ca2) deposits in the Grotów Peninsula (Gorzów Wielkopolska region, western Poland) (Marek Jasionowski: PGI, and Paweł Zdanowski, POGC)

Zechstein (Upper Permian) carbonates of the Stassfurt cyclothem (PZ2), known as the Main Dolomite (Ca2), comprise both shallow-platform and basin facies in the Gorzów Wielkopolski region (western Poland) (**Figure 8.85**). The Ca2 carbonate platform is a succession of oolitic, oncolitic, peloidal grainstones/packstones and lagoonal mudstones up to 80 m thick. The platform developed on an older sulphate platform and probably formed part of a highstand or transgressive systems tract. Within the basin, dark-coloured, finely-laminated, deep-water mudstones were deposited at the same time.

Pervasive dolomitisation is the most important type of diagenetic alteration affecting the Ca2 deposits in the Gorzów Wielkopolski area; others include dissolution, recrystallisation, anhydrite cementation/anhydritisation and de-dolomitisation. Although porosity can be well developed within the oolitic deposits (grainstones/packstones) of both platform and toe-of-slope/basin areas, it usually varies widely because of differences in the distribution of diagenetic alteration. The porosity of the platform deposits is generally low and is typically of intergranular type. In most cases, the primary pore space is completely occluded, usually by anhydrite (both cement and replacive) and less commonly by dolomite (**Figure 8.86**). In the barrier grainstone facies, early marine diagenesis produced synsedimentary fibrous isopachous cements. There is some evidence of emergence (pendant cement). A similar pattern of dolomitisation is found in fine-grained lagoonal mudstone/wackestone facies.

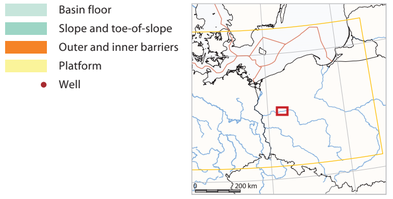

Figure 8.85 Palaeogeography during deposition of the Main Dolomite (Ca2) in the Grotów Peninsula (after Jaworowski & Mikolajewski, 2007) with locations of selected wells.

Porosity in the toe-of-slope deposits is generally much higher (up to 40%) than in the platform and is usually of secondary (oo)moldic type (**Figure 8.87**). In places, the molds are occluded by later large (often saddle) dolomite crystals. Due to replacement of the matrix by mosaics of fine- or medium-crystalline planar-s dolomite, high intercrystalline porosity connects the molds and improves permeability. The basinal mudstone/wackestone facies has a similar type of dolomitisation (**Figure 8.88a**). Locally, the planar dolomites recrystallised into coarse-crystalline saddle dolomite mosaics with complete destruction of the former fabric (**Figure 8.88b**). Saddle dolomite cements occur in some pores and fractures, whereas anhydrite cementation and replacement is of minor importance compared to the platform. De-dolomitisation is only encountered locally in the basin and toe-of-slope areas, where it resulted in coarse-crystalline calcite mosaics with relics of dolomite solid inclusions (**Figure 8.89**).

C and O isotopic signatures are quite homogeneous (**Figure 8.90**). The very high $\delta^{13}C$ values in dolomites (+6 to +8‰ PDB) are typical of the Zechstein Basin. In the lowermost parts of some sections, $\delta^{13}C$ can be much lower (as low as +1‰ PDB). Carbon isotopes show that there has been no input of light biogenic carbon and consequently there is no meteoric-water influence. $\delta^{18}O$ values are also very consistent. Both platform and toe-of-slope deposits have completely homogenised $\delta^{18}O$ values that are close to 0‰ (PDB). Dedolomites have slightly lower isotopic signatures of both C and O compared to parent dolomites. $\delta^{13}C$ values plot between +4 to +6‰ (PDB) and $\delta^{18}O$ between –2 to –1‰ (PDB).

The pervasive dolomitisation of the Ca2 deposits in the Gorzów Wielkopolski area is related to reflux of highly evaporated marine waters during burial in an environment with slightly elevated temperatures. The strontium-isotope values typical of the uppermost marine Permian ($^{87}Sr/^{86}Sr$ = 0.707010 to 0.707030)

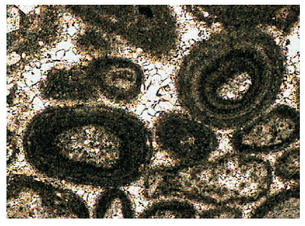

a.

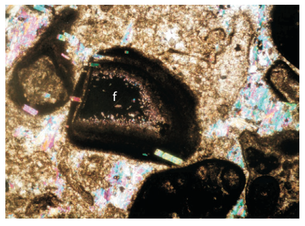

b.

Figure 8.86 Dolomitised oolitic grainstone of the highstand platform: a. intergranular porosity completely occluded with dolosparite, parallel polars, Grotów 6 well; b. abundant anhydrite occurring as cement and euhedral replacive crystals, f – fluorite crystals replacing ooid nucleus, crossed polars, Międzychód 4 well.

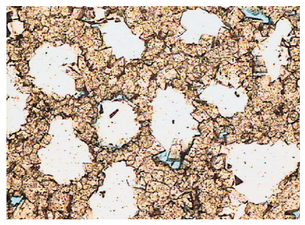

a.

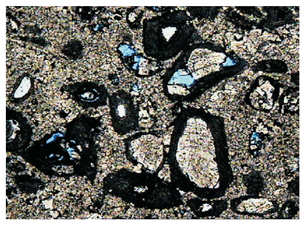

b.

Figure 8.87 Packstone/grainstone from the toe-of-slope: a. (oo)moldic porosity – grains, probably ooids were completely leached and matrix replaced by planar-s dolomite, parallel polars, Lubiatów 2 well; b. cortices of ooids are partly dolomitised, nuclei leached and filled with saddle dolomite, parallel polars, Sowia Góra 2K well.

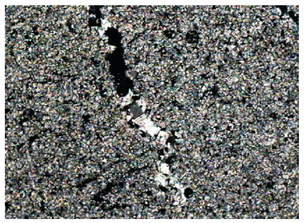

a.

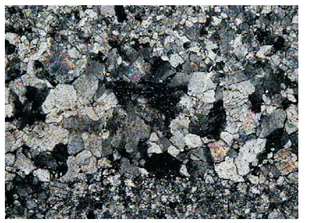

b.

Figure 8.88 Dolomitised mudstone facies: a. fine-grained crystalline planar-s mosaic with fracture partly occluded with coarser-grained dolomite, crossed polars, Sowia Góra 2K well; b. coarse-grained crystalline (non-planar) saddle dolomite mosaic with finer-grained dolomite, crossed polars, Sowia Góra 2K well.

a.

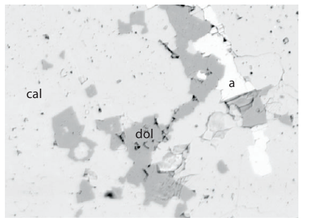

b.

Figure 8.89 De-dolomitised (lower part of the picture) mudstone facies in the toe-of-slope setting: a. crossed pollars, stained with alizarin, crossed polars, Lubiatów 2 well; b. SEM backscattering image; cal – calcite, dol – dolomite, a – anhydrite, Sowia Góra 2 well.

provide evidence for the marine origin of the diagenetic fluids. Fluid-inclusion data from dolomite crystals indicate temperatures in the range of 70 to 100°C and very high salinities. The inferred isotopic composition of water is in the range of +5 to +10 ‰ (SMOW).

Studies of fluid inclusions suggest that de-dolomitisation probably took place during burial at temperatures of about 100 to 120°C. Deep burial is also indicated by the development of large calcite crystals that transect dissolution seams/initial stylolites. The origin of the dedolomitising fluid is uncertain.

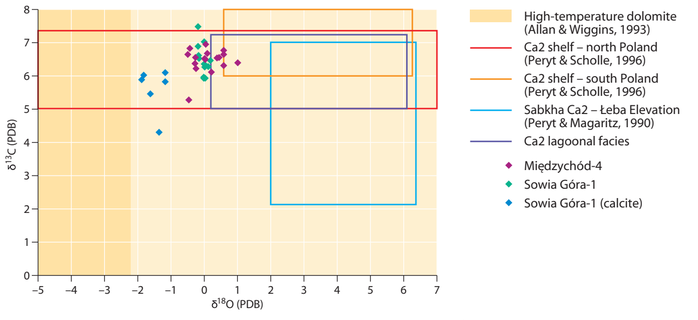

Figure 8.90 C and O stable isotopes of the Ca2 dolomites and de-dolomites from the Międzychód-4 and Sowia Góra-1 wells plotted against Ca2 dolomites from other locations in Poland.

Acknowledgements

The authors would like to acknowledge Marek Hajto (AGH University of Science & Technology), Rafał Kudrewicz (POGC), Anna Sowiżdżał (AGH University of Science & Technology) and Grzegorz Machowski (AGH University of Science & Technology) for their major contribution to the map compilations. Leszek Skowroński (PGI), Krzysztof Chłódek (POGC), Zbigniew Mikołajewski (POGC) and Maciej Kozłowski (POGC) provided valuable input to the chapter. The Ministry of Science and Higher Education and National Fund National Fund for Environmental Protection and Water Management are acknowledged for the support of work carried out by the Polish contributors.